



The University of  
**Nottingham**

**MOISTURE DAMAGE OF AGGREGATE-  
BITUMEN BONDS**

By

Jizhe Zhang

Thesis submitted to the University of Nottingham

For the degree of Doctor of Philosophy

November 2015

# Abstract

Moisture damage of the asphalt mixture is defined as the loss of strength, stiffness and durability due to the presence of moisture (in a liquid or vapour state) leading to adhesive failure at the aggregate-bitumen interface and/or the cohesive failure within the bitumen or bitumen-filler mastic. The presence of moisture can accelerate the distress of asphalt pavement in several different modes, such as rutting, fatigue cracking, thermal cracking and the formation of potholes. In the field, the moisture damage normally happens first at the interface of two pavement layers or at the bottom of pavement layers and develops gradually upward. Once moisture has come into contact and interacted with the asphalt mixture, moisture damage could be developed by the following mechanisms: detachment, displacement, spontaneous emulsification, pore pressure, and hydraulic scour. It should be mentioned that moisture damage is not limited to only one mechanism but is the result of a combination of several mechanisms.

As mentioned previously, the common modes of moisture damage of asphalt mixtures are a loss of adhesion between the aggregate and bitumen and/or a loss of cohesion in the mixture. Among these two failures, the adhesive failure is recognised as the main mode of moisture damage. Hence, the physico-chemical interactions between aggregates and bitumen in the presence of moisture are believed to partially govern the moisture sensitivity of asphalt mixtures, which can also affect the serviceability, performance and durability of the asphalt pavement.

This thesis describes the work that was carried out with regard to the moisture damage evaluation of aggregate-bitumen bonds through different procedures. The fundamental properties of the individual material such as the chemical composition and rheological properties of bitumen, moisture absorption, surface morphology and mineralogical composition of aggregates were first characterised. Two types of equipment, namely the dynamic contact angle (DCA) analyser and dynamic vapour sorption (DVS) system were used for determining the surface energy of the bitumen and aggregates, respectively. The obtained surface energy results were then combined thermodynamically to determine the work of adhesion between aggregate and bitumen, and the reduction in the adhesive properties if water is introduced into the system. Three established mechanical tests consisting of the standard peel test, Pneumatic

Adhesion Tensile Testing Instrument (PATTI) test and a pull off test were developed and redesigned to make sure that these tests are practical, reliable and feasible to measure the bonding strength of aggregate-bitumen combined specimens. The composite substrate peel test (CSPT) was developed to prepare composite substrates using crushed coarse aggregates as a more practical replacement for the aggregate substrates prepared from aggregate boulders. Finally, the moisture damage results from mechanical tests and thermodynamic results were compared and correlated with the basic physico-chemical properties of the original materials.

The results showed that in the dry condition, all techniques used in this research, including the mechanical tests and the surface energy tests led to similar results, with bitumen rather than aggregates dominating the bonding properties of aggregate-bitumen systems. After moisture conditioning, the four mechanical tests, including standard peel test, CSPT, PATTI test and pull-off test showed similar moisture sensitivity ranking and failure surface results demonstrating the good correlation between these four tests. In addition, based on the comparison conducted, the four mechanical tests are all considered to be reliable to evaluate the moisture sensitivity of different aggregate-bitumen systems. However, based on the aggregates considered in this research, the moisture sensitivity parameters obtained from the surface energy tests are suggested unreliable to evaluate the moisture sensitivity of aggregate-bitumen systems.

# Dedication

I dedicate this dissertation to my mom

# Acknowledgement

I would like to thank all the people who have provided their assistance, advice, encouragement and funding without which this research would not have been possible.

This research was conducted under the supervision of Professor Gordon Dan Airey, to whom I am deeply grateful for his guidance and assistance throughout my research period in the University of Nottingham. He has given careful reviews and individual guidance and comments on my reports and papers during my PhD study. His high expectations and continuous support are greatly appreciated and will never be forgotten.

Secondly, I would like to express my sincere gratitude to my second supervisor, Dr. James Grenfell, for his help and support throughout my research. His extensive comments and advice on my reports and papers were extremely valuable. I would also like to thank Dr. Alex Apeageyi for providing valuable suggestions and generous help in this research. Special thanks are also given to Mr. Martyn Barrett for his kind help in the testing design and sample preparation.

I sincerely thank all the technical staff in Nottingham Transportation Engineering Centre (NTEC), for their kind help during the experimental work, particularly Jonathan Watson, Richard Blakemore and Lawrence Pont. I am also very grateful to all my colleagues in NTEC for their support during my PhD research.

Special thanks is given to my lovely wife, Juan Jin and my little princess, Suyang Zhang who always give encouragement and support that made my education possible and always stood by me through its rough and smooth patches. Lastly I would like to thank my parents for their support during my over 22 years studying period. Their encouragement, expectation and love are the origin of my inspiration.

# Declaration

The research described in this thesis was conducted at the University of Nottingham, Department of Civil Engineering between November 2012 and November 2015. I declare that the work is my own and has not been submitted for a degree of another university.

Jizhe Zhang

Nottingham

November 2015

# Glossary

$\gamma_s^+$	Lewis acid component
$\gamma_s^-$	Lewis base component
$\gamma_s^{LW}$	Lifshitz-Van der Waals component
AASHTO	American Association of State Highway and Transportation Officials
ASTM	American Society for Testing and Materials
BET	Brunauer-Emmett-Teller
BSE	Back-scattered Electron
CA	Contact Angle
CSPT	Composite Substrate Peel Test
CV	Coefficient of Variability
DCA	Dynamic Contact Angle
DCB	Double Cantilever Beam
DSR	Dynamic Shear Rheometer
DVS	Dynamic Vapour Sorption
EDX	Energy Dispersive X-ray
FTIR	Fourier Transform Infrared Spectroscopy
HWTD	Hamburg Wheel Tracking Device
IRS	Index of Retained Strength
ITS	Indirect Tensile Strength

IWP	Impact Wedge Peel
LEFM	Linear-Elastic-Fracture-Mechanics
LVE	Linear Visco-Elastic
MLA	Mineral Liberation Analyser
NAT	Nottingham Asphalt Tester
NIST	National Institute of Standards and Technology
NTEC	Nottingham Transportation Engineering Centre
PATTI	Pneumatic Adhesion Tensile Testing Instrument
PET	Polyethylene Terephthalate
POTS	Pull-off Tensile Strength
PTFE	Poly Tetra Fluoro Ethylene
$R^2$	Coefficient of Determination
SATS	Saturation Ageing Tensile Stiffness
SD	Standard Deviation
SEM	Scanning Electron Microscopy
SHRP	Strategic Highway Research Program
SSA	Specific Surface Area
T	Absolute temperature
TDCB	Tapered Double Cantilever Beam
TS	Tensile Strength
TTSP	Time-Temperature Superposition Principle

UTM	Universal Testing Machine
$W_a$	Work of Adhesion
$W_{AWB}$	Work of debonding with the presence of water
$W_{BA}$	Work of adhesion between bitumen and aggregate
WLF	Williams-Landel-Ferry
$\Delta G$	Gibbs free energy
$\Delta H$	Enthalpy
$\Delta S$	Entropy

# Table of Contents

<b>Abstract .....</b>	<b>i</b>
<b>Dedication.....</b>	<b>iii</b>
<b>Acknowledgement.....</b>	<b>iv</b>
<b>Declaration .....</b>	<b>v</b>
<b>Glossary .....</b>	<b>vi</b>
<b>List of Figures .....</b>	<b>xv</b>
<b>List of Tables.....</b>	<b>xxi</b>
<b>1. Introduction .....</b>	<b>1</b>
1.1 Background .....	1
1.2 Problem statement .....	3
1.3 Research objectives and scope.....	4
1.4 Thesis organisation .....	5
References.....	7
<b>2. Literature review .....</b>	<b>9</b>
2.1 Introduction.....	9
2.2 Moisture damage mechanisms.....	10
2.2.1 Detachment.....	10
2.2.2 Displacement .....	11
2.2.3 Spontaneous Emulsification.....	11

2.2.4 Pore Pressure .....	12
2.2.5 Hydraulic Scour.....	13
2.3 Adhesion of Aggregate-Bitumen Interface.....	13
2.3.1 Chemical Bonding Theory .....	14
2.3.2 Electrostatic Theory .....	17
2.3.3 Mechanical Adhesion Theory .....	20
2.3.4 Thermodynamic Theory.....	22
2.4 Testing methods related to moisture damage evaluation.....	24
2.4.1 Tests on loose coated aggregates .....	24
2.4.2 Tests on compacted mixtures .....	26
2.4.3 Other representative tests for moisture damage evaluation .....	29
2.5 Summary.....	36
References.....	38
<b>3. Materials.....</b>	<b>48</b>
3.1 Introduction.....	48
3.2 Aggregates .....	48
3.2.1 Mineralogical composition of aggregate.....	48
3.2.2 Moisture absorption of aggregates .....	51
3.3 Bitumen.....	55
3.3.1 Dynamic shear rheometer test.....	55
3.3.2 Fourier Transform Infrared Spectroscopy (FTIR) test.....	57

3.4 Conclusions.....	58
References.....	60
<b>4. Surface energy testing of bitumen and aggregate .....</b>	<b>62</b>
4.1 Introduction.....	62
4.2 Surface energy evaluation of bitumen .....	63
4.2.1 Dynamic contact angle (DCA) technique .....	63
4.2.2 Test protocol.....	67
4.3 Surface energy evaluation of aggregate .....	69
4.3.1 Dynamic vapour sorption (DVS) technique .....	69
4.3.2 Test protocol.....	72
4.4 Work of adhesion and moisture sensitivity .....	73
4.4.1 Bond energy parameters .....	74
4.4.2 Moisture sensitivity parameters .....	75
4.5 Results.....	77
4.5.1 Surface free energy of bitumen .....	77
4.5.2 Surface free energy of aggregate .....	79
4.5.3 Aggregate-bitumen adhesion and moisture sensitivity .....	80
4.6 Conclusions.....	83
References.....	85
<b>5. Fracture energy - Peel test.....</b>	<b>87</b>
5.1 Introduction.....	87

5.2 Theory of fracture energy .....	88
5.3 Experimental procedure of peel test .....	92
5.3.1 Sample preparation.....	92
5.3.2 Fracture energy evaluation.....	94
5.3.3 IC Peel software introduction.....	95
5.4 Results.....	98
5.4.1 Parameters calculation.....	98
5.4.2 Influence of bitumen and aggregate in the dry condition.....	104
5.4.3 Influence of film thickness .....	108
5.4.4 Influence of moisture damage .....	109
5.5 Conclusions.....	114
References.....	115
<b>6. Tensile strength - PATTI test and Pull-off test.....</b>	<b>117</b>
6.1 Introduction.....	117
6.2 Pneumatic Adhesion Tensile Testing Instrument (PATTI) test .....	117
6.3 Pull-off test .....	121
6.4 Results for PATTI test .....	124
6.4.1 PATTI cohesive and adhesive bond strength measurements in dry condition .....	124
6.4.2 Cohesive and adhesive bond strength measurements after moisture damage .....	130
6.5 Results for Pull-off test.....	133

6.5.1 Influence of aggregate and bitumen on tensile strength in dry condition ....	133
6.5.2 Influence of moisture damage on Pull-off test.....	134
6.6 Conclusions.....	141
References.....	143
<b>7. Composite Substrate Peel Test (CSPT) .....</b>	<b>145</b>
7.1 Introduction.....	145
7.2 Experimental program .....	145
7.2.1 Substrate preparation.....	145
7.2.2 Adhesion specimen fabrication .....	148
7.2.3 Moisture conditioning .....	150
7.2.4 Parameter evaluation.....	150
7.3 Results.....	152
7.3.1 Fracture energy calculation for CSPT.....	152
7.3.2 Fracture energy in dry condition .....	154
7.3.3 Failure behavior after moisture conditioning .....	155
7.3.4 Retained fracture energy .....	158
7.4 Correlation between CSPT and standard peel test.....	160
7.5 Conclusions.....	161
References.....	163
<b>8. Correlation between different tests.....</b>	<b>164</b>
8.1 Introduction.....	164

8.2 Correlations of different tests in dry conditions .....	165
8.3 Correlations of different mechanical tests after moisture damage .....	166
8.3.1 Sensitivity of different mechanical tests on moisture damage .....	166
8.3.2 Correlations between different tests in terms of failure surface .....	170
8.4 Correlation between surface energy test and mechanical test .....	172
8.5 Conclusions.....	176
References.....	178
<b>9. Conclusions and Recommendations .....</b>	<b>179</b>
9.1 Overview.....	179
9.2 Conclusions.....	180
9.3 Recommendations.....	182
References.....	185
<b>Appendix A.....</b>	<b>186</b>
<b>Appendix B.....</b>	<b>187</b>
<b>Appendix C.....</b>	<b>188</b>
<b>Appendix D.....</b>	<b>189</b>
<b>Appendix E.....</b>	<b>190</b>

# List of Figures

Figure 2-1 Chemical functional groups in bitumen (1) naturally occurring and (2) formed on oxidative aging [31] .....	16
Figure 2-2 Schematic illustration of the stern layer and diffuse layer with thickness [26]. .....	18
Figure 2-3 Zeta potential of different types of bitumen with granite aggregate (a) and limestone aggregate (b) at different pH values [40] .....	19
Figure 2-0-4 Summary of aggregate physical properties and how they affect stripping [34] .....	21
Figure 2-5 Test equipment for determination of indirect tensile strength or stiffness ...	26
Figure 2-6 Hamburg wheel tracking device for determination of permanent deformation .....	27
Figure 2-7 Image and schematic of goniometer [70] .....	29
Figure 2-8 Image and schematic of dynamic contact angle test procedure [70] .....	30
Figure 2-9 Image of the Dynamic Vapour Sorption equipment .....	31
Figure 2-10 Image of the Microcalorimeter equipment .....	31
Figure 2-11 Schematic diagram of pull-off test [71] .....	33
Figure 2-12 Test equipment for pull-off test using UTM [75] .....	33
Figure 2-13 Configuration of different peel tests [84] .....	34
Figure 2-14 Equipment used for the SATS test.....	35
Figure 3-1 Mineral mosaic of five aggregates. L1 and L2 are classified as limestone while G1, G2 and G3 are granite .....	50

Figure 3-2 Moisture absorption values versus conditioning time for five different aggregates. Moisture conditioning testing was conducted at 20 °C.....	52
Figure 3-3 DSR test setup and applied signal .....	55
Figure 3-4 Master curves of shear complex modulus and phase angle at a reference temperature of 30 °C for two types of bitumen B1 and B2. Data shows that B1 is stiffer than B2.....	57
Figure 3-5 FTIR test result of B1 (40/60 pen) and B2 (70/100 pen) bitumen.....	58
Figure 4-1 Schematic of dynamic contact angle analyser [3] .....	64
Figure 4-2 Relationship between wetting force and depth of immersion during DCA test [5].....	65
Figure 4-3 Typical sorption isotherm obtained for L1 aggregate using octane vapour as probe liquid for partial vapour pressures ranging from 0% to 95% .....	70
Figure 4-4 Plot of $\gamma L \cos\theta$ versus $\gamma L$ for B1 and B2 .....	78
Figure 5-1 Deformation process of the peel arm. (a) deformation process of the peel arm. (b) large-displacement beam-theory model of the peel test [4]. .....	90
Figure 5-2 Schematic of the bilinear model for the stress-strain curve [4]......	90
Figure 5-3 Details of peel test equipment.....	94
Figure 5-4 Interface of the ICPeel software [7].....	98
Figure 5-5 Stress-strain curve of peel arm test.....	99
Figure 5-6. Tensile stress-strain curve fitted using bilinear model .....	100
Figure 5-7 Tensile stress-strain curve fitted using power law model.....	100
Figure 5-8 Relationship between elastic and frequency modulus of 40/60 pen bitumen .....	103

Figure 5-9 Relationship between elastic and frequency modulus of 70/100 pen bitumen .....	103
Figure 5-10 Measured tensile force-displacement curve for specimen prepared with 40/60 pen bitumen and L1 substrate with 0.25mm film thickness .....	104
Figure 5-11 Fracture energy of bitumen-limestone specimens at different film thicknesses .....	108
Figure 5-12 Relationship between normalised toughness and film thickness of bitumen .....	109
Figure 5-13 Effect of moisture conditioning time on retained fracture energy of different aggregate-bitumen combinations. (a) bitumen B1, (b) bitumen B2. ....	111
Figure 5-14 Failure surfaces of sample prepared with B1 bitumen in dry and after 14 days moisture condition.....	112
Figure 6-1 Pull-stub in profile and bottom views (a) and the prepared specimen (b) ..	118
Figure 6-2 Equipment associated with PATTI test .....	120
Figure 6-3 Cross-section view of piston attached to pull-stub [5] .....	120
Figure 6-4 The PATTI equipment connected with environmental chamber to control temperature .....	121
Figure 6-5 Sample preparation and pull off test procedures .....	123
Figure 6-6 PATTI tensile strength versus loading time (B1 + G1). ....	125
Figure 6-7 PATTI tensile strengths from PATTI test at different temperatures .....	126
Figure 6-8 Bitumen tensile strength versus stiffness modulus reported by Heukelom and Wijga [9]......	127
Figure 6-9 Failure surfaces of B1 bitumen with G1 aggregate samples at different temperatures: (a) -10 °C, (b) 0 °C, (c) 10 °C, (d) 20 °C, (e) 30 °C (f) 40 °C. The red area showed the adhesive failure.....	128

Figure 6-10 Retained bonding strength obtained from the PATTI test after moisture conditioning showing the effect of aggregate type on moisture sensitivity of aggregate-bitumen bonds at 20 °C: (a) bitumen B1, (b) bitumen B2. ....	132
Figure 6-11 Sample failure surfaces for dry and moisture-conditioned aggregate-bitumen bonds tested in the PATTI test. Note: moisture conditioning time for all specimens in this Figure is 14 days. ....	133
Figure 6-12 Effect of moisture on load-displacement behaviour of aggregate-bitumen combined samples before and after moisture conditioning. Samples were conditioned in water at 20 °C; loading rate was 10 mm/min (Pull-off test). ....	136
Figure 6-13 Effect of moisture conditioning time on tensile strength of different aggregate-bitumen combinations obtained from pull-off test. In general acidic aggregate performed worse than basic aggregates. The combination of bitumen B1 with aggregate G2 performed worst: (a) bitumen B1, (b) bitumen B2. ....	138
Figure 6-14 Failure surface of aggregate-bitumen bonds exposed to moisture: top bitumen B1; bottom bitumen B2. The effect of bitumen type is minimal compared with the effect of aggregate type .....	140
Figure 7-1 Aggregate substrate and coarse aggregates: (a) substrate must be prepared from large boulders, while (b) coarse aggregates are readily available in most labs...	146
Figure 7-2 Schematic of the aluminium mould used for composite substrate preparation .....	147
Figure 7-3 Procedures for aggregate substrate preparation: (a) trimming saw, (b) aggregates after trimming, (c) release compound, (d) assembled mould, (e) epoxy resin, (f) combine trimmed aggregates in the mould and fill the gaps with epoxy resin, (g) cured composite aggregate, (h) composite substrate used for peel test.....	148
Figure 7-4 Prepared adhesion specimens used for peel test.....	149
Figure 7-5 Moisture conditioning of adhesion specimens .....	150
Figure 7-6 Details of peel test equipment.....	151

Figure 7-7 Measured tensile load-displacement curve of: (a) B1-G2 in dry condition using CSPT and (b) B1-G2 after 14 days conditioning using CSPT. The three fluctuations presented in Figure 7-7b is because the epoxy resin segments between two aggregates result in high bond strength with bitumen even after moisture conditioning. .... 154

Figure 7-8 Failure surface of specimens prepared with G2 coarse aggregates in dry condition ..... 155

Figure 7-9 Failure surfaces and loading behavior of two specimens (B1-G1 and B1-G2) after 14 days of moisture conditioning using the CSPT ..... 157

Figure 7-10 Loading behavior of two samples (B1-G1 and B1-G2) after 14 days of moisture conditioning obtained using both standard peel test and CSPT ..... 158

Figure 7-11 Retained fracture energy with respect to moisture damage achieved from CSPT..... 160

Figure 7-12 Plots of standard peel test retained fracture energy and CSPT retained fracture energy of specimens prepared with B1 bitumen showing good agreement between these two tests ..... 161

Figure 8-1 Plots of CSPT retained fracture energy and standard peel test retained fracture energy of specimens prepared with B1 bitumen showing good agreement between these two tests ..... 168

Figure 8-2 Plots of retained fracture energy and retained tensile strength obtained from the standard peel test and PATTI test showing good agreement between these two tests. Note: The data in red colour (B2-G2 after 7 days conditioning) is far away the trend line. .... 169

Figure 8-3 Plots of retained fracture energy and retained tensile strength obtained from standard peel test and pull-off test. Note: The data in red colour (B1-G2 after 7 days conditioning) is far away the trend line. .... 170

Figure 8-4 Failure surfaces of B1-G2 specimens before and after moisture conditioning obtained from the standard peel test, the newly developed peel test, the PATTI test and

the pull-off test. Note: specimens of the standard peel test, CSPT and PATTI test were moisture conditioned for 14 days, while the pull-off specimen was moisture conditioned for 7 days. .... 171

Figure 8-5 Plots of retained fracture energy and moisture sensitivity parameter obtained from CSPT and surface energy test ..... 173

Figure 8-6 Plots of retained fracture energy and moisture sensitivity parameter obtained from standard peel test and surface energy test ..... 174

Figure 8-7 Moisture sensitivity parameter ER4 versus Wet to Dry Ratio of Fatigue Life [4] ..... 175

Figure 8-8 SATS Moisture Factors versus SE Bond Ratios [5] ..... 175

# List of Tables

Table 2-1 Mineral types and their relation to stripping .....	17
Table 2-2 Detailed introduction of tests on loose coated aggregates .....	25
Table 2-3 Detailed introduction of tests on compacted asphalt mixtures .....	28
Table 3-1 Testing conditions of frequency sweep tests.....	56
Table 4-1 Surface energy components of the probe liquids .....	77
Table 4-2 The average advancing and receding contact angle values.....	77
Table 4-3 Surface energy components of bitumen. ....	79
Table 4-4 Surface energy components and SSA of aggregates.....	79
Table 4-5 Work of adhesion and cohesion in dry condition .....	81
Table 4-6 Work of debonding in wet condition .....	81
Table 4-7 Moisture sensitivity parameters of all aggregate-bitumen combinations .....	83
Table 5-1 Plastic bending parameters of the peel arm .....	101
Table 5-2 Tensile force results for all specimens in the dry condition .....	105
Table 5-3 Three output parameters of all specimens in the dry condition .....	107
Table 6-1 Dry tensile strength (kPa) of aggregate-bitumen bonds at 20 °C (PATTI). .	130
Table 6-2 Dry tensile strength (MPa) of aggregate-bitumen in the dry state at 20 °C..	134
Table 7-1 Plastic bending parameters of the peel arm based on bi-linear model fit ....	152
Table 7-2 Dry fracture energy ( $J/m^2$ ) of aggregate-bitumen bonds in the dry state at 20 °C using the newly designed CSPT.....	155
Table 8-1 Aggregate-bitumen bonding values in dry condition.....	166

# 1. Introduction

## 1.1 Background

The total road length in the UK is estimated to be approximately 250 thousand miles with most of these roads being surfaced with asphalt mixtures [1]. Asphalt mixture is a composite material consisting of aggregates (coarse and fine), bitumen and filler, mixed in a predetermined ratio at high temperatures followed by compaction in order to produce a flexible pavement. When subjected to loading traffic, asphalt pavements deteriorate gradually with the passage of time because of repeated traffic loading and environmental attack. In England and Wales, about 2.8 billion pounds been spent every year by local authorities on road maintenance [2]. It is generally accepted that moisture damage is one of the major causes of pavement deterioration. Due to the wet climate in UK, distress and deterioration in a large number of pavements as a result of moisture damage is an indication of the significance and the severity of the problem.

Moisture damage in asphalt pavements can generally be classified as the gradual deterioration of strength, stiffness and durability due to the presence of moisture in a liquid or vapour state. Although the moisture cannot directly disrupt the asphalt mixtures, its presence accelerates the distress of asphalt pavement in several different modes, such as rutting, fatigue cracking, thermal cracking and the formation of potholes [3, 4]. Recent research studies have also shown that moisture damage maybe reversible under certain conditions [5]. In the field, moisture damage normally happens first at the interface of two pavement layers or at the bottom of pavement layers and then develops gradually upward. In addition, it has been observed that moisture damage is more prone to occur in the wheel path in comparison with locations between the wheel paths or on the shoulder [6].

Moisture induced damage is a particularly complicated mode of distress and can result in two different forms of failure including adhesive at the aggregate-bitumen (mastic) interface and cohesive within the bitumen (mastic) film. The adhesion between aggregate and bitumen can be defined as the attraction of these two materials in the area

of contact due to molecular forces holding the materials together and resisting separation. The bitumen cohesion can be defined as the attraction within the bitumen film due to the intermolecular forces and is influenced by factors such as modulus and viscosity [7].

Numerous testing methods have been developed for evaluating the moisture sensitivity of asphalt mixtures. Typically, many of these methods can be divided into two categories, which are tests conducted on loose coated aggregates and tests conducted on compacted mixtures. Tests on loose coated aggregates are normally conducted by immersing bitumen coated aggregates in water either at room temperature or high temperature for a specified period of time under static or dynamic conditions and finally assessing the stripping percentage of bitumen from the aggregate surface by visual inspection. Tests on compacted mixtures generally conditioned the samples, which are prepared in the laboratory or cored from existing pavements, in water to simulate the moisture damage process and evaluated the moisture sensitivity by calculating the ratio of conditioned to unconditioned strength or stiffness [8, 9].

There are several factors which may influence the development of moisture damage or moisture sensitivity of an asphalt pavement, such as aggregate mineralogy, surface texture of aggregate, bitumen chemistry and the compatibility between bitumen and aggregate. In addition, factors such as permeability of the asphalt mixture, volumetric properties of the mixture and the ambient conditions are all important when considering the susceptibility of asphalt mixtures to moisture damage [10]. Based on previous research, moisture damage is mainly characterised as the adhesive failure between aggregate and bitumen or bitumen-filler (mastic) [11]. So, it has been suggested that the adhesion between aggregate and bitumen in the dry condition and its degradation with the presence of water are two main attributes which determine the moisture sensitivity of pavements. The adhesion between aggregate and bitumen can be described by four theories which are chemical bonding theory, electrostatic theory, mechanical theory, and thermodynamic theory. [12].

## 1.2 Problem statement

Moisture induced damage has been recognised as one of the major causes of distress in asphalt pavements since the early 1900s [13]. As mentioned previously, a common manifestation of moisture damage of asphalt mixtures is a loss of adhesion between the aggregate and bitumen and/or a loss of cohesion in the mixture. Among these two failures, the adhesive failure is recognised as the main mode of moisture damage. Hence, the physico-chemical interactions between aggregates and bitumen in the presence of moisture are believed to partially govern the moisture sensitivity of asphalt mixtures, which can also affect the serviceability, performance and durability of the asphalt pavement.

To evaluate the moisture damage of adhesion between aggregates and bitumen, efforts have been made through the development of numerous testing methods. Based on the literature review, the standard tests on loose coated aggregates, such as the boiling water and the rolling bottle tests are considered as direct methods to assess moisture sensitivity by visual inspection. However, these tests only rely on a comparative evaluation so the results cannot be used to explain the actual mechanisms that contribute to moisture damage and it is hard to correlate test data with field performance. So, it seems important to develop testing techniques and procedures that can directly measure the strength of the aggregate-bitumen adhesive bonds.

Over the past few years, several testing techniques used in other areas have been selected and developed to measure the adhesion between aggregate and bitumen in the dry condition and after moisture damage. Among the most commonly used testing techniques and procedures are the peel test and the pull-off test. The peel test is a method used to measure the adhesive fracture energy of a bonded interface of composite materials and has been successfully used to evaluate the moisture sensitivity of different aggregate-bitumen combinations. The peel test used for aggregate-bitumen adhesive testing requires the preparation of a large flat aggregate surface with regular shape. In this case, only large stone boulders could be used for the peel substrate preparation. In terms of the pull-off test, the tensile stress necessary to detach the adhesive materials in a direction perpendicular to the substrates is measured. However, the limitation of this test is also very obvious. Firstly, established pull-off tests typically

manually control the bitumen film thickness using micrometres or spacers making it hard to obtain the required thickness and resulting in big deviations in measured strength. Secondly, the bitumen film is too thick and hence cannot simulate the real bitumen thickness in asphalt mixtures.

According to the literature review, a number of tests have been used to evaluate the moisture sensitivity of asphalt mixtures with most of these only relating moisture damage to mechanical deterioration. The physical and chemical properties of bitumen and aggregate are not explained in detail and correlated with the mechanical tests. In fact, the physico-chemical properties of aggregate and bitumen, such as the mineralogical composition of aggregates and functional groups of bitumen, play a fundamental role in the generation of moisture damage. The mechanisms of moisture damage in asphalt mixture can be better understood if the physico-chemical properties of the individual material (aggregate and bitumen) are linked to the mechanical distress of the aggregate-bitumen bond.

### **1.3 Research objectives and scope**

The main aim of this research is to better understand the influence of moisture on the deterioration of the aggregate-bitumen interface. As mentioned before, the main causes of moisture damage in asphalt mixtures are related to the adhesion properties of the aggregate-bitumen interface and its degradation with the presence of water. In the presence of water, the bitumen film is removed from the aggregate surface because of the weak boundary between these two materials. According to the literature review, the physical and chemical properties of bitumen and aggregates play an important role in the bonding strength of the aggregate-bitumen interface. In this research, the fundamental properties of the individual material such as the chemical composition and rheological properties of bitumen, moisture absorption, surface morphology and mineralogical composition of the aggregates were characterised. Surface energy properties of different types of bitumen and aggregates were measured to calculate the adhesion between these two materials with and without the presence of water. The standard peel test was used to measure the adhesive fracture energy of aggregate-bitumen bonds. In addition, two established mechanical tests, namely the Pneumatic

Adhesion Tensile Testing Instrument (PATTI) test and pull-off test were developed and redesigned to make sure they are practical, reliable and feasible to measure the bonding strength of aggregate-bitumen combined specimens. Furthermore, a composite substrate peel test (CSPT) was designed based on the established peel test to combine several coarse aggregates together and get a flat surface that can be used for the peel test. These four mechanical tests were used to evaluate the moisture sensitivity of different aggregate-bitumen systems by measuring the bond strength of aggregate-bitumen interfaces in the dry condition and after moisture conditioning. Finally, the moisture damage results from mechanical tests and thermodynamic results were compared and correlated with the physico-chemical properties of the original materials.

## **1.4 Thesis organisation**

To achieve the main aim of this research, specific objectives need to be undertaken and have been separated into nine chapters.

Chapter 1 briefly introduces the background related to moisture induced damage of asphalt mixtures and the relative methods to evaluate the moisture damage. The organisation of the final thesis is also presented in this chapter.

Chapter 2 conducts a comprehensive literature review on several aspects related to moisture damage of asphalt mixtures which includes moisture damage modality, theories of aggregate-bitumen adhesion and various testing techniques used to measure the moisture sensitivity of asphalt mixtures.

Chapter 3 presents the fundamental properties of aggregates and bitumen that are used in this research.

Chapter 4 provides the surface energy measurement of aggregates and bitumen carried out by using dynamic vapour sorption (DVS) and dynamic contact angle (DCA) analyser, respectively. The results in terms of surface energy parameters, work of adhesion and work of debonding are also presented and analysed in this chapter.

Chapter 5 introduces the detailed procedures of using the standard peel test to measure the adhesive fracture energy of aggregate-bitumen bonds. The moisture sensitivity of different aggregate-bitumen combinations were evaluated by using the peel test.

Chapter 6 develops and redesigns the established Pneumatic Adhesion Tensile Testing Instrument (PATTI) and the pull off tests to make them more applicable to measure the tensile strength of aggregate-bitumen bonds. The moisture sensitivity of aggregate-bitumen bonds are measured and compared in this chapter.

Chapter 7 presents the development of a new procedure to prepare aggregate substrate by using coarse aggregates. The moisture sensitivity of aggregate-bitumen bonds were evaluated using the newly designed composited specimen.

Chapter 8 compares the moisture evaluation techniques used in this research. The correlation between the moisture sensitivity results obtained from the different methods and the reliability of each test are characterised.

Chapter 9 outlines the conclusions of this study and the recommendations for future work.

## References

1. Road lengths in Great Britain 2014. Department of Transport. (<https://www.gov.uk/government/statistics/road-lengths-in-great-britain-2014>) [accessed 01.10.15].
2. Annual Local Authority Road Maintenance (ALARM) Survey 2014. Asphalt Industry Alliance, ([http://www.asphaltindustryalliance.com/images/library/files/ALARM\\_Survey\\_2014.pdf](http://www.asphaltindustryalliance.com/images/library/files/ALARM_Survey_2014.pdf)) [accessed 03.07.14].
3. Kim Y.R., Little D.N. and Lytton R.L. Effect of moisture damage on material properties and fatigue resistance of asphalt mixtures. *Journal Transportation Research Record (TRB)*, 2004, 1891: 48–54.
4. Mehrara A. and Khodaii A. A review of state of the art on stripping phenomenon in asphalt concrete. *Construction and Building Materials*, 2013, 38: 423-442.
5. Apeageyi A.K., Grenfell J.R.A. and Airey G.D. Observation of reversible moisture damage in asphalt mixtures. *Construction and Building Materials*, 2014, 60: 73-80.
6. Lu Q. Investigation of conditions for moisture damage in asphalt concrete and appropriate laboratory test methods: PhD dissertation. University of California Transportation Center, 2005.
7. Copeland A.R. Influence of moisture on bond strength of asphalt-aggregate systems: PhD dissertation. Vanderbilt University, 2007.
8. Harrigan E.T., Leahy R.B. and Youtcheff J.S. The superpave mix design system: Manual of specifications, test methods and practices, SHRP-A-379, Strategic Highway Research Program, National Research Council, Washington DC, 1994.
9. Airey G.D. and Choi Y.K. State of the art report on moisture sensitivity test methods for bituminous pavement materials. *Road Materials and Pavement Design*, 2002, 3(4): 355-372.

10. Grenfell J., Ahmad N., Airey G.D., Collop A.C. and Elliott R. Optimising the moisture durability SATS conditioning parameters for universal asphalt mixture application. *International Journal of Pavement Engineering*, 2012, 13(5): 433–50.
11. Fromm H.J. The mechanisms of asphalt stripping from aggregates surfaces. *Journal of the Association of Asphalt Paving Technologists*, 1974; 43: 191-223.
12. Bhasin A. Development of Methods to Quantify Bitumen-Aggregate Adhesion and Loss of Adhesion due to Water: PhD dissertation, Texas A&M University, USA. 2006.
13. Huang B., Shu X., Dong Q. and Shen J. Laboratory evaluation of moisture susceptibility of hot-mix asphalt containing cementitious fillers. *Journal of Materials in Civil Engineering*, 2010, 22(7): 667-673.

## 2. Literature review

### 2.1 Introduction

Asphalt mixtures are widely used as pavement construction materials. During their service life, asphalt pavements have to sustain high traffic loads and harsh environmental conditions and deteriorate with the passage of time. One of the major causes of distress in asphalt pavements can be considered to be moisture damage with about 2.8 billion pounds being spent every year on road maintenance across England and Wales [1]. Moisture damage in asphalt pavement is defined as the loss of strength, stiffness and durability because of the presence of moisture resulting in adhesive failure at the aggregate-bitumen interface and/or cohesive failure within the bitumen film or mastic [2, 3, 4]. With the presence of moisture, water may enter the aggregate-bitumen interface through diffusion across bitumen films, seepage into the film through micro voids or cracks, and through direct access in partially coated aggregates [2, 5]. It is noticeable that the existence of moisture may also weaken the asphalt mixture by emulsifying or softening the bitumen film but without removing it from aggregate surfaces. Also, when the moisture is removed from the asphalt mixture, the stiffness loss may be reversible. However, when the pavement is loaded during the weakened condition, the moisture damage is accelerated and may become irreversible [6]. Although not all damage is caused directly by moisture, its presence increases the extent and severity of already existing distresses like cracking, potholes and rutting [7]. The resistance of asphalt mixtures to moisture attack has been related to aggregate mineralogy, surface texture of aggregate, bitumen chemistry and the compatibility between bitumen and aggregate [7, 8, 9]. In addition, factors such as permeability of the asphalt mixtures, volumetric properties of the binder and the ambient conditions are all important when considering the susceptibility of asphalt mixtures [10].

With the view to better understanding the deterioration of asphalt mixtures when exposed to moisture, this chapter presents the principal findings from a review of selected literature that is strongly related to the current study - moisture damage of asphalt mixtures. The literature review begins with a general introduction about the

phenomenon of moisture damage on asphalt pavement and its effect on pavement structure. The different failure modes induced by moisture damage are introduced in this section. In addition, the adhesion between aggregate and bitumen and its sensitivity to moisture damage are explained theoretically in several different aspects. Finally, various means of measuring moisture damage of asphalt mixture, including tests on loose aggregates, tests on compacted mixtures and tests on the aggregate-bitumen interface, are introduced.

## **2.2 Moisture damage mechanisms**

According to previous researchers [11, 12], moisture in either a liquid or vapour state infiltrates an asphalt mixture as well as the bitumen or mastic film and reaches the aggregate-bitumen interface so as to change the internal structure and finally results in the degradation of the mechanical properties of the material. In addition, moisture may also invade the asphalt mixture system by seeping through already existing cracks in the mixture or by diffusing outward from the aggregate pores. Once moisture has come into contact and interacted with the asphalt mixture, moisture damage could be developed by the following mechanisms: detachment, displacement, spontaneous emulsification, pore pressure, and hydraulic scour [7]. It should be mentioned that moisture damage is not limited to only one mechanism but is the result of a combination of several mechanisms. The detailed explanations of these five mechanisms are shown as follows:

### **2.2.1 Detachment**

Detachment is defined as a separation of bitumen film from the aggregate surface by a thin film of water but without an obvious break in the film [13, 12]. This phenomenon could be explained by different aspects. Firstly, bitumen is hydrophobic but aggregate is hydrophilic, it is therefore not easy to attach to a hydrophilic aggregate surface with a hydrophobic bitumen. However, moisture can attach to aggregate much easier so as to detach the aggregate-bitumen interface. In addition, researchers have identified that most bitumen has very low polar activity, therefore the interface formed between bitumen and aggregate is chiefly due to relatively weak nonpolar bonds [14]. On the

other hand, water molecules are highly polar and tend to form a strong polar bond with aggregate resulting in a detachment of bitumen from the aggregate-bitumen interface. Thirdly, studies on surface energy showed that the surface energy of bitumen is higher than water meaning the lower wettability of bitumen to aggregate surface in comparison with water [14]. Based on thermodynamic theory, water could reduce the free energy of the aggregate-bitumen system by replacing the bitumen film to form a thermodynamically stable condition. So, if moisture reaches the aggregate-bitumen interface, the detachment of the bitumen film from the aggregate surface is a spontaneous action.

### **2.2.2 Displacement**

Displacement is the deterioration of detachment which involves displacement of the bitumen film at the aggregate surface through a break in the bitumen film. When moisture diffuses to the aggregate-bitumen interface, some chemical bonds previously formed between bitumen and aggregate break in water so as to reduce the bond strength. Displacement maybe developed because of the combined action of detachment and traffic loading. Also, when water reaches the aggregate surface, the pH of the water changes because of the different mineralogical compositions of aggregate. These changes alter the type of polar groups adsorbed, leading to the build-up of opposing, negatively charged, electrical double layers on the aggregate and bitumen surfaces. The drive to reach equilibrium attracts more water and leads to physical separation of the bitumen from the aggregate [15, 16]. Various factors such as the incomplete coating of the aggregate surface, film rupture at sharp aggregate corners or edges, pinholes originating in the asphalt film because of poor coating of aggregate could also lead to water penetration and finally result in displacement.

### **2.2.3 Spontaneous Emulsification**

Spontaneous emulsification is a degradation process caused by the emulsification of the bitumen film in the presence of water so as to reduce the hardness of the asphalt mixture. This emulsion process is aggravated in mixtures containing specific clays or asphalt additives played as emulsifiers. Emulsification is a very slow process which

only occurs when bitumen films are immersed in water for a long time. In addition, the rate of emulsification depends on the nature of the bitumen and the presence of additives [17]. Kiggundu [18] demonstrated that mixture prepared with harder bitumen emulsified in distilled water much faster than the one with softer bitumen. Unlike the detachment and displacement mechanisms which result in adhesive failures, spontaneous emulsification leads to cohesive failures. This is because the presence of moisture changes the physico-chemical properties of the bitumen so as to reduce its cohesive strength. In the field, spontaneous emulsification failures are difficult to detect because no loss of bituminous coating can be observed [19]. Apeagyei et al. [20] found that the process is reversible as moisture conditioned asphalt mixtures that had lost up to 80% of their initial stiffness fully recovered upon subsequent drying. They also suggest that cohesive rather than adhesive failure dominates the durability of asphalt mixtures under long-term moisture exposure.

#### **2.2.4 Pore Pressure**

Pore pressure is considered to be a short-term moisture damage mechanism caused by the pumping action applied to the mixture due to dynamic traffic loads. When the macro pores and existing cracks in a pavement are saturated with water, an intense local water pressure region could be formed because of the dynamic traffic loads. Due to water being incompressible, additional stresses are developed within the material and result in more mechanical damage than the dry unsaturated case [21]. During this process, the pore pressure can cause the bitumen film to crack, which will accelerate the moisture diffusion towards the aggregate-bitumen interface resulting in detachment and displacement due to the abrasive action of water [22].

Bhairampally [23] demonstrated that a well-designed asphalt mixture tends to strain harden under repeated loading and results in the locking of the aggregate matrix caused by densification. In this case, water finds it hard to penetrate into the asphalt mixture and therefore avoids pore pressure. On the other hand, for some poorly-designed asphalt, micro-cracking is exhibited in the mastic under traffic loading and results in progressive cohesive and/or adhesive failure. The rate of this damage is accelerated in the presence of water as the pore pressure is developed in the micro-cracks. With a view to avoid pore pressure damage of asphalt pavement, the concept of pessimum air

voids was described by Terrel and Al-Swailmi [7] and was found to be between 8% and 10%. Above this level the air voids are interconnected and moisture can flow out under a stress gradient developed by traffic loading. Below this value the air voids are relatively impermeable and cannot be saturated with water. In the pessimum range, water can enter the voids but cannot escape freely and the pore pressure builds up under repeated traffic loading.

### **2.2.5 Hydraulic Scour**

Hydraulic scour is the washing away of the outer layers of mastic from the pavement surface due to the presence of water flow [24]. Stripping results from the action of tyres on the pavement surface where the saturation level is high and water may remain trapped for long periods of time. Osmosis and pull-back have been suggested as possible mechanisms of scour [17]. Cheng et al. [25] have demonstrated that the diffusion of moisture through an asphalt mixture is considerable and that pavements can hold large amounts of water. In addition, the presence of salts and salt solutions in aggregate pores causes an osmotic pressure gradient to suck water through the bitumen film. With the presence of water in asphalt mixtures, the cohesive and adhesive strength maybe reduced and finally totally stripped because of the hydraulic scour. This type of damage is considered to be a mechanical damage following other processes, such as detachment or spontaneous emulsification. The level of damage is also considered to be related to the water held by the mixtures.

## **2.3 Adhesion of Aggregate-Bitumen Interface**

In an asphalt mixture, bitumen and aggregate stick together, and the aggregate-bitumen adhesion is defined at their boundaries. With the presence of moisture, asphalt mixtures could be damaged by several modes and generate cracks in the materials. The damage in asphalt mixtures can occur either within the bitumen film or at the aggregate-bitumen interface resulting in cohesive and adhesive failure, respectively. Normally, the development of cohesive failure is due to the softening of the bitumen film. Water can affect the bituminous cohesion through intrusion into the bitumen film or through saturation of the void system resulting in pavement distress [8]. Compared to cohesive

bonds, the adhesive bonds between bitumen and aggregate are considered to be much more complicated but play a more important role in moisture damage manifested as stripping of the bitumen from the aggregate [12]. So, it is of importance to review the fundamental theories and associated mechanisms of the aggregate-bitumen adhesive bond. Hefer et al. [26] described four theories that are often used to explain the aggregate-bitumen adhesion consisting chemical bonding theory, electrostatic theory, mechanical theory, and thermodynamic theory. The detailed explanations of these four theories are presented as follows:

### **2.3.1 Chemical Bonding Theory**

The two main constituents of an asphalt mixture are bitumen and aggregate. The chemical reaction is based on the premise that acidic and basic components of both bitumen and aggregate react to form water-insoluble compounds that resist stripping. During mixing, hot bitumen with a low viscosity coats the aggregate surface and tends to enter any available crevice or pore. When in contact with the aggregate surface, the short-range chemical interactions of bitumen are feasible because of electrostatic interactions between the charged aggregate surface and the molecules attracted to the surface. It is considered that the bonds formed by chemical sorption might be useful to minimise the stripping potential of the aggregate-bitumen interface. But in theory, the chemical bonds between aggregate and bitumen are highly complex and vary among different systems primarily due to the complex and variable composition of the materials involved [27].

After bonding has formed, the bond strength between bitumen and aggregate depends on the absorption of aggregate surface to bitumen functional groups, and its relative desorption by water. The polar molecules in bitumen exhibit specific points interacting with specific sites of the bulk bitumen and on the aggregate surface. At a molecular level, basic nitrogen compounds adhere tenaciously to aggregate surfaces and are hard to strip with the presence of water [28]. The double charged salts of acids, such as calcium salts in limestone, are resistant to the action of water. It is noticeable that not all aggregate-bitumen chemical bonds can sustain moisture damage. Carboxylic acids for example, are quite polar and adhere strongly to dry aggregate. However, the bonds formed with sodium and potassium can be easily removed from aggregate surface due

to the break of bonds with the presence of water. With a view to understand the reactions that might take place, the functional groups of bitumen and aggregate should be explained.

### ***2.3.1.1 Functional Groups of Bitumen***

The chemical composition of bitumen is extremely complex and it varies widely according to the source of the crude oil from which the bitumen originates [29]. In general, bitumen is mainly composed of large amount of hydrocarbons with a content of about 90%-95% by weight. However, the remaining atoms which contain oxygen, nitrogen, sulphur, nickel, vanadium and iron are considered very important to the interaction with aggregate and hence the performance of asphalt mixtures [30]. Figure 2-1 shows the chemical structures of the naturally occurring functional groups of bitumen and those formed during oxidation [31]. It is considered that the functional groups which are most strongly adsorbed on aggregate surfaces, are also those displaced most easily by water [32]. Take carboxylic acids and sulfoxides for example, although the components are very small in bitumen, they account for almost half of the total chemical functionality in the strongly adsorbed fractions. However, water has stronger hydrogen bond (the electrostatic attraction between polar groups that occurs when a hydrogen (H) atom bound to a highly electronegative atom) with some aggregate surfaces compared to the carboxylic acids. This may contribute to their ease of displacement by water. However, poly-functional molecules which contain ketones, anhydrides, and nitrogen are strongly adsorbed by aggregate even with the presence of moisture as suggested by water displacement studies.

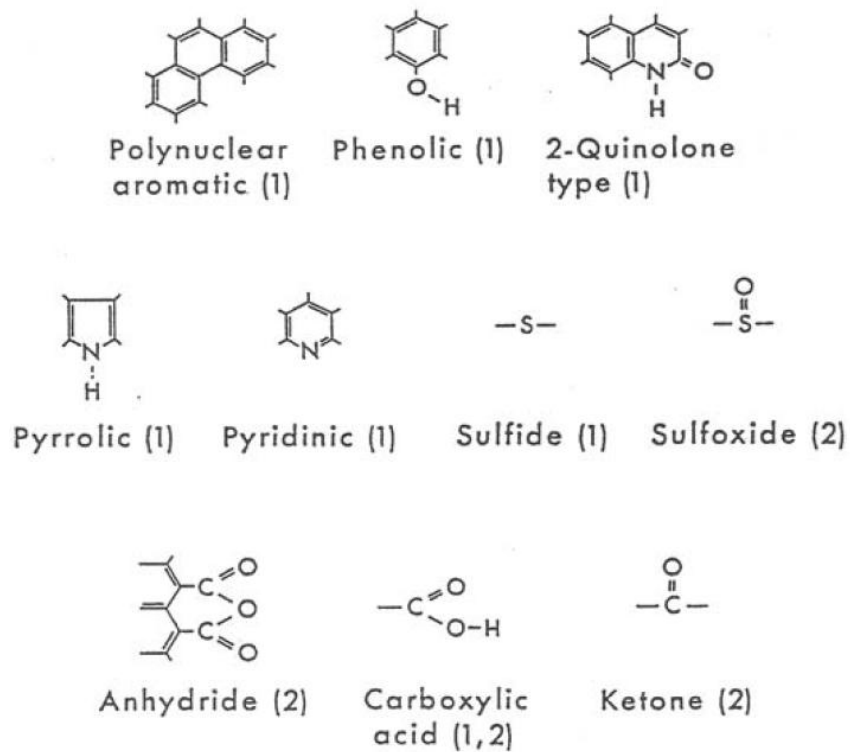


Figure 2-1 Chemical functional groups in bitumen (1) naturally occurring and (2) formed on oxidative aging [31]

### 2.3.1.2 Functional Groups of Aggregate

Aggregates constitute the biggest part of asphalt mixtures so have an important effect on the moisture damage properties. Although the aggregates are classified as limestone, granite, or basalt, each of those materials is composed of a variety of mineralogical compositions. The mineralogical composition of the aggregate has a much stronger influence on the aggregate-bitumen adhesion than the bitumen.

Aggregate surfaces provide electrostatic and Lewis acid/basic sites for interaction with bitumen polar components [33]. Bonding studies have shown that adsorbing groups of bitumen are mainly naphthenic acids meaning they tend to form stronger bonds with basic aggregates. In addition, these bonds are typically formed on minerals where metals, such as magnesium, iron and calcium, are present. Table 2.1 shows different types of minerals and their relation to stripping [34]. With regard to stripping, Fe, Ca, Mg, and Al are generally beneficial because the bonds formed with acid polar bitumen are insoluble in water. However, alkali metals are detrimental due to the soluble bonds formed with bitumen. Based on the research from Bagampadde et al. [35], mixtures

with aggregates containing alkali metal elements, such as sodium and potassium, or aggregates with high contents of quartz and alkali feldspars are more prone to moisture damage. However, mixtures with aggregates containing calcium, magnesium and iron are found to be moisture resistant. Similar results were also found by Airey et al. [36].

Table 2-1 Mineral types and their relation to stripping [34]

Category	Mineral Type	Rock	Comment
Silica	Quartz – $\text{SiO}_4$	Granite Phyolite Sandstone Quartzite	Poor adherence as water attaches due to H-bonding.
Ferro - magnesian	Olivine – $(\text{MgFe})_2\text{SiO}_4$ Augite - $(\text{Ca,Mg,Fe})(\text{Si,Al})_2\text{O}_6$ Hornblende - $(\text{Ca,Na})_2\text{-}$ $3(\text{Mg,Fe}^{2+},\text{Fe}^{3+},\text{Al})_5(\text{Al,Si})_8\text{-}$ $\text{O}_{22}(\text{OH})_2$ Biotite - $\text{K}(\text{Mg,Fe}^{2+})_3(\text{Al,Fe}^{3+})\text{-}$ $\text{Si}_3\text{O}_{10}(\text{OH})_2$	Gabbro Diabase Andesite Basalt Diorite Mica	Olivine and augite form insoluble Mg and Ca salts while biotite gives soluble K salt. Hornblende is intermediary in character.
Limestone	Calcite – $\text{CaCO}_3$ Dolomite - $\text{CaMg}(\text{CO}_3)_2$	Limestone Chalk Dolomite	Generally good adherence but are friable. Undergo strong acid-base and electrostatic interactions with bitumen. Some have soluble salts.

### 2.3.2 Electrostatic Theory

Solid surfaces can be characterised as electropositive or electronegative due to the assembly of atoms and the consequent formation of molecular dipoles. A charged aggregate surface attracts an oppositely charged or partially charged species of bitumen. The part of the attracted bitumen molecule is then available to attract other oppositely charged bitumen molecules through electrostatic interaction. If this build-up of interlinked molecules caused by induced polarisation occurs, the build-up would taper off rather quickly with distance from the aggregate surface due to the decreasing influence of the polar surface with increasing distance. During interfacial failure of the aggregate-bitumen system, separation of the two phases leads to an increasing potential difference up to a point where discharge occurs. The adhesive strength can therefore be attributed to the strength required to separate the charged surfaces in overcoming the Coulombic forces [37, 38].

Interactions between solid surfaces and liquid media containing dissolved ions, such as water, are considered important to explain moisture damage of asphalt mixtures [39, 40]. For aggregates, most surfaces are charged in the presence of water due to the high dielectric constant of water making it a good solvent for ions. Ions of opposite charge, bind directly to the surface to neutralise the surface charge, known as the Stern Layer. Thermal motion prevents ions to accumulate on the surface so that a diffuse layer of counter-ions and co-ions is formed. As shown in Figure 2-2, the electric potential at the surface decreases with distance into the bulk water. The electric potential at the solid surface ( $\psi_0$ ) decrease with the distance into the bulk water. The  $\delta$  represents the thickness of Stern Layer.

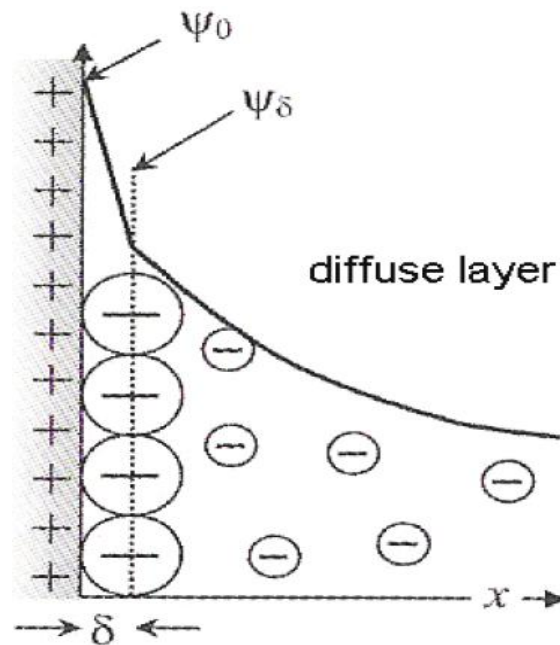


Figure 2-2 Schematic illustration of the stern layer and diffuse layer with thickness [26].

Based on electrostatic theory, the zeta potential which is the potential difference between the dispersion medium and the stationary layer of fluid attached to the dispersed particle has been used to analyse debonding of bitumen film from the aggregate in the presence of moisture [40]. Figure 2-3(a) shows the zeta potential of three types of bitumen on granite. It can be seen that depending on the pH value, the zeta potentials of bitumen and aggregate have the same polarity meaning net repulsion of these two materials and this results in debonding in the presence of water. However, the zeta potentials of bitumen and limestone aggregate tend to have opposite polarity in a wide range of pH values, as shown in Figure 2-3(b). In this case, adhesion between

bitumen and aggregate is favoured due to the net attraction between these two oppositely charged surfaces.

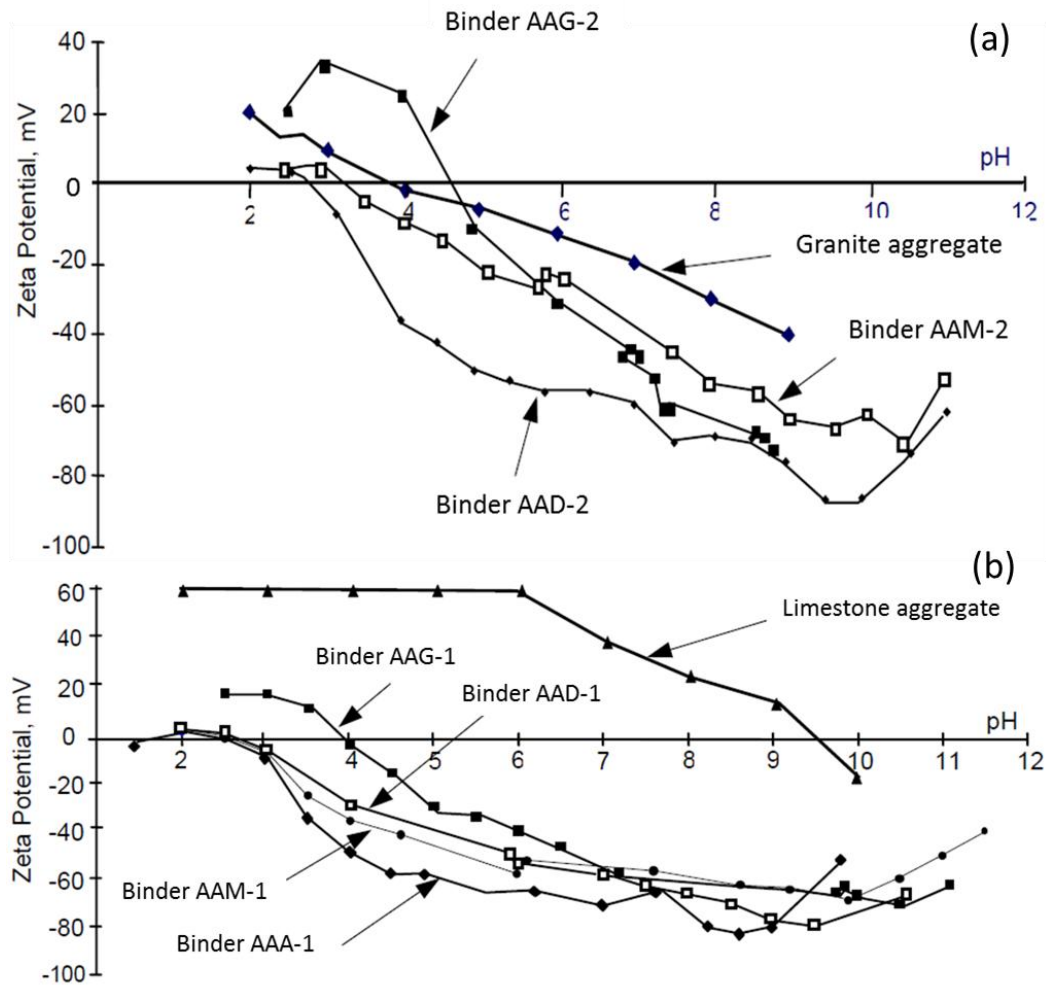


Figure 2-3 Zeta potential of different types of bitumen with granite aggregate (a) and limestone aggregate (b) at different pH values [40]

According to work by Yoon and Tarrer [39], with the presence of water, carboxylic acid ( $R-COOH$ ) separates into the carboxylate anion ( $R-COO^-$ ) and the proton ( $H^+$ ). This causes bitumen to have a negative polarity at the surface. Solid surfaces in contact with water usually acquire charges through chemical reactions at the solid surface and adsorption of complex ions from the solution. A high pH value of water in contact with the mineral surface will cause the surface to be more negative charged. Aggregates with water present are negatively charged, and as a result, a repulsive force develops between the aggregate and bitumen at the interface.

### 2.3.3 Mechanical Adhesion Theory

Mechanical adhesion theory involves the mechanical gripping of the adhesive into the cavities, pores and asperities of the solid surface on a macroscopic scale and it has been realised as the most intuitive adhesion phenomenon [37]. This theory assumes that the bitumen is forced into the irregularities of the aggregate surface, producing a mechanical interlock. Based on this theory, the aggregate-bitumen adhesion relies on physical aggregate properties, including surface texture, porosity or absorption, surface coating, surface area, and particle size [7]. It is generally accepted that aggregate with a porous, slightly rough surface could provide a strong mechanical interlocking to promote adhesion [41].

The influence of aggregate properties on mechanical adhesion of the aggregate-bitumen interface and its resistance to moisture damage has been widely analysed. Figure 2-4 shows a summary of the effects of aggregate physical properties on the resistance and susceptibility to stripping [34]. According to this Figure, it is vital to maximise the surface area and texture of aggregate to get a strong physical bonding between bitumen and aggregate. A strong physical bonding could also contribute to improve the nature of the chemical bond between bitumen and aggregate even in the presence of water.

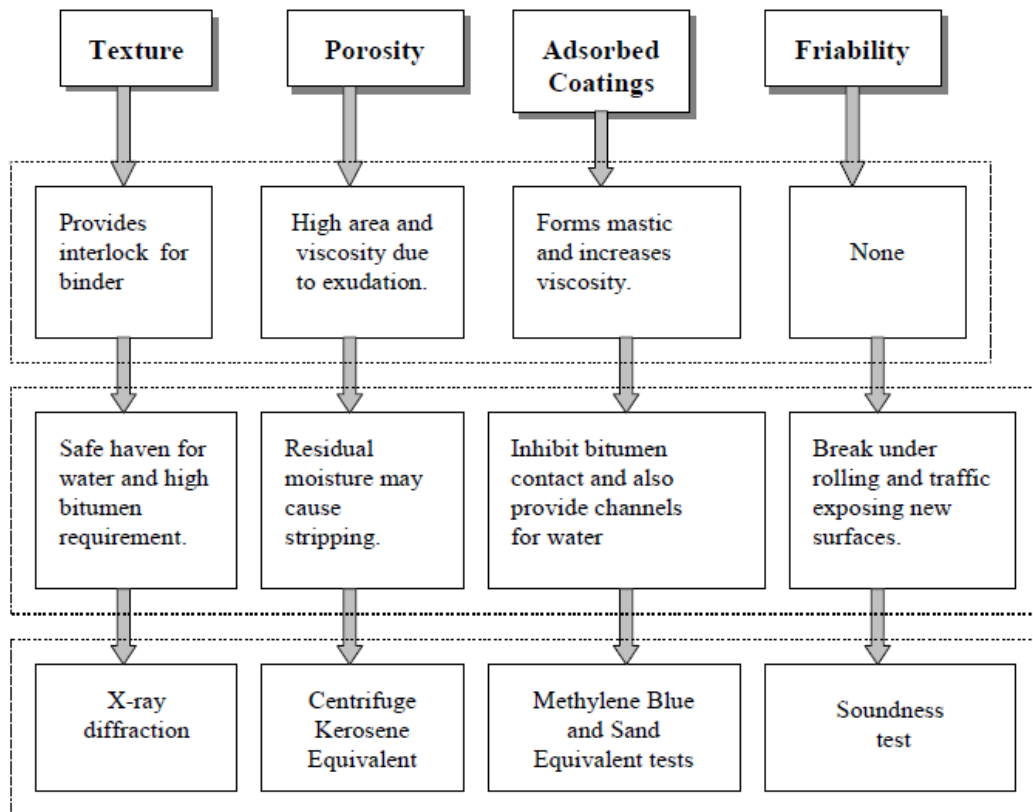


Figure 2-4 Summary of aggregate physical properties and how they affect stripping [34]

In terms of angularity, aggregates with good angularity have been normally considered beneficial in producing a better mechanical interlock [5]. However, for more angular aggregate, debonding has been determined to be more severe because the angularity may promote the stripping between bitumen/mastic and aggregate, leaving a point of intrusion for the water.

The effects of crushing of the aggregate are also very important. Tarrer and Wagh [42] pointed out that newly crushed aggregates tend to strip faster than stockpiled aggregates. They state that newly crushed aggregate surfaces can attract one or more layers of water molecules which strongly adsorb on the aggregate surface as a result of electrochemical attraction. After aging, the outermost adsorbed water molecules may become partially replaced or covered by organic contaminants present in air that reduce stripping potential.

### 2.3.4 Thermodynamic Theory

Thermodynamic theory is based on the concept that an adhesive will adhere to a substrate due to established intermolecular forces at the interface provided that intimate contact is achieved. The magnitude of these fundamental forces can generally be related to thermodynamic quantities, such as surface free energies of the materials involved in the adhesive bond or the Gibbs free energy of the system.

In thermodynamics, the Gibbs free energy is a thermodynamic potential that measures the process-initiating work obtainable from a thermodynamic system at a constant temperature and pressure [43]. It represents the energy change between the initial and final state. Such a process occurs due to an imbalance between two natural tendencies. The first tendency is the spontaneous conversion of potential energy into work and heat, known as enthalpy, and the second tendency being the spontaneous increase in randomness of the system, known as entropy. In order to relate enthalpy and entropy, the Gibbs free energy (G) is defined at constant temperature and pressure as:

$$\Delta G = \Delta H + T\Delta S \quad (2-1)$$

where  $\Delta G$  is Gibbs free energy,  $\Delta H$  is Enthalpy,  $T$  is the absolute temperature and  $\Delta S$  is Entropy.

According to thermodynamic theory, the surface energy ( $\gamma$ ), is the reversible work required to create a unit area of new surface. The work of adhesion ( $W_a$ ) and the Gibbs free energy is equal in magnitude, but the relationship of these two parameters should be interpreted as follows [44]:

$$W_a = -\Delta G_a \quad (2-2)$$

If the material is completely brittle, the work done on the sample is dissipated only through the propagation of a crack, thereby creating two new surfaces. The total work expended per unit of surface area in forming the two surfaces ( $W_c$ ) is then equal to twice the surface energy per unit of surface area:

$$W_c = 2\gamma \quad (2-3)$$

or

$$\Delta G_c = -2\gamma \quad (2-4)$$

When two dissimilar materials form an interface, such as aggregate and bitumen, a tensile force can be applied to split the materials into dissimilar parts. However, because dissimilar materials are separated, some of the intermolecular forces present during intimate contact, are now missing. The interfacial energy should be accounted for by subtracting it from the energy done to create the two new surfaces. The relationship is:

$$W_a = \gamma_A + \gamma_B - \gamma_{AB} \quad (2-5)$$

or,

$$\Delta G_a = \gamma_{AB} - \gamma_A - \gamma_B \quad (2-6)$$

where  $\gamma_A$  and  $\gamma_B$  are the surface energies of the aggregate and bitumen, and  $\gamma_{AB}$  is the interfacial energy between the two materials in contact. A higher magnitude of work of adhesion indicates higher resistance of the interface to an adhesive failure [45].

Moisture damage susceptibility of an aggregate-bitumen system can be quantified based on the free energy change when water displaces bitumen film from the aggregate surface. The work required for water to displace a unit of the interface and create a new unit of water-bitumen interface and water-aggregate interface is expressed by:

$$W_{AWB} = \gamma_{AW} + \gamma_{BW} - \gamma_{AB} \quad (2-7)$$

where the subscript  $w$  corresponds to water.

The values of  $W_{AWB}$  are normally negative meaning the debonding of the aggregate-bitumen interface is a spontaneous process in the presence of water. A large magnitude of  $W_{AWB}$  implies a greater potential for water to displace the bitumen from aggregate [45]. Thermodynamic theory provides a well-grounded moisture damage interpretation [46]. It allows not only the determination of compatible combinations of aggregates and bitumen but also provides fundamental parameters by which to explain moisture damage in fracture mechanics based models [12, 47, 48].

## **2.4 Testing methods related to moisture damage evaluation**

Since the 1930s, efforts have been made to develop tests to evaluate the water sensitivity of asphalt mixtures [49]. Since then, numerous testing methods have been developed with a view to assess the susceptibility of asphalt mixtures to moisture damage. Generally, many of these developed moisture damage methods can be divided into two categories, which are tests conducted on loose coated aggregates and tests subjected to compacted mixtures. Tests on loose coated aggregates normally consist of immersing bitumen coated aggregates in water either at room temperature or high temperature for a specified period of time under static or dynamic conditions and finally assessing the stripping percentage of bitumen from the aggregate surface by visual inspection. Tests on compacted mixtures generally condition samples, which are prepared in the laboratory or cored from existing pavements, in water to simulate the moisture damage process and evaluate the moisture sensitivity by calculating the ratio of conditioned and unconditioned strength or stiffness [50, 51]. In addition, there are several tests with specimens prepared by combining two flat aggregate surfaces with bitumen and evaluating their loss of tensile strength or fracture energy after moisture damage. Furthermore, other methods based on thermodynamic theory could measure the surface energy of bitumen and aggregate so as to evaluate moisture sensitivity of different aggregate-bitumen combinations by calculating the work of adhesion in dry conditions and work of debonding in the presence of water.

### **2.4.1 Tests on loose coated aggregates**

The principle of these tests is to assess the percentage of the aggregates surface that have maintained their bitumen coating after immersion in water or chemical solution. These tests are performed under similar procedures with loose coated aggregates first immersed in water or chemical solution. Then immersion is carried out for specified time at room or elevated temperature in static, shaking or rolling conditions. Finally, the separation of bitumen from aggregate surface is assessed by visual inspection. Generally, these methods with a simple test procedure are considered easy to perform. However, these test rely on the basis of comparative evaluation so that the results cannot be used to explain the actual mechanisms that contribute to moisture damage

and it is hard to correlate data with field performance [52]. The laboratory based tests on loose coated aggregates to assess the moisture damage are presented in Table 2-2.

Table 2-2 Detailed introduction of tests on loose coated aggregates

Test method	Extra feature	Test description
Static immersion test (AASHTO T182, ASTM D1664)	Distilled water for 16-18 hours	Visually assess the percent of aggregates surface that have maintained their bitumen coating after immersion [49]
Dynamic immersion test	Distilled water for 16-18 hours with mechanical agitation	Visually assess the percent of aggregates surface that have maintained their bitumen coating after agitation [53]
Chemical immersion test	Solutions containing sodium carbonate	Visually assess the percent of aggregates surface that have maintained their bitumen coating after soaking [53]
Rolling bottle test (Cen prEN 12697-11)	Rotate at 40 rpm for three days	The percentage of bitumen retained on aggregate surface is visually determined
Boiling water test (ASTM D3625)	Boiling water for 1 to 10 minutes	The amount of bitumen loss is determined by visual assessment [54]
Ancona stripping test	Immerse the coated aggregates in a beaker distilled water and then put the beaker in boiling water for 45 minutes	The amount of bitumen loss is determined by visual assessment [55]
Boiling water stripping test	Boiling water 10 minutes followed by chemical attack	The proportion of exposed aggregate surface is evaluated through a chemical attack. The stripping ratio is determined with reference to a calibration curve [56]
Ultrasonic method	Immerse in water with ultrasonic attack	Measuring the ratio of stripped surface by weighing the stripped test piece or by visual assessment [57]
Net adsorption test (SHRP, M001)	Shaking aggregate in bitumen-toluene solution for 6 hours followed by adding 2ml water and shaking for another 8 hours	The amount of bitumen adsorbed on the aggregate and desorbed from the coated aggregate is measured using a spectrophotometer [58]
Modified net adsorption test	Following the same test procedure as the net adsorption test	The initial adsorption value is calculated by providing an indicator to assess the affinity and resistance to stripping of the aggregate-bitumen system [59]

## 2.4.2 Tests on compacted mixtures

The tests on compacted mixtures generally involve the measurement of mechanical properties of compacted asphalt mixture before and after immersion in water and evaluate their changes due to the moisture damage. The compacted mixture specimens could be prepared in the laboratory or cored from existing pavements. Mechanical parameters such as indirect tensile strength or stiffness are normally used as indicators to assess the moisture damage [2]. The equipment used to measure the indirect tensile strength or stiffness of the compacted mixture is known as the Nottingham Asphalt Tester (NAT) and is shown in Figure 2-5. The permanent deformation (rutting) of asphalt mixture substrates under repeated loading is also used to evaluate the moisture damage. Figure 2-6 shows the Hamburg Wheel Tracking Device (HWT) used to evaluate the pavement rutting development. The laboratory based tests on compacted mixtures to assess moisture damage are presented in Table 2-3.



Figure 2-5 Test equipment for determination of indirect tensile strength or stiffness



Figure 2-6 Hamburg wheel tracking device for determination of permanent deformation

Table 2-3 Detailed introduction of tests on compacted asphalt mixtures

Test method	Extra feature	Test description
Texas freeze-thaw pedestal test	Specimens 14mm in diameter by 19mm in height are prepared from a single gradation (0.5-0.85mm). The specimen is first cured at 23 °C for 3 days followed by thermal cycling of -12 °C for 15hours, 23 °C for 45 minutes and 49 °C for 9 hours in water.	The number of thermal cycles recorded when crack observed. Moisture susceptible: thermal cycles < 10 Moisture resistance: thermal cycles > 20 [60]
Immersion compression test (AASHTO T165, ASTM D1075)	The specimen is first cured at 23 °C for 4 hours followed by immersion in water at 49 °C for 4 days and then at 23 °C for 4 hours before compressive strength testing.	The index of retained strength (IRS) is measured to evaluate the moisture sensitivity with 75% retention as the indicator [51].
Marshall Stability test (AASHTO T245)	Specimens are first vacuum treated under water and then immersed in water at 60 °C for 48 hours [53].	The ratio of Marshall stability of conditioned specimens to unconditioned specimens is used to assess the moisture sensitivity.
Duriez test (NF P 98-251-1)	Moisture conditioning at 18 °C for 7 days [61]	Moisture sensitivity is assessed as the retained unconfined compression strength at 18 °C and 1 mm/s loading
Lottman procedure	Vacuum treated in water with 600 mm Hg for 30 minutes to simulate the short-term performance. Freeze-thaw procedure was applied to simulate the field performance up to 4 years.	The indirect tensile strength and stiffness before and after conditioning were used to characterise the moisture resistance [62].
Tunncliff and Root procedure	Partial vacuum to make sure the saturation degree between 55% and 80% followed by water bath at 60 °C for 24 hours.	The retained indirect tensile strength was used to justify the moisture resistance [63].
Immersion wheel tracking	Asphalt mixture slab immersed in water at 40 °C and subjected to a 20Kg wheel tracking at 25 cycles/minute [64].	The failure is indicated by a sudden increase in plastic deformation of the slab. The rutting depth and the loading replications will be used as indicators to evaluate moisture sensitivity.
Hamburg wheel tracking	Slab submerged in water at 50 °C and subjected to a repeated steel wheel load with 50 passes per minute [65].	Testing is undertaken for 20000 passes or until a 20mm rut depth. The required number of wheel passes to induce 1 mm rutting is used to characterise the moisture damage.

## 2.4.3 Other representative tests for moisture damage evaluation

### 2.4.3.1 Surface energy tests

Based on the thermodynamic theory as presented in Section 2.3.4, the work of adhesion between aggregate and bitumen could be determined if their surface free energies are known. This theory can also be applied to evaluate the moisture damage susceptibility of the aggregate-bitumen system when water displaces the bitumen film from the aggregate surface. Furthermore, previous researchers have determined the correlations between thermodynamic parameters and moisture sensitivity of asphalt mixtures [66, 67]. Therefore, it is possible to evaluate the moisture sensitivity of asphalt mixtures by measuring the surface free energy of the aggregate and bitumen.

There are two commonly used methods, known as the ‘Sessile drop method’ and ‘Wilhelmy plate method’, applied to measure the contact angle of specific probe liquids with bitumen so as to derive the surface free energy of bitumen [68]. The ‘Sessile Drop Method’ is a direct method of measuring the static contact angle of a probe liquid dropped onto the bitumen substrate using a camera fixed in the Goniometer, as shown in Figure 2-7 [68]. The ‘Wilhelmy Plate Method’ is an indirect method to calculate the contact angle from the measured dynamic force change using the dynamic contact angle (DCA) analyser, as shown in Figure 2-8 [69]. Previous researchers have demonstrated that it is difficult to get consistent results with the goniometer whilst the repeatability of the DCA is comparatively better [70].

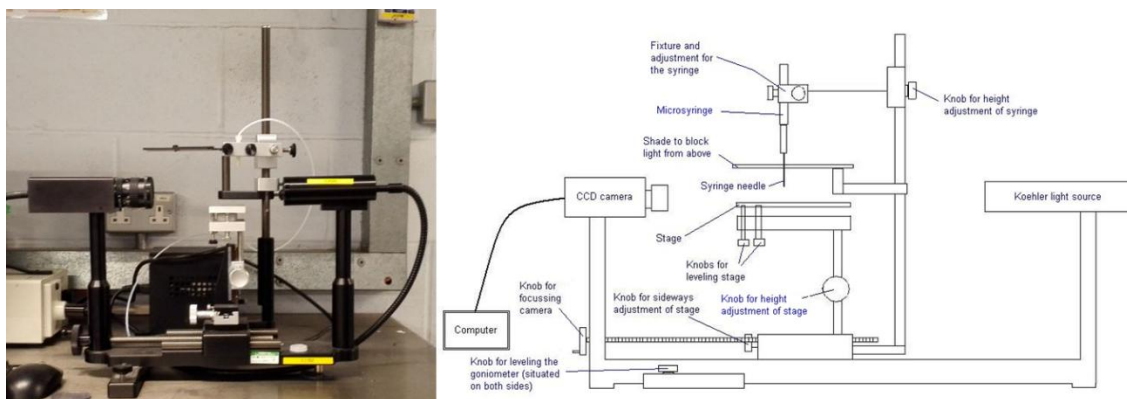


Figure 2-7 Image and schematic of goniometer [70]

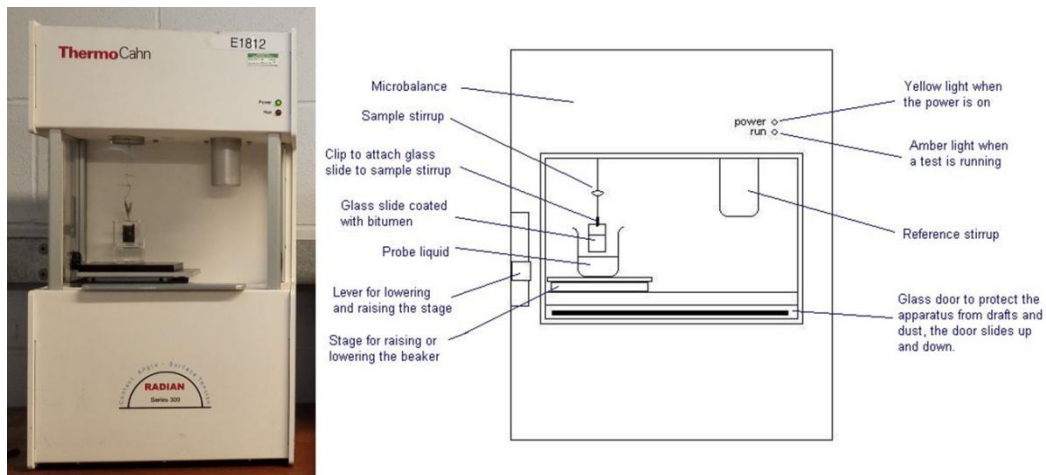


Figure 2-8 Image and schematic of dynamic contact angle test procedure [70]

Because of the high surface energy of aggregate, it is difficult to use the contact angle technique as the probe liquids readily spread on the aggregate surface and it is difficult to obtain accurate contact angles. So, two other methods, namely the dynamic vapour sorption (DVS) test and the microcalorimeter technique can be used to measure the surface energy of aggregates [67]. Images of these two pieces of equipment are shown in Figures 2-9 and 2-10, respectively. The DVS test measures the mass increase of aggregate when probe vapours are passed through the sample under controlled temperature and pressure conditions and the results used to determine the surface free energy components of the aggregate [7]. Microcalorimetry is a technique to measure the heat change when aggregates are immersed in the probe liquids with the help of integrated software and the results are used to calculate the surface energy of aggregate [67]. The surface energy results of bitumen and aggregates were used to identify parameters based on thermodynamic theory that can quantify their work of adhesion in dry conditions and work of debonding in the presence of water. The thermodynamic parameters were shown to correlate well with the moisture sensitivity of asphalt mixtures based on laboratory tests [67].



Figure 2-9 Image of the Dynamic Vapour Sorption equipment



Figure 2-10 Image of the Microcalorimeter equipment

### ***2.4.3.2 Mechanical tests on aggregate-bitumen interface***

The bond strength of the aggregate-bitumen interface is recognised as one of the most important contributing factors that affect the main mechanical properties of the asphalt mixture. By measuring the adhesive bond strength of coatings between bitumen and aggregate, several testing techniques have been developed but the most commonly used methods include the pull-off test and peel test. These two methods have also been successfully used to evaluate the moisture sensitivity of the aggregate-bitumen bond by immersing specimens in water for a period of time before testing.

#### **Pull-off test**

The pull-off test is a widely used mechanical test to measure the tensile strength of coatings and interface strength of composite materials [71]. Normally, the pull-off test is conducted by measuring the tensile stress necessary to detach the adhesive materials in a direction perpendicular to the substrates, as shown in Figure 2-11. In the pavement research area, the pull-off test specimen is generally produced by combining two rigid aggregate substrates using bitumen or mastic as the adhesive material and the adhesive layer is tested using a universal testing machine (UTM), as shown in Figure 2-12 [71]. The advantage of this method is that the testing factors such as substrate dimensions, adhesive thickness, loading rate and temperature can be changed based on the requirements. Previous researchers demonstrated that a slower loading rate resulted in a smaller tensile stress to failure [72]. An increase in testing temperature results in a decrease in failure tensile strength with other testing conditions held constant [73]. In addition, this method can also be used to evaluate the moisture sensitivity of the aggregate-bitumen interface as the adhesive bond is generally affected by moisture [74]. The retained tensile strength defined as the ratio of strength after moisture conditioning to the strength in the dry condition is commonly used to evaluate the moisture resistance of asphalt mixtures.

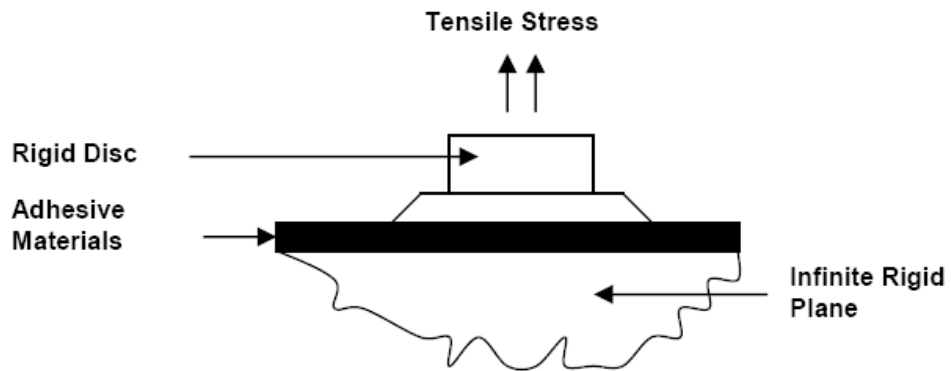


Figure 2-11 Schematic diagram of pull-off test [71]



Figure 2-12 Test equipment for pull-off test using UTM [75]

The pneumatic adhesion tensile testing instrument (PATTI) is a device using generated air pressure from the equipment to detach the bond between aggregate and bitumen. The maximum tensile pressure to separate the bitumen from substrate is captured and converted to its pull-off tensile strength [76]. This method has been successfully used by many researchers to measure the moisture resistance of different aggregate-bitumen combinations and is recognised to be an accurate method to not only determine the

mechanical tensile strength of bitumen or bitumen-aggregate interface, but also identify the type of failure, either adhesive or cohesive [77, 78, 79, 80].

### Peel test

The peel test is a well-developed standard (ASTM D6862-11) method to measure the adhesive strength of the bonded interface of composite materials and is widely used in various engineering applications [81]. Figure 2-13 illustrates the different configurations for several peel methods. For a typical peel test, a thin flexible peel arm and a rigid substrate are bonded using the adhesive material. During testing, the peel arm is pulled from the substrate at a specified angle and speed with the peel force recorded. The recorded peel force in steady state conditions is then used to calculate the fracture energy of the adhesive. In the pavement research area, aggregates are used as the rigid substrate and bonded to the flexible peel arm with bitumen as the adhesive. Horgnies et al. [82] undertook the peel test to peel bitumen from aggregate surface by using polyethylene terephthalate (PET) as a peel arm to evaluate the influence of interfacial composition on aggregate-bitumen adhesion. Blackman et al. [83] undertook a similar peel test but replaced the PET with aluminium alloy as the peel arm to measure the moisture-induced damage of different aggregate-bitumen combinations. This test is considered to be a reliable method to measure the peel strength (fracture energy) of the aggregate-bitumen interface if suitable corrections for plastic work can be performed.

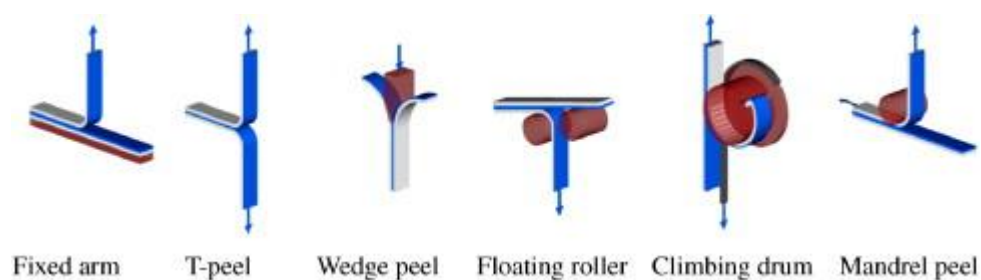


Figure 2-13 Configuration of different peel tests [84]

### 2.4.3.3 Saturation Ageing Tensile Stiffness (SATS) Test

The saturation ageing tensile stiffness (SATS) test, as shown in Figure 2-14, is the first method that combines both ageing and moisture damage mechanisms by conditioning

pre-saturated asphalt mixture specimens at an elevated temperature and pressure in the presence of moisture. The retained stiffness modulus and the retained saturation are two parameters used as an indication of the sensitivity of the compacted mixture to the combined effects of ageing and moisture damage [2]. Airey et al. [2] evaluated the influence of aggregate, filler and bitumen on moisture damage of asphalt mixtures. It was found that the air voids and binder content have negligible effect on the retained stiffness values when tested in the SATS test. The filler may have affected the moisture sensitivity of acidic aggregate mixtures. By using the SATS test, Collop et al. [85] found that mixture prepared with acidic aggregates was more sensitive to moisture damage than those prepared with basic aggregates. The SATS test showed the same ranking in terms of the moisture sensitivity of asphalt mixtures as the AASHTO T283 procedure [86]. In addition, it has been considered that the SATS test could correctly predict the performance of asphalt mixtures in the field [87].



Figure 2-14 Equipment used for the SATS test

## 2.5 Summary

Bitumen, as one of the world's most widely used construction materials, has been selected as a binder in pavement construction for almost 100 years. Long-term research has demonstrated that moisture-induced damage in asphalt mixtures plays a very significant role in the performance of asphalt pavements during its service life and serious attention needs to be paid to this mechanism. When moisture damage occurs, the loss of cohesion in the mixture and/or the loss of adhesion between the bitumen and the aggregate interface will reduce the ability of a pavement to support traffic-induced stresses and strains, which can promote the development of cracks and rutting so as to accelerate the deterioration of the pavement. This chapter gave a comprehensive introduction about moisture damage in aspects of definition, mechanisms, theories and evaluation methods with the main points showing the following:

Moisture damage, defined as the degradation of the mechanical properties of asphalt mixtures because of the presence of moisture, is considered to be a major cause of the deterioration of asphalt pavements. For the asphalt pavement itself, the compatibility between bitumen and aggregate, and the volumetric properties of the mixture are important factors that influence the moisture sensitivity. In addition, other factors such as ageing of binders, traffic loading and environmental changes will combine with moisture damage so as to accelerate the pavement degradation.

As introduced in Section 2.2, moisture could damage the asphalt mixture via five main mechanisms namely: detachment, displacement, spontaneous emulsification, pore pressure and hydraulic scour. The development of the moisture damage is determined by the fundamental properties of a mixture and by the changes in the moisture state.

Because the aggregate-bitumen interface is a vulnerable boundary to moisture damage and is the research focus of this thesis, the adhesion between aggregate and bitumen was explained by several different theories. These theories are fundamental to understand why aggregate and bitumen can bond together in dry conditions, and some of the bonds deteriorate with the presence of moisture. By using these theories, it is helpful to select compatible aggregate and bitumen combinations before producing an

asphalt mixture and carrying out pavement design, so as to make sure of the performance during its service life.

Many laboratory testing methods to evaluate the moisture susceptibility of asphalt mixtures are presented in this chapter. Tests related to moisture damage of asphalt mixtures can be broadly divided into tests performed on the loose coated aggregates and tests performed on compacted asphalt mixtures. The most commonly used methods for loose coated aggregate are the static immersion test, rolling bottle test and boiling water test assessing the loss of the bitumen coating from the aggregate visually to evaluate the moisture susceptibility. In terms of the compacted asphalt mixtures, mechanical evaluation by measuring the loss of strength and stiffness of specimens before and after moisture conditioning is the main procedure to evaluate their moisture sensitivity. In addition, other methods such as surface energy tests, the peel test, the pull-off test and the SATS test are also recognised as feasible to evaluate the moisture sensitivity of asphalt mixtures.

## References

1. Annual Local Authority Road Maintenance (ALARM) Survey 2014. Asphalt Industry Alliance, ([http://www.asphaltindustryalliance.com/images/library/files/ALARM\\_Survey\\_2014.pdf](http://www.asphaltindustryalliance.com/images/library/files/ALARM_Survey_2014.pdf)) [accessed 03.07.14]
2. Airey G.D., Collop A.C., Zoorob S.E. and Elliott R.C. The influence of aggregate, filler and bitumen on asphalt mixture moisture damage. *Construction and Building Materials*, 2008, 22(9): 2015-2024.
3. Qiao Y., Flintsch G., Dawson A. and Parry T. Examining Effects of Climatic Factors on Flexible Pavement Performance and Service Life. *Transportation Research Record: Journal of the Transportation Research Board*, 2013, 2349: 100-107.
4. Apegyei A.K., Grenfell J.R.A. and Airey G.D. Evaluation of moisture sorption and diffusion characteristics of asphalt mastics using manual and automated gravimetric sorption techniques. *Journal of Materials in Civil Engineering*, 2013, 26(8): 04014045.
5. Stuart K.D. *Moisture Damage in Asphalt Mixture-a State of the Art Report*, Report No. FHWA-RD-90-019, Federal Highway Administration, Virginia, 1990.
6. Santucci L. *Moisture Sensitivity of Asphalt Pavements*. Technical Transfer Program, Institute of Transportation Studies, University of California, Berkeley, 2002.
7. Grenfell J.R.A., Ahmad N., Liu Y., Apegyei A.K., Large D. and Airey G.D. Assessing asphalt mixture moisture susceptibility through intrinsic adhesion, bitumen stripping and mechanical damage. *Road Materials and Pavement Design*, 2014, 15(1): 131-152.
8. Terrel R.L. and Al-Swailmi S. *Water sensitivity of asphalt-aggregate mixes: test section*. SHRPA-403, Strategic Highway Research Program. National Research Council, Washington DC, 1994.

9. Abo-Qudais S. and Al-Shweily H. Effect of aggregate properties on asphalt mixtures stripping and creep behaviour. *Construction and Building Materials* 2007, 21(9): 1886-1898.
10. Grenfell J.R.A., Ahmad N., Airey G.D., Collop A. and Elliott R. Optimising the moisture durability SATS conditioning parameters for universal asphalt mixture application. *International Journal of Pavement Engineering*, 2012, 13(5): 433-450.
11. Kakar M.R., Hamzah M.O. and Valentin J. A review on moisture damages of hot and warm mix asphalt and related investigations. *Journal of Cleaner Production*, 2015, 99: 39-58.
12. Caro S., Masad E., Bhasin A. and Little D.N. Moisture susceptibility of asphalt mixtures, Part 1: mechanisms. *International Journal of Pavement Engineering*, 2008, 9(2): 81-98.
13. Majidzadeh X. and Brovold P.N., State of the Art: Effect of Water on Bitumen-Aggregate Mixtures. Special HRB Report No.98, Highway Research Board, Washington DC, USA, 1968.
14. Road Research Laboratory, Department of Scientific and Industrial Research. Bituminous Materials in Road Construction, Her Majesty's Stationery Office, London, 1962.
15. Hicks R.G., Santucci L. and Aschenbrener T., Moisture Sensitivity of Asphalt Pavements: A National Seminar, Proceeding of Transportation Research Board, San Diego, California, 2003.
16. Scott J.A.N., Adhesion and disbonding mechanisms of asphalt used in highway construction and maintenance, Association of Asphalt Paving Technologists 1978, 47: 19-48.
17. Formm H.J., The Mechanisms of Asphalt Stripping from Aggregate Surfaces. Association of Asphalt Paving Technologists, 1974, 43: 191-223.

18. Kiggundu B.M, Stripping in HMA mixtures: State-of-the-art and critical review of test methods. Auburn, AL: National Center for Asphalt Technology, 1988.
19. Martin J.S., Cooley Jr. L.A. and Hainin M.R., Production and construction issues for moisture sensitivity of hot-mix asphalt pavements, Proceeding of Transportation Research Board National Seminar. San Diego, California, 2003: 209-222.
20. Apeagyei A.K., Grenfell J.R.A. and Airey G.D., Observation of reversible moisture damage in asphalt mixtures. *Construction and Building Materials*, 2014, 60: 73-80.
21. Kringos N., Scarpas A., and De Bondt A., Determination of moisture susceptibility of mastic-stone bond strength and comparison to thermodynamical properties. *Journal of the Association of Asphalt Paving Technologists* 2008, 77, 435–478.
22. Varveri A., Avgerinopoulos S. and Scarpas A., Experimental evaluation of long-and short-term moisture damage characteristics of asphalt mixtures. *Road Materials and Pavement Design*, 2016, 17(1): 168-186.
23. Bhairampally R.K, Lytton R.L. and Little D.N., Numerical and Graphical Method to Assess Permanent Deformation Potential for Repeated Compressive Loading of Asphalt Mixtures. *Transportation Research Record: Journal of the Transportation Research Record*, 2000, 1723: 150-158.
24. Kringos N. and Scarpas A. Raveling of asphaltic mixes due to water damage: computational identification of controlling parameters. *Transportation Research Record: Journal of the Transportation Research Board*, 2005, 1929: 79–87.
25. Cheng D.X., Little D.N., Lytton R.L. and Holste J.C., Surface free energy measurement of aggregates and its application to adhesion and moisture damage of asphalt-aggregate systems, Proceeding of International Center for Aggregates Research 9th Annual Symposium: Aggregates-Concrete, Bases and Fines, Texas, 2001.

26. Hefer A.W., Little D.N. and Lytton R.L., A Synthesis of Theories and Mechanisms of Bitumen-Aggregate Adhesion Including Recent Advances in Quantifying the Effect of Water. *Journal of the Association of Asphalt Paving Technologists*, 2005, 74: 139-196.
27. Petersen J.C., Plancher H. and Ensley E.K., Miyake G and Venable R L, Chemistry of Asphalt-Aggregate Interaction Relationship with Moisture Damage Prediction Test, *Transportation Research Board*, 1982, 843: 95-104.
28. Robertson R.E., *Chemical Properties of Asphalts and Their Effects on Pavement Performance*, *Transportation Research Circular No. 499*. Washington DC, 2000.
29. Read J. and Whiteoak D. *The Shell Bitumen Handbook*, 5th Edition, Shell Bitumen UK, Chertsey, 2003.
30. Romberg J.W., Nesmitts S.D. and Traxler R.N. Some Chemical Aspects of the Components of Asphalt, *Journal of Chemical and Engineering Data*, 1959, 4(2): 159-161.
31. Peterson C.J. Quantitative Functional Group Analysis of Asphalt Using Differential Infrared Spectrometry and Selective Chemical Reactions –Theory and Application, *Transportation Research Record*, 1986, 1096: 1-11.
32. Petersen J.C., Ensley E.K. and Barbour F.A. Molecular interactions of asphalt in the asphalt-aggregate interface region. *Transportation Research Record*, 1974, 515: 67-78.
33. Curtis C.W., Lytton R.L. and Brannan C.J. Influence of Aggregate Chemistry on the Adsorption and Desorption of Asphalt, *Transportation Research Record*, 1992, 1362, 1-9.
34. Bagampadde U., Isacson U. and Kiggundu B.M. Classical and contemporary aspects of stripping in bituminous mixes. *Road Materials and Pavement Design*, 2004, 5(1): 7-43.

35. Bagampadde U., Isacson U., Kiggundu B.M. Influence of aggregate chemical and mineralogical composition on stripping in bituminous mixtures. *The International Journal of Pavement Engineering*, 2005, 6(4): 229-239.
36. Airey G.D., Collop A.C., Zoorob S.E. and Elliot R.C. Moisture damage assessment of asphalt mixtures using the UK SATS test. *Proceeding of 86<sup>th</sup> Transportation Research Board Annual Meeting*, Washington DC, 2007.
37. Schultz J. and Nardin M. Theories and mechanisms of adhesion. In A. Pizzi and K.L. Mittal (Eds.), *Handbook of Adhesive Technology*. New York: Marcell Dekker, Inc. 1994.
38. Allan K.W. Mechanical theory of adhesion. In: D.E. Packham, ed. *Handbook of Adhesion*. London: Longman Group, UK Ltd, 273-275.
39. Yoon H.H. and Tarrar A.R. Effect of aggregate properties on stripping. *Transportation Research Record: Journal of the Transportation Research Board* 1988, 1171: 37-43.
40. Labib M.E. Asphalt-aggregate interactions and mechanisms for water stripping. *American Chemical Society, Division of Fuel Chemistry*, 1992, 37: 1472-1481.
41. D' Angelo J. and Anderson R.M. Material production, mix design and pavement design effects on moisture damage. *Proceeding of Moisture Sensitivity of Asphalt Pavement: a National Seminar*, San Diego, Washington DC, 2003: 187-201.
42. Tarrar A.R. and Wagh V.P. The Effect of the Physical and Chemical Characteristics of the Aggregate on Bonding. *Strategic Highway Research Program*, National Research Council, Washington, DC, 1991.
43. Gibbs free energy, Wikipedia, [https://en.wikipedia.org/wiki/Gibbs\\_free\\_energy](https://en.wikipedia.org/wiki/Gibbs_free_energy) [accessed 03.07.14].
44. Good R.J. and van Oss C.J. The modern theory of contact angles and the hydrogen bond component of surface energies. *Modern Approaches to Wettability-Theory and Applications*, Springer US, 1992.

45. Bhasin A., Masad E., Little D. and Lytton R. Limits on adhesive bond energy for improved resistance of hot mix asphalt to moisture damage. Transportation research record: Journal of The Transportation Research Board, 2006, 1970: 3-13.
46. Bhasin A. and Little D.N. Characterization of aggregate surface energy using the universal sorption device. Journal of Materials in Civil Engineering, 2007, 19(8): 634-641.
47. Lytton R.L., Masad E.A., Zollinger C., Bulut R. and Little D.N. Measurements of surface energy and its relationship to moisture damage, National Technical Information Service, Alexandria, 2005.
48. Arambula E., Masad E. and Martin A.E. Influence of air void distribution on the moisture susceptibility of asphalt mixes. Journal of Materials in Civil Engineering, 2007, 19(8): 655-664.
49. Terrel R.L. and Shute J.W. Summary report on water sensitivity, SHRP-A/IR-89-003, Strategic Highway Research Program, National Research Council, Washington DC, 1989.
50. Harrigan E.T., Leahy R.B. and Youtcheff J.S. The superpave mix design system: Manual of specifications, test methods and practices, SHRP-A-379, Strategic Highway Research Program, National Research Council, Washington DC, 1994.
51. Airey G.D. and Choi Y.K. State of the art report on moisture sensitivity test methods for bituminous pavement materials. Road Materials and Pavement Design 2002, 3(4): 355-372.
52. Liu Y., Apeageyi A., Ahmad N., Grenfell G. and Airey G. Examination of moisture sensitivity of aggregate-bitumen bonding strength using loose asphalt mixture and physico-chemical surface energy property tests. International Journal of Pavement Engineering, 2014, 15(7): 657-670.
53. Whiteoak D. The Shell Bitumen Handbook. Thomas Telford, 1991.

54. Kennedy T.W., Roberts F.L. and Lee K.W. Evaluation of moisture effects on asphalt concrete mixtures, *Transportation Research Record*, 1983, 911: 134-143.
55. Bocci M. and Colagrande S. The adhesiveness of modified road bitumen. *Proceeding of the 5<sup>th</sup> Eurobitumen Congress, Vol 1A, Stockholm, 1993*
56. Choquet F. and Verhasselt A. An objective method of measuring bitumen-aggregate adhesion-the boiling water stripping test. *Proceeding of the 5<sup>th</sup> Eurobitumen Congress, Stockholm, 1993.*
57. Vuorinen M.J. and Valtonen J.P. A New Ultrasonic Method for Measuring the Resistance to Stripping, *Proceeding of the Eurobitumen Workshop 99, Paper No. 023, Luxembourg, 1999.*
58. Curtis C.W., Ensley K. and Epps J. Fundamental properties of asphalt-aggregate interactions including adhesion and absorption, *National Research Council. Strategic Highway Research Program, Washington DC, 1993.*
59. Walsh G., Jamieson I., Thornton J. and O'Mahony M. A modified SHRP net adsorption test. *Proceeding of Europhalt & Eurobitumen Congress, Starsbourg 1996.*
60. Kennedy T.W., Roberts F.L. and Lee K.W. Evaluation of moisture susceptibility of asphalt mixtures using the Texas freeze-thaw pedestal test. *Proceedings of the Association of Asphalt Paving Technologists, 1982, 51: 327-341.*
61. Corte J.F. and Serfass J.P. The French approach to asphalt mixture design: a performance-related system of specifications, *Proceeding of Association of Asphalt Paving Technologists, 2000: 794-834.*
62. Lottman R.P. Laboratory test methods for predicting moisture-induced damage to asphalt concrete, *Transportation Research Record*, 1982, 843: 88-95.
63. Tunnicliff D.G. and Root R.E. Use of antistripping additives in asphalt concrete mixtures, *NCHRP 274, Transportation Research Board, Washington DC, 1984.*

64. Mathews D.H. and Colwill D. M. The immersion wheel-tracking test. *Journal of Applied Chemistry*, 1962: 505-509.
65. Aschenbrener T. Evaluation of Hamburg wheel-tracking device to predict moisture damage in hot-mix asphalt. *Transportation Research Record*, 1995, 1492: 193-201.
66. Cheng D. Surface Free Energy of Asphalt-Aggregate Systems and Performance Analysis of Asphalt Concrete Based on Surface Free Energy. Ph.D. dissertation. Texas A&M University, College Station, 2002.
67. Bhasin A. Development of methods to quantify bitumen-aggregate adhesion and loss of adhesion due to water. Ph.D. dissertation. Texas A&M University, 2006.
68. Little D.N. and Jones D.R. Chemical and mechanical mechanisms of moisture damage in hot mix asphalt pavements. *National Seminar in Moisture Sensitivity*, San Diego, California, 2003.
69. Adamson A.W. and Gast A.P. *Physical chemistry of surfaces* (6th edition). New York: John Wiley & Sons, 1997.
70. Ahmad N. Asphalt mixture moisture sensitivity evaluation using surface energy parameters. Ph.D. dissertation. University of Nottingham, 2011.
71. Hunter R. N., Self A., Read J., Gerlis R. and Taylor R. *The Shell Bitumen Handbook 6<sup>th</sup> Edition*. ICE Publishing. 2015.
72. Kim Y.R., Freitas A.C. and Allen D.H. Experimental characterization of ductile fracture-damage properties of asphalt binders and mastics. Presented at the 87th Annual Meeting of Transportation Research Board, Washington DC, 2008.
73. Harvey J.A.F. and Cebon D. Failure mechanisms in viscoelastic films. *Journal of Materials Science*, 2003, 38: 1021–1032.
74. Apegyei A.K., Grenfell J.R.A. and Airey G.D. Moisture-induced strength degradation of aggregate–asphalt mastic bonds. *Road Materials and Pavement Design*, 2014, 15(1): 239-262.

75. Mohd Jakami F. Adhesion of asphalt mixtures. PhD dissertation, University of Nottingham, 2012.
76. Zhang J., Airey G.D. and Grenfell J.R.A. Experimental evaluation of cohesive and adhesive bond strength and fracture energy of bitumen-aggregate systems. *Materials and Structures*, 2015: 1-15.
77. Kim Y.R., Pinto I. and Park S.W. Experimental evaluation of anti-stripping additives in bituminous mixtures through multiple scale laboratory test results. *Construction and Building Materials*, 2012, 29: 386–393.
78. Cho D.W., Bahia H.U. and Kamel N.I. Critical evaluation of use of the procedure of superpave volumetric mixture design for modified binders. *Transportation Research Record: Journal of the Transportation Research Board* 2005, 1929, 114–125.
79. Copeland A.R., Youtcheff J. and Shenoy A. Moisture sensitivity of modified asphalt binders: Factors influencing bond strength. *Transportation Research Record*, 2007, 1998: 18–28.
80. Kanitpong K. and Bahia H.U. Evaluation of Hma moisture damage in Wisconsin as it relates to pavement performance. *International Journal of Pavement Engineering*, 2008, 9(1): 9–17.
81. Standard Test Method for 90 Degree Peel Resistance of Adhesives. D6862-11. ASTM International, US. (<http://www.astm.org/Standards/D6862.htm>) [accessed 03.07.14].
82. Horgnies M., Darque-Ceretti E., Fezai H. and Felder E. Influence of the interfacial composition on the adhesion between aggregates and bitumen: Investigations by EDX, XPS and peel tests. *International Journal of Adhesion and Adhesives* 2011; 31(5): 238–247.
83. Blackman B.R.K., Cui S., Kinloch A.J. and Taylor A.C. The development of a novel test method to assess the durability of asphalt road-pavement materials. *International Journal of Adhesion and Adhesives*, 2013; 42: 1-10.

84. Moore D.R. An introduction to the special issue on peel testing. *International Journal of Adhesion and Adhesives*, 2008, 28(4): 153-157.
85. Collop A.C., Choi Y. and Airey G.D. Effects of pressure and aging in SATS test. *Journal of Transportation Engineering*, 2007, 133(11): 618-624.
86. Anon, 'Resistance of compacted bituminous mixtures to moisture induced damage.' AASHTO T283-99, American Association of State Highways and Transportation Officials, USA, 2000
87. Airey G.D., Choi Y.K., Collop A.C. and Elliott R.C. Development of an accelerated durability assessment procedure for high modulus base (HMB) materials, *Proceeding of Sixth International RILEM Symposium on Performance Testing and Evaluation of Bituminous Materials*. RILEM Publications SARL, 2003: 160-166.

## **3. Materials**

### **3.1 Introduction**

The main objectives of this thesis are to evaluate the susceptibility of aggregate-bitumen bonds to moisture damage based on the values achieved from different techniques followed by comparing the correlations between these techniques. Aggregates which were commonly used in UK with known field performance from five different sources were selected for testing. They included two limestone aggregates (L1 and L2) and three granite aggregates (G1, G2 and G3). Two types of bitumen with different penetration grades were used to prepare aggregate-bitumen adhesive specimens with the aggregates mentioned above. Before characterising the moisture susceptibility of the aggregate-bitumen bond, it is of importance to understand the properties (including physical and chemical properties) of the original materials.

### **3.2 Aggregates**

Aggregates constitute the dominant part of asphalt mixtures with the percentage by weight ranging from 92% for wearing course asphalt to about 96% for continuously graded macadam [1]. It is reasonable to consider that aggregate has important effects on the moisture sensitivity of asphalt mixtures due to its high proportion. So, properties of aggregates, including mineralogical composition and moisture absorption, were measured in this part.

#### **3.2.1 Mineralogical composition of aggregate**

The mineralogy of the different aggregates was studied using a mineral liberation analyser (MLA) in order to understand the effect of their mineralogical compositions on moisture damage resistance of aggregate-bitumen bonds. The experimental procedures used for the MLA included the following steps. Aggregates were first washed in water and then dried in an oven at 40 °C for 24 hours. The oven-dried

aggregates were cast in resin moulds with 25mm diameter and 20mm height, followed by polishing of the surface using a rotary polishing machine. Then, carbon coating was applied to get an electron conductive surface. An FEI Quanta 600 scanning electron microscopy (SEM) with MLA capability was used for the mineral analysis. During testing, the SEM collects back-scattered electron (BSE) images and energy dispersive X-ray data for a series of frames step by step across the specimen surface. Measurement of the backscattered electron intensities allows for the segmentation of mineral phases within each particle section, while energy dispersive X-ray (EDX) analysis of a given phase allows for phase identification [2]. The final result is like a map with different colours representing different mineralogical compositions.

The MLA scans and the detailed mineral compositions for the five aggregates are presented in Figure 3-1 and Table 3-1, respectively. It should be mentioned that as the amount of aggregate used for the MLA test is very little, the variability of the final result is inevitable. In this research, several small aggregates were combined in one sample so as to improve the representativeness of the result. As shown in this Figure, minerals in the granite samples (G1, G2 and G3) exhibit considerable texture and their distribution is more complex, while the limestone surface is simple and calcite makes up almost all of the area. For the limestone (L1 and L2) samples, calcite is the predominant phase when compared to the other minerals present, with 96.98% and 99.48% by weight, respectively. However, granite is made up of a number of different mineral phases. Chlorite, albite and quartz are the common dominant minerals for these three granite aggregates with quantities higher than 10%. There are three other minerals, epidote, anorthite and k-feldspar which are detected in G1, G2 and G3, respectively, with quantities higher than 10%. It is believed that large proportions of the albite and quartz phases have the potential to lead to moisture damage, due to the poor adhesion between quartz and bitumen. Although albite can form a strong bond with bitumen in the dry condition, this bond is quickly broken in the presence of water [3]. There is also evidence that feldspar is responsible for interfacial failure at aggregate-bitumen interface [4].

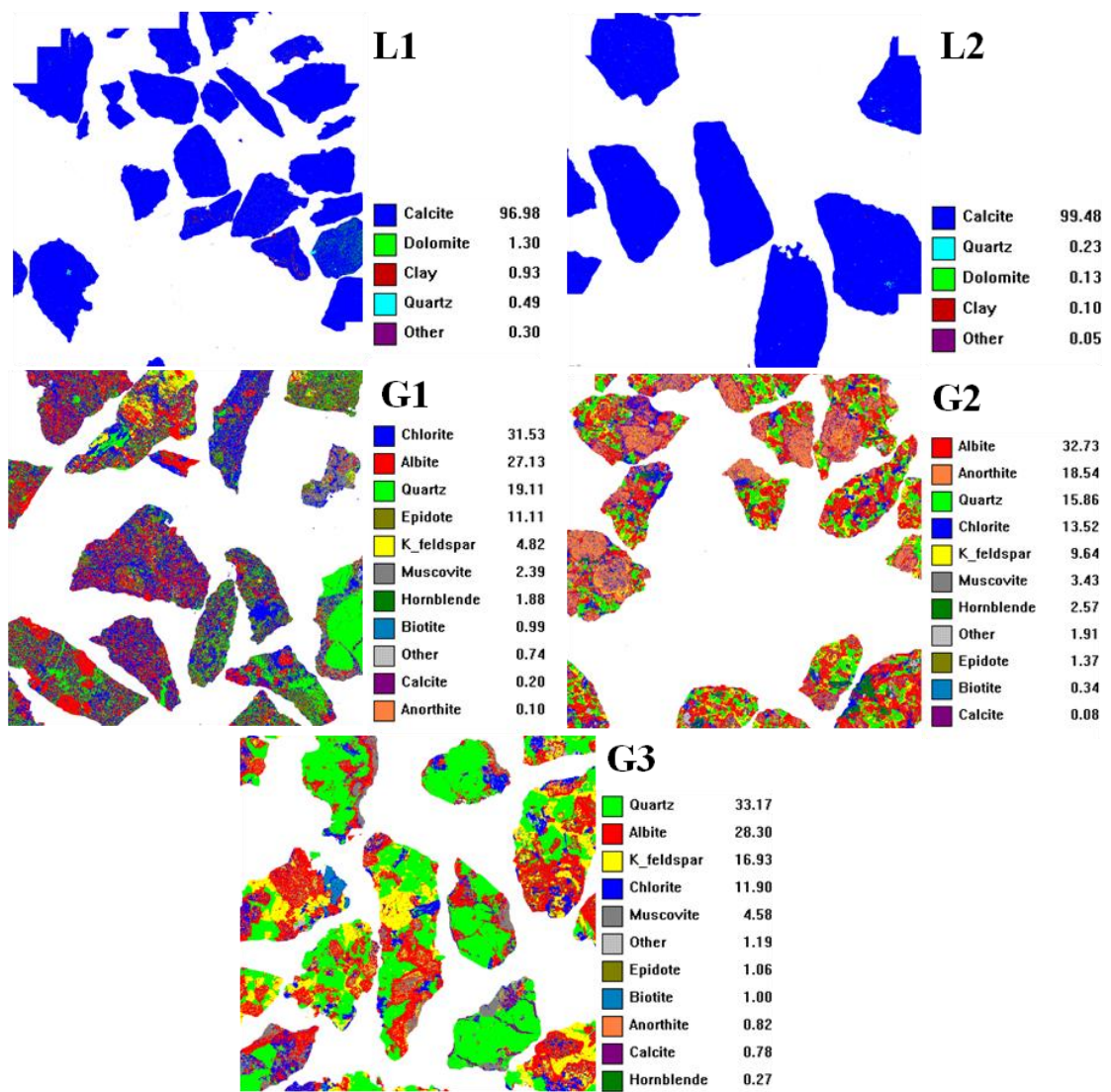


Figure 3-1 Mineral mosaic of five aggregates. L1 and L2 are classified as limestone while G1, G2 and G3 are granite

Table 3-1. Mineral composition of aggregates identified by MLA analysis

Mineral type	Composition (Wt %)				
	L1	L2	G1	G2	G3
Chlorite	-	-	31.53	13.52	11.90
Albite	-	-	27.13	32.73	28.30
Quartz	0.49	0.23	19.11	15.86	33.17
Epidote	-	-	11.11	1.37	1.06
K-feldspar	-	-	4.82	9.64	16.93
Muscovite	-	-	2.39	3.43	4.58
Hornblende	-	-	1.88	2.57	0.27
Biotite	-	-	0.99	0.34	1.00
Other	0.30	0.05	0.74	1.91	1.19
Calcite	96.98	99.48	0.20	0.08	0.78
Anorthite	-	-	0.10	18.54	0.82
Dolomite	1.30	0.13	-	-	-
Clay	0.93	0.10	-	-	-
Total	100	100	100	100	100

### 3.2.2 Moisture absorption of aggregates

The presence and amount of moisture present at the aggregate-bitumen interface reduces the structural strength due to the loss of the adhesive bond between the bitumen and the aggregate, and/or the loss of the cohesive bond within the bitumen film. An important parameter that influences moisture-induced damage in asphalt mixtures is the rate and amount of water absorption of the aggregates. Therefore, it is of importance to quantify the absorption properties of the aggregates. This approach of considering the moisture absorption properties of the aggregate is in contrast to most previous studies that only consider conditioning time when evaluating moisture damage [4]. The current approach recognises the differences in moisture absorption characteristics of different aggregates. To perform the moisture absorption experiments, rectangular aggregate beams with dimensions of 100 mm × 20 mm × 10 mm were first cut from boulders. Then the beams were cleaned using deionised water and dried in an oven at 40 °C for 24 hours to remove all the moisture. The weight of each beam in the dry condition was measured using a balance with precision of 0.1 µg. All aggregates were moisture conditioned by placing them in baths containing deionised water at 20 °C and weighing

them periodically until steady stable conditions were reached. The results were used to calculate the mass uptake of aggregates as a percentage of the dry aggregate weight (Equation (3-1)) [4].

$$\text{Mass uptake (\%)} = M_t = \frac{w_t - w_0}{w_0} \times 100 \tag{3-1}$$

where  $M_t$  is the moisture uptake at time  $t$ ,  $w_0$  is the initial mass of the aggregate in dry condition,  $w_t$  is the mass of aggregate after time  $t$ .

The amount of moisture absorbed as well as the conditioning time was monitored for aggregates when submersed in water at 20 °C for up to 14 days and the results are depicted in Figure 3-2. The results show that the total amount of moisture absorbed ranged from about 0.13% for aggregate G1 to about 2.21% for aggregate L1. The results suggest that the rather large differences in water absorption could be due to the different mineralogy and structure of the aggregates.

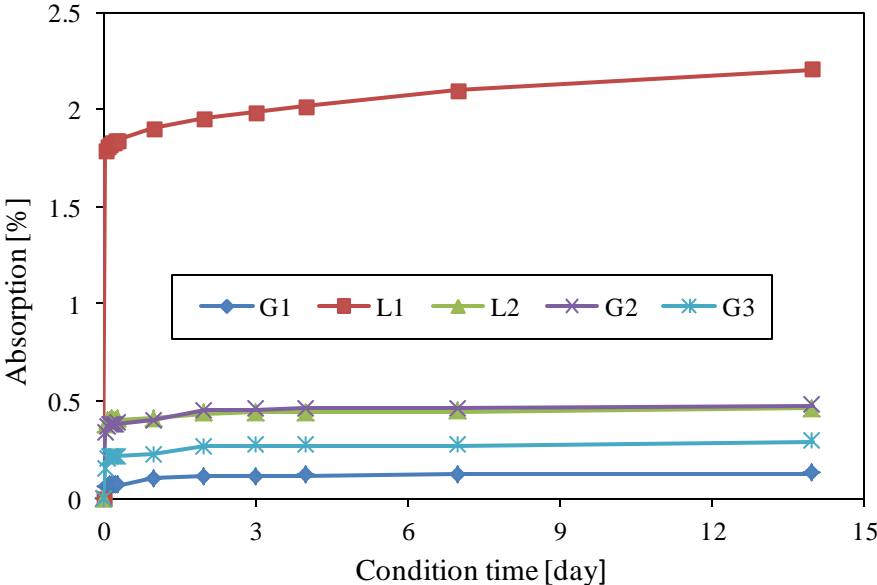


Figure 3-2 Moisture absorption values versus conditioning time for five different aggregates. Moisture conditioning testing was conducted at 20 °C.

A regression analysis was performed to develop a statistical model by relating the aggregate mineralogical data presented in Table 3-1 with the aggregate moisture absorption (14 days) depicted in Figure 3-2. In this regression, the top three minerals in each aggregate were selected as shown in Table 3-2. Then, nine parameters were combined with the mineral compositions of each aggregate to form linear equations

with the result  $M_1$  representing the predicted water absorption, as shown in Equation 3-2. In the beginning, these nine parameters can endow any constant number. Then, the gaps between the predicted water absorption values and the measured results were then squared and summed as shown in Table 3-3. Finally, the summed value as shown in Table 3-3 (red color) is the objective. During regression, the objective was defined to be minimizing by changing the nine parameters as shown in Equation 3-2 and then obtain the values of the nine parameters as shown in Equation 3-3.

Table 3-2. The minerals selected for data regression.

Aggregate	Mineral composition (%)							
	Calcite	Dolomite	Clay	Quartz	Albite	Anorthite	K-feldspar	Chlorite
L1	96.98	1.3	0.93	0.49	0	0	0	0
L2	99.48	0.13	0.1	0.23	0	0	0	0
G1	0.2	0	0	19.11	27.13	0.1	4.82	31.53
G2	0.08	0	0	15.86	32.73	18.54	9.64	13.52
G3	0.78	0	0	33.17	28.3	0.82	16.93	11.9
Parameters								
<b>a</b>	<b>x<sub>1</sub></b>	<b>x<sub>2</sub></b>	<b>x<sub>3</sub></b>	<b>x<sub>4</sub></b>	<b>x<sub>5</sub></b>	<b>x<sub>6</sub></b>	<b>x<sub>7</sub></b>	<b>x<sub>8</sub></b>

Note: The red colored cells are parameters need to be regressed.

$$M_1 = a + x_1 * \text{Calcite} + x_2 * \text{Dolomite} + x_3 * \text{Clay} + x_4 * \text{Quartz} + x_5 * \text{Albite} + x_6 * \text{Anorthite} + x_7 * \text{Kfeldspar} + x_8 * \text{Chlorite}$$

(3-2)

where  $M_1$  is the predicted moisture absorption at 14 days; calcite is the amount of calcite mineral mass (%); dolomite is the amount of dolomite mineral mass (%); clay is the amount of clay minerals (%); quartz is the amount of quartz (%); albite is the amount of albite (%); anorthite is the amount of anorthite (%); kfeldspar is the amount of k-feldspar (%) and chlorite is the amount of chlorite (%).

Table 3-3. The measured and predicted water absorption results

Aggregate	M <sub>0</sub> (%)	M <sub>1</sub> (%)	(M <sub>0</sub> -M <sub>1</sub> ) <sup>2</sup>
L1	2.21	2.209981	3.5E-10
L2	0.46	0.460093	8.6E-09
G1	0.13	0.129997	7.69E-12
G2	0.47	0.469973	7.34E-10
G3	0.29	0.290034	1.17E-09
Sum			1.08593E-08

Note: M<sub>0</sub> is the measured water absorption, M<sub>1</sub> is the predicted water absorption and the red colored cell is objective to be minimized.

The results of regression analysis identified four mineral components – dolomite, clay, anorthite and k-feldspar as the most significant factors that influence aggregate moisture absorption, as shown in Equation 3-3. When inputting the mineral compositions of each aggregate in the equation, the predicted water absorption (as shown in Table 3-3) is very similar to the measured results meaning the reliability of this equation based on these five aggregates. As shown in this equation, of these four factors, dolomite and clay appear to be the most significant factors in limestone while anorthite and k-feldspar are the dominant factors in granite.

$$M_1 = 3.877E - 08 + 0.003 * Calcite + 0.998 * Dolomite + 0.707 * Clay + 0.005 * Quartz + 0 * Albite + 0.0178 * Anorthite + 0.006 * Kfeldspar + 3.416E - 06 * Chlorite \quad (3-3)$$

where M<sub>1</sub> is the predicted moisture absorption at 14 days; calcite is the amount of calcite mineral mass (%); dolomite is the amount of dolomite mineral mass (%); clay is the amount of clay minerals (%); quartz is the amount of quartz (%); albite is the amount of albite (%); anorthite is the amount of anorthite (%); kfeldspar is the amount of k-feldspar (%) and chlorite is the amount of chlorite (%).

### 3.3 Bitumen

Bitumen is the material which binds the graded aggregates together to form asphalt mixtures. It is considered that the performance of an asphalt pavement is largely determined by the rheological (physical) properties and the chemical composition of the bitumen [5]. Two types of bitumen (B1 and B2) with penetration grades of 40/60 and 70/100, respectively, were used in the study.

The physical properties of the bitumen were characterised using softening point and penetration tests. Based on the tests, the softening points (ASTM D36/D36M) [5] of B1 and B2 were 51.2 °C and 45.2 °C respectively, whereas the measured penetration (ASTM D5) [7] of B1 at 25 °C was 46 (0.1mm) compared with 81 (0.1mm) for B2. Apart from that, the rheological properties and chemical composition of the bitumen were characterised as follows.

#### 3.3.1 Dynamic shear rheometer test

The dynamic shear rheometer (DSR) was adopted to characterise the visco-elastic behaviour of bitumen from low to high service temperatures. A thin bitumen specimen is sandwiched between two parallel metal plates held in a constant temperature medium. During the test, the bottom plate remains fixed while the top one oscillates at a controlled sinusoidal shear stress or strain, as shown in Figure 3-3. The two plates are submerged in a liquid bath (20% Ethylene Glycol + 80% Water) to control the temperature of the bitumen.

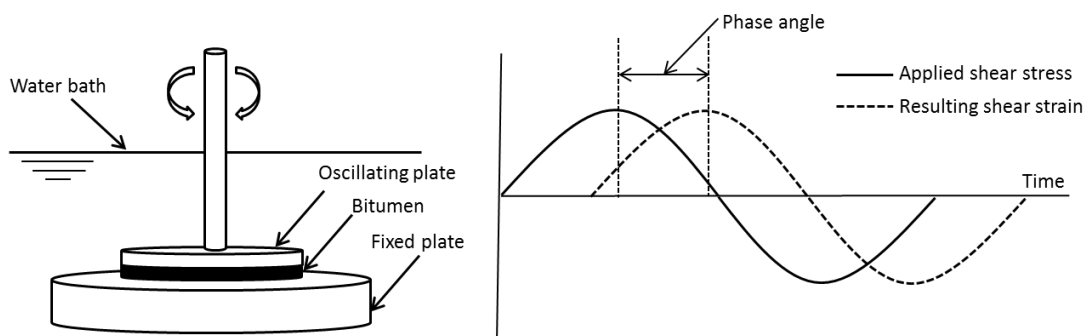


Figure 3-3 DSR test setup and applied signal

The DSR tests were performed in the temperature range from 10 °C to 80 °C. Before the frequency sweep test, a strain sweep test needs to be done so as to define the linear visco-elastic region (LVE) at each temperature. Based on the strain sweep tests, the strain levels were defined for the frequency sweep tests. Table 3-1 shows the testing conditions at different temperatures for the frequency sweep tests.

The main rheological parameters obtained from the DSR test are the complex shear modulus and the phase angle. The complex modulus,  $G^*$ , represents the shear stiffness of the bitumen under the conditions of testing. While the phase angle, represents the time delay between the applied stress and the measured strain. The complex modulus ( $G^*$ ) increases with decreasing temperature and/or increasing frequency. However, the phase angle increases as the temperature increases and/or the frequency decreases.

The frequency sweep test results were analysed based on the time-temperature superposition principle (TTSP) [8]. Master curves of complex modulus and phase angle were built according to the Williams-Landel-Ferry (WLF) theory which is as follows:

$$\text{Log}a_t = -\frac{C_1(T-T_{ref})}{C_2+(T-T_{ref})} \quad (3-3)$$

where  $a_t$  is the shift factor value,  $C_1$  and  $C_2$  are constants,  $T$  is temperature measurement and  $T_{ref}$  is reference temperature (30 °C).

Table 3-1 Testing conditions of frequency sweep tests

Sample	Bitumen							
Temperature ( °C)	10	20	30	40	50	60	70	80
Target Strain (%)	0.5	0.5	0.5	1	1	1	1	1
Parallel Plate Diameter	8mm			25mm				
Sample thickness	2mm			1mm				
Frequency	0.1-10 Hz							

Figure 3-4 shows the shear complex modulus and phase angle master curves for the two types of bitumen used in this research. Data in this figure were produced by means of DSR testing performed within the linear visco-elastic range. The reference temperature is 30 °C. According to the time-temperature superposition principle (TTSP), low shear frequencies correspond to high temperatures while the high frequencies correspond to low temperatures. It was found that bitumen B1 exhibits a higher shear complex

modulus than bitumen B2 from low to high shear frequency. With respect to the phase angle, the data seems to overlap as the frequency becomes lower than 10 Hz. However, the phase angle of bitumen B1 is somewhat higher than that of bitumen B2 as the frequency becomes greater than 10 Hz, but the difference is relatively minor. Bitumen showing higher complex modulus is likely to form a stiffer bond to resist the direct tensile forces.

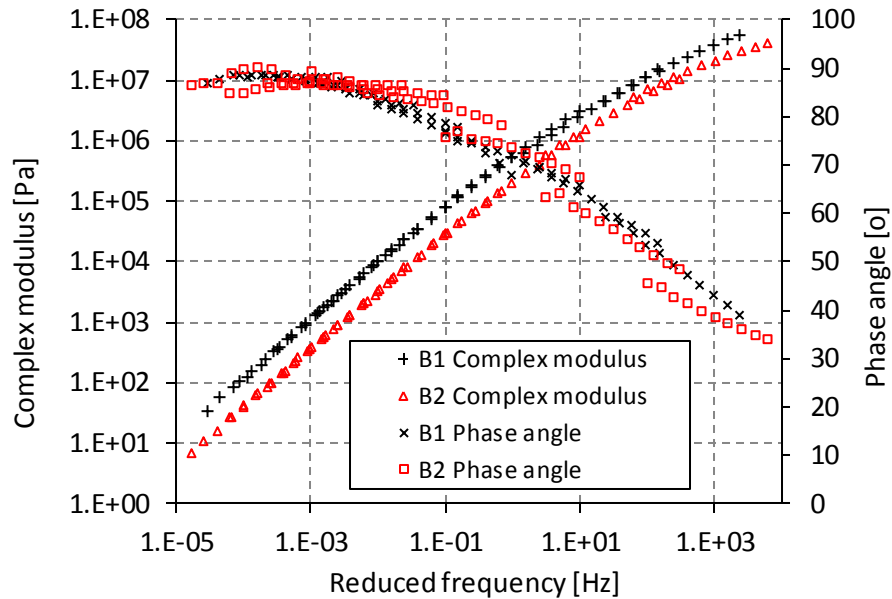


Figure 3-4 Master curves of shear complex modulus and phase angle at a reference temperature of 30 °C for two types of bitumen B1 and B2. Data shows that B1 is stiffer than B2.

### 3.3.2 Fourier Transform Infrared Spectroscopy (FTIR) test

The functional groups of the bitumen were characterised by means of Fourier Transform Infrared Spectroscopy (FTIR) using an Agilent 670 FTIR spectrometer and the procedure suggested by Marsac et al. [9]. The process involved firstly placing a small amount of bitumen (10mg) onto the scanning window of the apparatus. During testing, the beam used in the FTIR test is generated by starting with a broadband light source which contains the full spectrum of wavelengths to be measured. This beam containing multiple frequencies of light was shone at the specimen with the detector used to measure how much of that beam was absorbed by the sample. This process is repeated a number of times and the data analysed to determine the absorption at each wavelength.

Figure 3-5 illustrates the infrared spectroscopy curves of the 40/60 pen and 70/100 pen bitumen at 25 °C. According to previous research [10], the absorption peaks at  $2921\text{cm}^{-1}$  and  $2852\text{cm}^{-1}$  correspond to C-H asymmetrical stretching. The absorption peak of S=O is at  $1030\text{cm}^{-1}$ , which is used to detect the existence of sulfoxides. In terms of carboxylic acids, their C=O and C-O stretch absorption peaks are at  $1730\text{-}1700\text{cm}^{-1}$  and  $1320\text{-}1210\text{cm}^{-1}$ , respectively. The  $1265\text{cm}^{-1}$  band can be assigned to C-O bending vibrations. The vibration at  $2360\text{cm}^{-1}$  is the absorption doublet band of  $\text{CO}_2$  and in this research this peak can be neglected. In this Figure, the absorbance peaks of C-H ( $2852\text{cm}^{-1}$ ) were fixed at the same height. It can be seen that the absorbance of these two types of bitumen nearly overlap. If considering specific sections, the difference in terms of absorbance can be identified. The absorption peak in the region of  $1030\text{ cm}^{-1}$  for 70/100 pen bitumen is higher than 40/60 pen bitumen, demonstrating higher amounts of sulfoxides may present in 70/100 pen bitumen. Furthermore, the 70/100 pen bitumen may contain more carboxylic acids due to the higher absorbance values of 70/100 pen bitumen than 40/60 pen bitumen at  $1730\text{cm}^{-1}$ . The functional groups which can contribute to the bitumen-aggregate bonding, such as sulfoxides and carboxylic acids, can be detected from FTIR curves, but their components are very small.

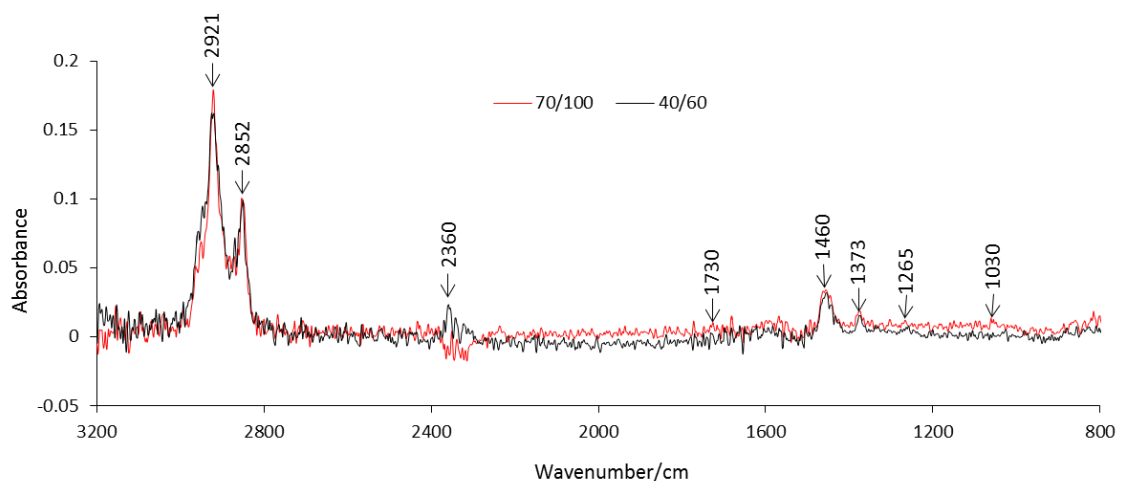


Figure 3-5 FTIR test result of B1 (40/60 pen) and B2 (70/100 pen) bitumen

### 3.4 Conclusions

This chapter reports findings from an investigation of the physical and chemical properties of aggregates and bitumen. Several test techniques, which include MLA,

water absorption, DSR and FTIR, were used in this part. Factors such as the mineralogical compositions and water absorptions of aggregates as well as rheological properties and functional groups of bitumen were evaluated.

MLA is a reliable method to characterise the mineralogical properties of aggregate which could not only detect the percentage of each mineral but also give their distributions on the aggregate surface. The water absorption properties of aggregates were obtained by measuring their moisture uptake with the duration of conditioning time. It can be seen that aggregates from different sources show obviously different mineralogical compositions and moisture absorption properties. The rather large differences in water absorption could be due to the different mineralogy and structure of the aggregates. There are specific minerals which could influence the moisture absorption of aggregates.

According to the DSR test, the two types of bitumen have almost the same visco-elastic behaviour due to their nearly overlapped phase angle plots. B1 bitumen seems to be much stiffer in comparison with B2 bitumen because of its higher complex modulus. In terms of the FTIR test, nearly identical absorption peaks demonstrated similar functional groups of the two types of bitumen.

## References

1. Wu J. The influence of mineral aggregates and binder volumetrics on bitumen ageing. PhD dissertation, University of Nottingham, UK, 2009.
2. Grenfell J.R.A., Ahmad N., Airey G.D., Collop A. and Elliott R.C. Optimising the moisture durability SATS conditioning parameters for universal asphalt mixture application. *International Journal of Pavement Engineering* 2012; 13(5): 433-450.
3. Bagampadde U, Isacsson U, Kiggundu B M. Influence of aggregate chemical and mineralogical composition on stripping in bituminous mixtures. *The international journal of pavement engineering*, 2005, 6(4): 229-239.
4. Apeageyi A.K., Grenfell J. and Airey G.D. Moisture-induced strength degradation of aggregate–asphalt mastic bonds. *Road Materials and Pavement Design* 2014, 15(1): 239-262.
5. Read J. and Whiteoak D. *The Shell Bitumen Handbook*, 5th Edition, Shell Bitumen UK, Chertsey, 2003.
6. Standard Test Method for Softening Point of Bitumen (Ring-and-Ball Apparatus). ASTM D36/D36M, ASTM International, US. (<http://www.astm.org/Standards/D36>) [accessed 03.07.14].
7. Standard Test Method for Penetration of Bituminous Materials. ASTM D5, ASTM International, US. (<http://www.astm.org/Standards/D5>) [accessed 03.07.14].
8. Ferry J.D. *Viscoelastic properties of polymers*, Wiley, New York 1971.
9. Marsac P., Piéard N., Porot L. et al. Potential and limits of FTIR methods for reclaimed asphalt characterisation. *Materials and Structures*, 2014, 47(8): 1273-1286.

10. Wu S.P., Pang L., Mo L.T., Chen Y.C. and Zhu G.J. Influence of aging on the evolution of structure, morphology and rheology of base and SBS modified bitumen. *Construction and Building Materials* 2009, 23: 1005-1010.

# 4. Surface energy testing of bitumen and aggregate

## 4.1 Introduction

As presented in Chapter 2, thermodynamic theory is considered to be a widely used and practicable method to evaluate the adhesive/cohesive bonding. According to this theory, adhesive and cohesive bonds of aggregate-bitumen combinations are directly related to surface energy properties of both materials [1]. So, it is of importance to select the most reliable techniques to measure the surface energies of bitumen and aggregates.

For liquid materials, the parameters “surface tension” and “surface energy” are interchangeable with the equivalent units and values. Because of this, the surface energy of a liquid can be obtained by measuring its surface tension. Surface tension for a liquid can be directly achieved by using the following classical techniques: Wilhelmy Plate Device, Du-Nouy ring method, Drop Weight method, Pendant Drop method, and Sessile Drop method [2].

For solid materials, however, the surface tension and surface energy are not equal. Normally, stretching of solid materials not only expend much work related to elastic and sometimes plastic deformation, but also changes the surface structure. Direct mechanical measurement of solid surface energy only limited to a few solid like mica and diamond as the surface stretching is avoided during cleavage, and the work of cleaving yields surface energy. For most of the solids, it is becomes impossible to achieve the surface free energy by measuring the surface tension directly as the surface stretching is not avoided [2]. So, indirect techniques are therefore used to measure the surface energy of solids. The work of adhesion of a solid with different probe liquids of known surface free energy components is measured which is then used to calculate the surface energy components of the solid. Two techniques, which are the contact angle and the vapour/gas adsorption, are considered to be the most popular methods to measure the interaction of a solid with a probe liquid.

Explanation about the techniques used for measuring the surface energy properties of bitumen and aggregate are first presented in this chapter. The surface free energy components of materials as mentioned in Chapter 3, including bitumen and aggregates, were then measured. Furthermore, the interfacial work of adhesion between the two materials was calculated by combining these surface energy results based on thermodynamic theory. Finally, the effect of water/moisture on the interfacial work of adhesion was also studied by comparing the moisture sensitivity parameters.

## **4.2 Surface energy evaluation of bitumen**

As the bitumen used in this research is in a solid state at room temperature, the surface energy properties should be measured through an indirect method by measuring the contact angle of the bitumen with different probe liquids with known surface free energy components. Two contact angle methods, which are the Sessile Drop/Static Contact Angle Technique and the Dynamic Contact Angle Technique, are usually used for contact angle measurement. According to Ahmad's research [3], the repeatability and reliability of the static contact angle technique is poor in comparison with the dynamic contact angle method. So, in this section, the dynamic contact angle technique was selected to measure the surface energy components of bitumen.

### **4.2.1 Dynamic contact angle (DCA) technique**

In 1863, Wilhelmy developed a contact angle evaluation method by immersing a plate into a liquid and calculating the contact angle from the measured force [2]. The principle of this Wilhelmy plate method is the force interaction changes of the plate as it is immersed and withdrawn from a liquid with a very slow and constant speed. This method is considered to be a fast and efficient technique to measure the contact angles of bitumen with different probe liquids [4].

A Cahn Model dynamic contact angle (DCA) analyser was used to measure the contact angles of the probe liquids on bitumen coated glass slides under dynamic conditions. Figure 4-1 illustrates a schematic of the equipment used in this research. Because there are three unknown surface energy parameters for bitumen, at least three probe liquids

(one non-polar and two polar) are used. A beaker containing a type of probe liquid is placed on a movable stage positioned under the balance. The bitumen coated glass plate is suspended from the balance of the equipment with the help of a crocodile clip and it is necessary to make sure the bottom edge of the plate is parallel to the surface of the probe liquid. During testing, the bitumen coated plate is immersed and then withdrawn from the probe liquid at a constant speed while continuously recording the force involved.

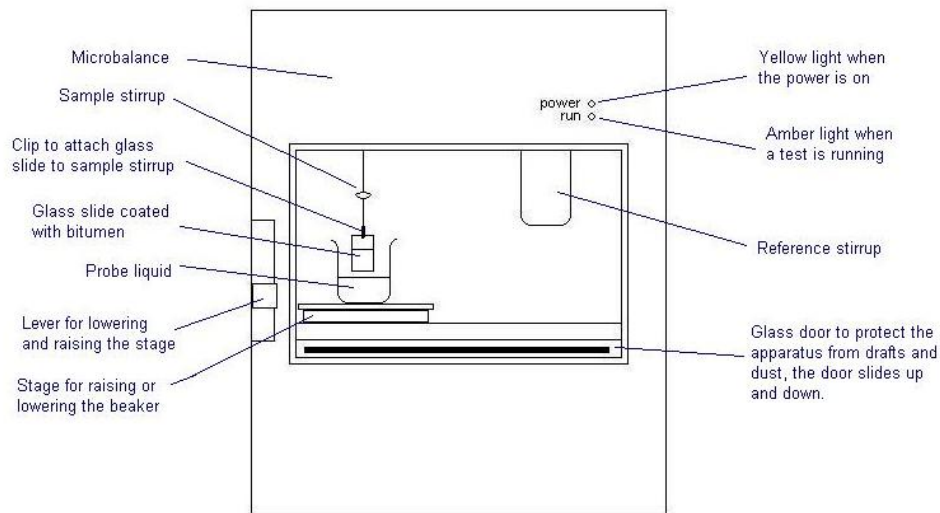


Figure 4-1 Schematic of dynamic contact angle analyser [3]

Figure 4-2 illustrates the force-depth relationship model of the DCA experiment. The dynamic contact angle between bitumen and a probe liquid measured during the immersing process (process 3) is called the advancing contact angle; while the dynamic contact angle during the withdrawal process (process 4) is called the receding contact angle.

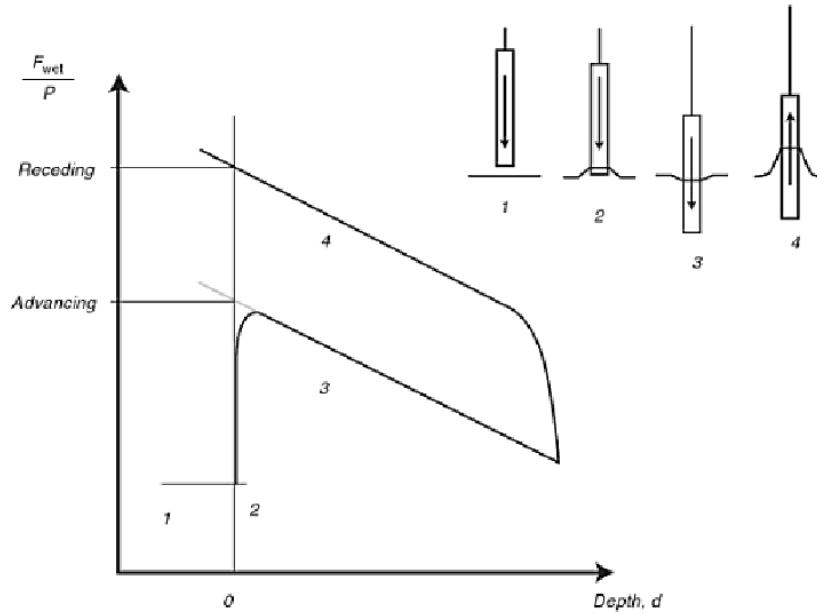


Figure 4-2 Relationship between wetting force and depth of immersion during DCA test [5]

The procedure for deriving the contact angle from the measured force is presented as follows.

When a plate is suspended in air, equation 4-1 is valid:

$$F_1 = Wt_{plate} + Wt_{bitumen} - V\rho_{air}g \quad (4-1)$$

where  $F_1$  is the force measured by the balance of the equipment before immersed in the liquid, which is also the force required to hold the plate;  $Wt_{plate}$  and  $Wt_{bitumen}$  represent the weight of the glass plate and the bitumen film, respectively;  $V$  is the volume of the bitumen coated plate;  $\rho_{air}$  is the density of the air and  $g$  is the local acceleration of gravity.

As the plate is partially immersed in a liquid, the balance measures the force according to equation 4-2:

$$F_2 = Wt_{plate} + Wt_{bitumen} + P_t\gamma_L \cos\theta - V_{im}\rho_L g - (V - V_{im})\rho_{air}g \quad (4-2)$$

where  $F_2$  is the force measured by the balance of the equipment after immersed in the liquid,  $P_t$  is the perimeter of the bitumen coated plate,  $\gamma_L$  is the total surface energy of the probe liquid,  $\theta$  is the dynamic contact angle between bitumen and the liquid,  $V_{im}$  is

the volume of plate immersed in the liquid, and  $\rho_L$  is the density of the liquid. Equation 4-3 was obtained by subtracting equation 4-1 from equation 4-2.

$$\Delta F = P_t \gamma_L \cos\theta - V_{im} \rho_L g + V_{im} \rho_{air} g \quad (4-3)$$

Then the contact angle between the bitumen surface and the probe liquid is calculated as follows:

$$\cos\theta = \frac{\Delta F + V_{im}(\rho_L - \rho_{air}g)}{P_t \gamma_L} \quad (4-4)$$

To obtain surface energy values for the bitumen, contact angle values of the probe liquids are measured and applied to the Young-Dupre equation for the work of adhesion ( $W_{SL}$ ) between the two materials. Based on the relationship between the Young-Dupre equation and the work of adhesion, equation 4-5 is obtained:

$$W_{SL} = \gamma_{Li} (1 + \cos\theta_i) = 2\sqrt{\gamma_S^{LW} \gamma_{Li}^{LW}} + 2\sqrt{\gamma_S^- \gamma_{Li}^+} + 2\sqrt{\gamma_S^+ \gamma_{Li}^-} \quad (4-5)$$

where  $\gamma_{Li}$ ,  $\gamma_{Li}^{LW}$ ,  $\gamma_{Li}^+$ , and  $\gamma_{Li}^-$  are the surface energy parameters of the liquid,  $\theta_i$  is the contact angle measured by the Wilhemy plate method,  $\gamma_S^{LW}$  is the Lifshitz-Van der Waals component of bitumen,  $\gamma_S^+$  is the Lewis acid component of bitumen, and  $\gamma_S^-$  is the Lewis base component of bitumen. These parameters could be assumed as follows to simplify the calculation:

$$y_i(x) = 1 + \cos\theta_i$$

$$a_{1i} = 2\frac{\sqrt{\gamma_{Li}^{LW}}}{\gamma_{Li}}; a_{2i} = 2\frac{\sqrt{\gamma_{Li}^+}}{\gamma_{Li}}; a_{3i} = 2\frac{\sqrt{\gamma_{Li}^-}}{\gamma_{Li}}, \text{ and} \quad (4-6)$$

$$x_1 = \sqrt{\gamma_S^{LW}}; x_2 = \sqrt{\gamma_S^-}; x_3 = \sqrt{\gamma_S^+}$$

Because three probe liquids were used in this research, the following matrix form of a linear simultaneous equation is established:

$$\begin{bmatrix} a_{11} & a_{12} & a_{13} \\ a_{21} & a_{22} & a_{23} \\ a_{31} & a_{32} & a_{33} \end{bmatrix} \begin{bmatrix} x_1 \\ x_2 \\ x_3 \end{bmatrix} = \begin{bmatrix} y_1 \\ y_2 \\ y_3 \end{bmatrix} \quad (4-7)$$

Equation 4-7 is easy to solve and its results provide the surface energy components of bitumen [6].

#### 4.2.2 Test protocol

As introduced before, the Wilhelmy plate method could be used for measuring the contact angle between bitumen and the probe liquids. The surface energy parameters of the probe liquid and the contact angle values are then used to calculate the surface energy parameters of bitumen. In order to determine the surface energy characteristics of bitumen, selection of suitable probe liquids is of great importance and several factors should be considered:

1. The three surface energy parameters of the probe liquid must be known.
2. The probe liquid does not interact (chemically react or dissolve) with the bitumen.
3. The probe liquid should be homogenous and pure.

According to Bhasin's research [6], it is better to use five probe liquids as it reduces the chance of getting a negative number from the square root of the surface energy components. However, Ahmad found that the result achieved from three probe liquids remains similar with the one achieved from five liquids. So, three probe liquids, namely distilled water, glycerol and diiodomethane were used [3].

Before measuring the contact angle, the bitumen coated plate specimen should be prepared. In this research, microscope glass slides with the dimensions of 40 mm × 24 mm × 0.45 mm (No. 15) are selected. The detailed procedures for preparing the bitumen coated plate are as follows:

1. Glass slides are first cleaned with acetone and followed by rinsing using distilled water. Then, a blue flame was used to remove any moisture or organic matter from both sides of the slide.

2. A small steel can filled with bitumen is placed in an oven at the mixing temperature of the bitumen under consideration for around 30 minutes. The molten bitumen is thoroughly stirred using a stick to ensure its homogeneity.
3. The clean glass slide is dipped into and out of the molten bitumen with the depth of no less than 15mm. The slide is inverted immediately to make sure the bitumen drains down to get a uniform layer.
4. The bitumen coated slides are then carefully inserted onto a slide holder and conditioned in a desiccator at room temperature for 24 hours.

To measure the contact angle, the following procedure is followed:

1. Turn on the DCA equipment and open the Win DCA software.
2. Fill a 50 ml beaker with the required probe liquid up to a depth of 20 mm and place it on the stage of the equipment. A dark beaker is required for diiodomethane due to its light sensitive properties.
3. Input the relative factors to the Win DCA software which include the surface energy parameters of the probe liquid and the dimensions of the bitumen coated slide.
4. The bitumen coated slide is attached with a copper clip and then hung on the sample stirrup which is connected with the balance.
5. Adjust the hung glass slide to make sure its bottom edge is kept parallel to the surface of the liquid in the beaker. Then manually move the height of the stage so that the distance between the bottom of the slide and the surface of the liquid is within approximately 5 mm.
6. Close the front cover of the equipment. After the slide stops swinging and become stable, start the test by pressing the button in the software.
7. The weight of the slide is recorded continuously during the whole advancing and receding testing process by the microbalance. An immersion depth of 5 mm is selected in this test.

8. After getting the final data, manual analysis of the force-distance plot was performed to achieve the advancing and receding contact angle based on the principle as shown in equation 4-4.
9. The surface energy components of bitumen are finally calculated with the help of an Excel spread sheet provided with the software.

### **4.3 Surface energy evaluation of aggregate**

Due to the high surface energy of aggregate materials, the contact angle technique cannot be used to measure the surface energy components. With high surface energy, the probe liquid could readily spread on aggregate surfaces resulting in a zero degree contact angle and a high spreading pressure. So, a vapour sorption method was used to determine the surface energy of aggregate by measuring the spreading pressure of the probe vapour on the aggregate.

#### **4.3.1 Dynamic vapour sorption (DVS) technique**

For this study, a dynamic vapour sorption system (DVS Advantage 2, Surface Measurement Systems, Middlesex, UK) was used to determine the surface energy of the aggregates. To perform the test, probe vapours with known surface energy components are passed through the aggregate sample, under controlled temperature and pressure conditions, with the help of the inert carrier gas (dry nitrogen). During this process, the mass of the aggregate sample increases due to the probe vapour being adsorbed at their surface that is then measured using a sensitive balance. All the tests were performed at a temperature of 25°C. The change in mass of an aggregate sample was plotted against the increasing vapour pressure values, as shown in Figure 4-3, to generate sorption isotherms which were used to estimate specific surface area and equilibrium spreading pressures of the aggregates.

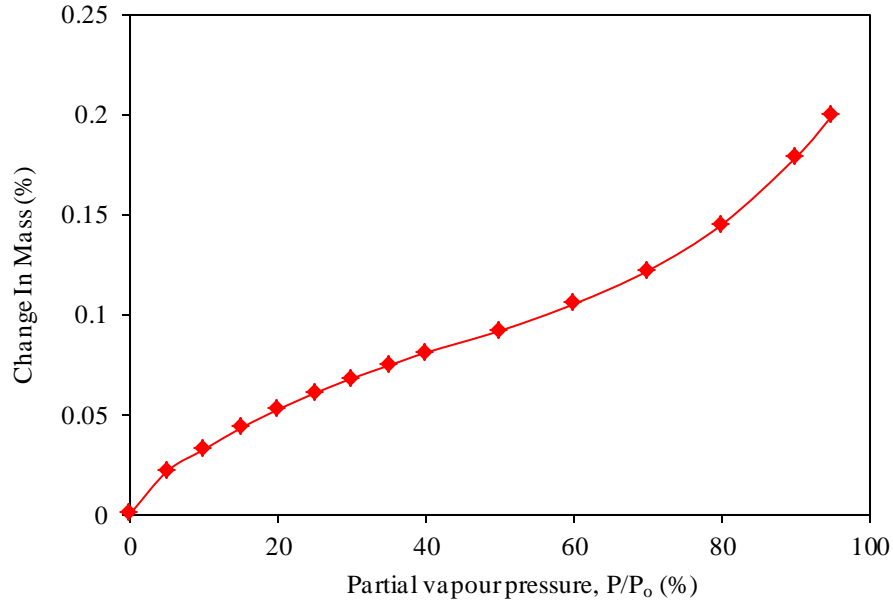


Figure 4-3 Typical sorption isotherm obtained for L1 aggregate using octane vapour as probe liquid for partial vapour pressures ranging from 0% to 95%

According to the original data achieved from the DVS test, the specific surface area of the aggregate is calculated by using the Brunauer-Emmett-Teller (BET) approach as shown:

$$SSA = \left( \frac{n_m N_o}{M} \right) \alpha \quad (4-8)$$

where  $SSA$  is the specific surface area of aggregate ( $m^2$ ),  $n_m$  is the monolayer specific amount of vapour adsorbed on the surface of aggregate (g),  $N_o$  is Avogadro's number ( $6.022 \times 10^{23} \text{ mol}^{-1}$ ),  $M$  is the molecular weight of the vapour (g/mol),  $\alpha$  is the projected or cross-sectional area of the vapour single molecule ( $m^2$ ).

The number of vapour molecules adsorbed on the solid surface is determined by using the Langmuir approach:

$$\frac{P}{n(P_o - P)} = \left( \frac{c-1}{n_m c} \right) \frac{P}{P_o} + \frac{1}{n_m c} \quad (4-9)$$

where  $P$  is the partial vapour pressure (Pa),  $P_o$  is the saturated vapour pressure of solvent (Pa),  $n$  is the special amount adsorbed on the surface of the absorbent (mg), and  $c$  is the BET constant (parameter theoretically related to the net molar enthalpy of adsorption).

Adsorption of vapour molecules on the aggregate surface reduces its surface energy. So, spreading pressure as a result of adsorption of the vapour molecules can be expressed as:

$$\pi_e = \gamma_S - \gamma_{SV} \quad (4-10)$$

where  $\pi_e$  is the spreading pressure at the maximum saturated vapour pressure or equilibrium spreading pressure ( $\text{mJ}/\text{m}^2$ ),  $\gamma_S$  is the aggregate surface energy in a vacuum, and  $\gamma_{SV}$  is the aggregate surface energy after exposure to vapour.

Spreading pressure at the maximum saturation vapour pressure for each solvent,  $\pi_e$ , is calculated by using the following Gibbs free energy model:

$$\pi_e = \frac{RT}{A} \int_0^{P_0} \frac{n}{P} dP \quad (4-11)$$

where  $R$  is the universal gas constant ( $83.14 \text{ cm}^3 \text{ bar}/\text{mol.K}$ ), and  $T$  is the absolute temperature (K).

By introducing spreading pressure,  $\pi_e$ , in the Young-Dupre relation, the following relationship is obtained:

$$W_{SL} = \pi_e + \gamma_{LV} (1 + \cos \theta) \quad (4-12)$$

The contact angle value for high energy solids such as aggregates is zero, therefore, equation 4-12 can be re-written as:

$$W_{SL} = \pi_e + 2\gamma_{LV} \quad (4-13)$$

By substituting the above relation in equation 4-5, the following equation is obtained

$$2\gamma_L + \pi_e = 2\sqrt{\gamma_S^{LW} \gamma_L^{LW}} + 2\sqrt{\gamma_S^+ \gamma_L^-} + 2\sqrt{\gamma_S^- \gamma_L^+} \quad (4-14)$$

Spreading pressures from three probe vapours are measured. Then, the three energy components of the aggregate ( $\gamma_S^{LW}, \gamma_S^+, \gamma_S^-$ ) can be determined by solving three simultaneous equations based on the same method as equation 4-7.

### 4.3.2 Test protocol

The surface energy components of aggregates are calculated by measuring the spreading pressure of probe vapours on the aggregate surface. Therefore carefully prepared aggregates and the selecting of suitable probe vapours are very important.

According to the holding capability of the sample chamber of the DVS equipment, aggregate fractions passing 5 mm and retained on 2.36 mm are used for testing. The sieved aggregates are first washed with deionised water. After cleaning, the aggregates are dried in an oven at 150°C for 4 hours and followed by cooling down to room temperature to make sure all the moisture is evaporated. The cleaned and dried aggregates are stored in glass vials.

With a view to get a uniform adsorption/monolayer of the probe vapour on the aggregate surface, the surface tension values of the probe vapours selected for aggregate analysis are generally lower in comparison with the ones that are used for testing the bitumen. So, the easily available distilled water cannot be used with DVS because of its high surface tension/surface energy/cohesion [3]. Based on this theory, three probe liquids which are octane, ethyl acetate and chloroform are selected for the DVS test.

The detailed procedures for measuring the surface energy of aggregate are described as follows:

1. Regulate the thumb screws provided at the bottom of the manifold to make sure the manifold base is horizontal so as to avoid the hang wires touching the walls of the sample or reference chamber.
2. Turn on the computer and the equipment system.
3. Check the pressure regular and the temperature to make sure these values are always 1.5 bar and 25°C, respectively.
4. Wash the sample and the reference pans with deionised water followed by ethanol and then dry them using lint free wipes.

5. The probe liquid used in this test is poured into the solvent bottle and screwed into the manifold.
6. Click on the DVS Advantage control software and create new DVS methods to be used in this test. The created methods are then added to a new DVS sequence by using the NEW Sequence menu item.
7. Load already saved sequence by using the sequence drop down menu.
8. Carefully hang the cleaned sample and reference pans in the respective chambers with the help of tweezers and close the chambers.
9. Take out the pans and add the required amount of aggregate (normally 2 to 3 grams) and counter weight/steel ball bearings in the respective pans. Both pans are then placed back on the hang wires and finally close the chamber.
10. After countering the weight of the steel balls, start the test by clicking the Run Sequence and save data button. During the test, the increase in mass of the aggregates because of adsorption of the probe vapours on the aggregate surface was measured.
11. The provided DVS Advantage Analysis Software is used to calculate the specific surface area and spreading pressure properties of the sample based on the mass sorption results obtained from different vapour probes, according to the principles as shown in equation 4-8 to equation 4-11. The surface energy components of the aggregate are then calculated from the obtained surface area and spreading pressure values.

#### **4.4 Work of adhesion and moisture sensitivity**

The main objective of measuring surface energy of bitumen and aggregates is to be able to predict the moisture sensitivity of aggregate-bitumen bonds using the principles of thermodynamics and physical adhesion. This objective was accomplished by using the surface free energy parameters of the bitumen and aggregates to calculate their interfacial work of adhesion (dry bond strength) and the work of debonding (energy reduction) of the system with the presence of water/moisture. The calculated bond

energy parameters are then incorporated and arranged into four different ratios for moisture sensitivity analysis of different aggregate-bitumen combinations.

#### 4.4.1 Bond energy parameters

There are three parameters, including dry work of adhesion, the work of debonding and the bitumen cohesion, which can be calculated from the surface energy properties of the bitumen and the aggregates.

##### *Work of adhesion*

The work of adhesion between bitumen and aggregate can be calculated by performing surface free energy calculations using equation 4-15. The bigger the value of this parameter means the greater the adhesion between the two materials and hence more resistance against debonding [3].

$$W_{BA} = 2\sqrt{\gamma_B^{LW}\gamma_A^{LW}} + 2\sqrt{\gamma_B^+\gamma_A^-} + 2\sqrt{\gamma_B^-\gamma_A^+} \quad (4-15)$$

where  $W_{BA}$  is the work of adhesion between bitumen and aggregate, the subscripts B and A represent bitumen and aggregate respectively.

##### *Work of debonding*

For the general case, the work of adhesion for two materials in contact within a third medium can be explained by the following equation. It is the reduction in bond strength of a bitumen-aggregate system when water displaces the bitumen from the aggregate surface [3].

$$W_{BWA} = \gamma_{BW} + \gamma_{WA} - \gamma_{BA} \quad (4-16)$$

where subscripts A, B and W represent aggregate, bitumen and water, respectively.

Then, if the surface energy parameters of water are entered into Equation 4-16, the equation can be expanded as follows [3]:

$$\begin{aligned}
W_{BWA} = & \left\{ \left( \left( \sqrt{\gamma_A^{LW}} - 4.67 \right)^2 \right) + \left( 2 \times \left( \sqrt{\gamma_A^+} - 5.05 \right) \times \left( \sqrt{\gamma_A^-} - 5.05 \right) \right) \right\} + \\
& \left\{ \left( \left( \sqrt{\gamma_B^{LW}} - 4.67 \right)^2 \right) + \left( 2 \times \left( \sqrt{\gamma_B^+} - 5.05 \right) \times \left( \sqrt{\gamma_B^-} - 5.05 \right) \right) \right\} - \left\{ \left( \left( \sqrt{\gamma_B^{LW}} - \right. \right. \right. \\
& \left. \left. \left. \sqrt{\gamma_A^{LW}} \right)^2 \right) + \left( 2 \times \left( \sqrt{\gamma_B^+} - \sqrt{\gamma_A^+} \right) \times \left( \sqrt{\gamma_B^-} - \sqrt{\gamma_A^-} \right) \right) \right\} \quad (4-17)
\end{aligned}$$

#### *Bitumen cohesion*

Bitumen cohesion is the work done to create a new unit area by fracture of the neat bitumen phase and is twice the total surface energy of the material.

#### **4.4.2 Moisture sensitivity parameters**

According to surface energy principles, the moisture sensitivity of asphalt mixture could be predicted by the relationship between work of debonding and work of adhesion. In order to improve the resistance to moisture damage, the work of adhesion ( $W_{BA}$ ) should be as high as possible and the work of debonding ( $W_{BWA}$ ) magnitude should be as small as possible [6]. Based on this reasoning, one of the energy parameters that can be used to assess the moisture damage is show as follows:

$$ER_1 = \left| \frac{W_{BA}}{W_{BWA}} \right| \quad (4-18)$$

$ER_1$  is the ratio of the dry to wet bond strength of the bitumen-aggregate combination. According to this equation, the higher the value of  $ER_1$ , the less moisture sensitive the mixture is likely to be.

Based on the literature review in Chapter 2, adsorption of bitumen into the aggregate may depend on several other factors including the total volume of permeable pore space, the size of the pore openings and surface texture of the aggregates. Rougher aggregate surfaces provide a good lock with bitumen and can have better adhesion properties. These factors can be slotted into the equation by including the surface area of the aggregate materials:

$$ER_2 = \left| \frac{W_{BA}}{W_{BWA}} \right| \times SSA \quad (4-19)$$

where SSA is the specific surface area of the aggregates. A rougher aggregate surface with a higher specific surface area may provide good interlocking spaces for the bitumen.

Apart from work of adhesion and debonding, wettability of aggregate by the bitumen should be considered in order to predict the moisture sensitivity. A material will wet the surface of another material if the cohesive bond energy of the former is less than the work of adhesion of the latter. So, for a given aggregate-bitumen combination, the wettability of bitumen on the aggregate surface is determined by the difference between aggregate-bitumen work of adhesion and the bitumen work of cohesion. An alternative energy parameter can therefore be proposed with the resistance of an asphalt mixture to moisture damage being directly proportional to the wettability of the bitumen with the aggregate and inversely proportional to the reduction in free energy when water causes debonding. This energy parameter can be mathematically expressed as:

$$ER_3 = \left| \frac{W_{BA} - W_{BB}}{W_{BWA}} \right| \quad (4-20)$$

where  $W_{BB}$  is the cohesive bond energy of the bitumen. For a given aggregate surface, bitumen with greater wettability will better coat the aggregate surface leaving fewer weak places for the water to penetrate and cause stripping.

If the influence of micro-texture of the aggregate surface on the moisture sensitivity is considered, specific surface area should be combined with equation 4-20. According to Bhasin [7], the rate of diffusion in micro porous materials is proportional to the square root of the specific surface area. It is believed that this parameter best simulates the moisture sensitivity results obtained through other laboratory tests. So, the energy parameter can be therefore defined as:

$$ER_4 = \left| \frac{W_{BA} - W_{BB}}{W_{BWA}} \right| \times \sqrt{SSA} \quad (4-21)$$

These four energy parameters will be used to characterise the moisture sensitivity of all bitumen-aggregate combinations.

## 4.5 Results

### 4.5.1 Surface free energy of bitumen

The surface energies of two different types of bitumen as mentioned in Chapter 3 were measured in this section. The surface energy properties of the probe liquids, which include distilled water, glycerol and diiodomethane, used in this research are shown in Table 4-1. Five replicate specimens of the same bitumen were tested with each probe liquid. The average advancing and receding contact angles of the two types of bitumen with three probe liquids are shown in Table 4-2. The results presented in this Table correlated well with previous research as the contact angle and coefficient of variability showed similar values [7]. It is observed that the advancing contact angle values are always bigger than the receding ones. This is because the bitumen coated plate was already been wetted by the probe liquid during the advancing movement. The receding contact angle obtained in this test cannot reflect the real relationship between bitumen and the probe liquid. Also, the repeatability of advancing contact angle results is much better than the receding results. So, the advancing contact angle values are selected for surface energy determination.

Table 4-1 Surface energy components of the probe liquids [3]

Probe liquid	Surface energy components (mJ/m <sup>2</sup> )			
	$\gamma^{LW}$	$\gamma^+$	$\gamma^-$	$\gamma$
Water	21.8	25.5	25.5	72.8
Glycerol	34.0	3.92	57.4	64.0
Diiodomethane	50.8	0	0	50.8

Table 4-2 The average advancing and receding contact angle values

Bitumen		Water		Glycerol		Diiodomethane	
		Adv	Rec	Adv	Rec	Adv	Rec
B1	Avg (degree)	84.9	43.6	75.7	26.2	44.1	16.5
	CV (%)	1.76	2.75	1.71	20.15	2.96	26.87
B2	Avg (degree)	88.8	68.6	77.0	54.3	52.4	16.0
	CV (%)	0.89	2.54	2.34	10.86	2.71	33.29

Note: Adv = advancing contact angle, Rec = receding contact angle, Avg = the average value, CV = coefficient of variation.

In order to analyse the reliability of the contact angle results, a plot of  $\gamma_L \cos\theta$  versus  $\gamma_L$  was produced for the contact angle values obtained with the three probe liquids. This method was designed by plotting  $\gamma_L \cos\theta$  versus  $\gamma_L$  to determine the anomalous behaviour in contact angle measurements [8]. Based on this method, contact angle results which lie on a straight line when  $\gamma_L \cos\theta$  is plotted versus  $\gamma_L$  are considered to be acceptable. However, results which are far from the curve are associated with anomalous behaviour and should not be used for the surface energy calculation. The plots of  $\gamma_L \cos\theta$  versus  $\gamma_L$  for two types of bitumen used in this research are depicted in Figure 4-4. It can be seen from this figure that for B1 and B2 bitumen considered, the data points for all three probe liquids lie very close to the trend line with R-squared values of 0.9902 and 0.9983, respectively. This demonstrated that the contact angle values measured from all the probe liquids can be used for the surface energy calculation.

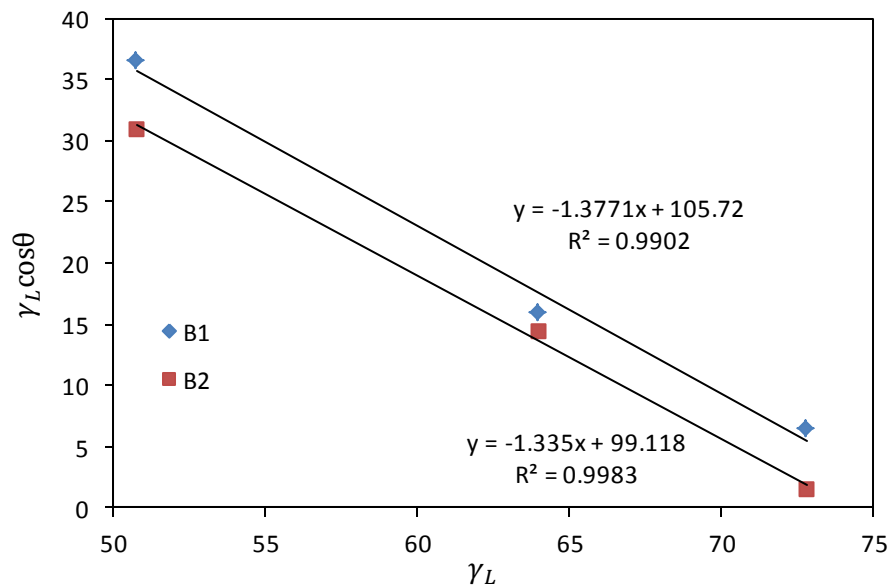


Figure 4-4 Plot of  $\gamma_L \cos\theta$  versus  $\gamma_L$  for B1 and B2

The calculated surface energy results of the two bitumens used in this research are presented in Table 4-3. From this Table it can be seen that the Lifshitz-van der Waals components ( $\gamma^{LW}$ ) of the surface energy are obviously higher than the acid ( $\gamma^+$ ) and base ( $\gamma^-$ ) components. This indicated that the Lifshitz-van der Waals component plays

a predominant part in the adhesion process. In terms of the acid and base components, the latter values are higher than the former. This phenomenon correlates well with Hefer's research [9]. The results for the B1 bitumen exhibited a comparatively higher total surface energy compared to the result for the B2 bitumen demonstrating that stiffer bitumen tends to have higher surface energy which in turn results in higher adhesion with aggregate [3]. The results of the surface energy components in Table 4-3 showed similar values in comparison with previous research [7].

Table 4-3 Surface energy components of bitumen.

Bitumen	Surface energy components (mJ/m <sup>2</sup> )			
	$\gamma^{LW}$	$\gamma^+$	$\gamma^-$	$\gamma$
B1	37.47	0.03	3.46	38.10
B2	32.94	0.06	2.07	33.62

#### 4.5.2 Surface free energy of aggregate

Five aggregates, including two limestones and three granites were tested and the results were used to estimate specific surface area (SSA) and spreading pressure from which the surface energy parameters were calculated. Octane was used as the probe vapour to measure the SSA of aggregates due to its non-polar nature which is supposed to give more accurate values [3]. The surface energy components and SSA of the five aggregates are shown in Table 4-4. From existing literature, the Lifshitz-van der Waals components of aggregates reported to be 35 - 80 ergs/cm<sup>2</sup>. The values obtained in this research are in agreement with this range [7].

Table 4-4 Surface energy components and SSA of aggregates

Aggregate	Surface energy components (mJ/m <sup>2</sup> )				SSA (m <sup>2</sup> /g)
	$\gamma^{LW}$	$\gamma^+$	$\gamma^-$	$\gamma$	
L1	75.3	108.9	49.7	222.4	0.1708
L2	82.2	6.7	59.3	122.0	0.0865
G1	69.1	17.3	568.3	267.5	0.3819
G2	68.3	16.4	40.8	120.0	0.3807
G3	68.0	163.9	122.7	351.6	0.4420

Specific surface area of the various aggregates showed large differences depending on aggregate type. It can be seen that the three granite aggregates showed similar SSA values, while the values for limestone are much smaller in comparison with the granite.

The results show that surface energy properties vary considerably, in terms of surface energy components as well as total surface energy. The test results indicate that the limestone aggregates have slightly higher van der Waals components (over  $75 \text{ mJ/m}^2$ ) than granite aggregates (under  $70 \text{ mJ/m}^2$ ). In contrast, granite aggregates tend to have higher total surface energy in comparison with limestone. Also, the acid-base components showed significant and irregular differences between these five aggregates. The differences can be attributed to different elemental and mineralogical compositions of the aggregates which in turn will influence the strength of aggregate-bitumen adhesion and their moisture sensitivity.

#### **4.5.3 Aggregate-bitumen adhesion and moisture sensitivity**

The objective of measuring the surface free energies of bitumen and aggregate is to be able to calculate their interfacial work of adhesion in dry conditions and the work of debonding with the presence of moisture. These two parameters can therefore be used to predict the moisture durability of aggregate-bitumen combinations based on the physical adhesion principles.

Work of adhesion results for the various aggregate-bitumen combinations and the work of cohesion results for bitumen are shown in Table 4-5. With the absence of moisture, work of adhesion/cohesion values are positive meaning that energy must be applied to debond the adhesion between aggregate and bitumen. From this Table it can be seen that B1 bitumen tends to have higher work of cohesion and work of adhesion results in comparison with B2 bitumen. In terms of the same bitumen, the aggregate also influences the work of adhesion with G1 having the highest values and G2 having the lowest results. It is important to notice the significantly higher value of work of adhesion between bitumen and aggregate compared to the bitumen cohesive strength in the dry state. Therefore, in the absence of moisture, the dominant failure mode in asphalt mixtures should be cohesive which is in accordance with experience [10].

Table 4-5 Work of adhesion and cohesion in dry condition

Bitumen	$W_{BB}$ (mJ/m <sup>2</sup> )	$W_{BA}$ (mJ/m <sup>2</sup> )				
		L1	L2	G1	G2	G3
B1	76.19	147.42	123.22	125.28	118.39	152.30
B2	67.24	132.95	115.14	118.59	109.52	136.70

Note:  $W_{BB}$  = work of cohesion result for bitumen,  $W_{BA}$  = work of adhesion result for aggregate-bitumen combinations

Work of debonding values for the aggregate-bitumen combinations and bitumen films are presented in Table 4-6. From this table it can be seen that the value of the work of debonding was aggregate type dependent, which suggests that the physico-chemical properties of the aggregates play a fundamental and more significant role in the generation of moisture damage, than the bitumen properties. In addition, specimens with positive work of debonding are considered more stable than those with negative work of debonding. For debonding results with negative values, the smaller magnitude values indicate better moisture resistance. According to this principle, specimens comprising of aggregate G2 and L2 would be expected to be more stable than the other three mixtures because of their positive work of debonding values. However, G1 and G3 seem to be the most sensitive aggregates to moisture damage due to their negative work of debonding. In terms of the same aggregate, B2 bitumen tends to result in lower work of debonding values in comparison with B1. So, the B2 bitumen seems more sensitive to moisture damage. The works of debonding results for bitumens are much higher than those for bitumen-aggregate combinations. This means in the presence of moisture, the failure mechanism tends to transform from cohesive to adhesive.

Table 4-6 Work of debonding in wet condition

Bitumen	$W_{BWB}$ (mJ/m <sup>2</sup> )	$W_{BWA}$ (mJ/m <sup>2</sup> )				
		L1	L2	G1	G2	G3
B1	66.51	-42.26	2.59	-167.17	3.76	-97.93
B2	71.83	-49.58	1.66	-166.72	2.03	-106.38

Note:  $W_{BWB}$  = work of debonding when water presence in bitumen cohesive bond,  $W_{BWA}$  = work of debonding when water presence in aggregate-bitumen adhesive bond

Moisture sensitivity parameters calculated according to the four equations presented in Section 4.4.2 are shown in Table 4-7. A higher moisture sensitivity parameter indicates

a better moisture resistance of the aggregate-bitumen combination under consideration. Little and Bhasin [11] defined a set of threshold values for the moisture sensitivity parameters based on an extensive field moisture damage performance versus surface energy results study, with the view to separate ‘good’ from ‘poor’ moisture damage performing aggregate-bitumen combinations. The threshold limits are 0.75 for ER<sub>1</sub>, 0.50 for ER<sub>2</sub>, 0.50 for ER<sub>3</sub> and 0.35 for ER<sub>4</sub>. Based on these threshold limits, aggregate-bitumen combinations which are classified as poor are coloured red as shown in Table 4-7. The magnitude of the moisture sensitivity parameter was found to be aggregate type dependent. All the parameters identified combinations B1-G1 and B2-G1 as moisture sensitive. In addition, L2 and G2 aggregates are considered to have good moisture damage performance due to their highest ratios. In terms of the same aggregate, B2 bitumen tends to achieve smaller moisture sensitivity parameters demonstrating its poor moisture damage properties in comparison with B1 bitumen.

Table 4-7 Moisture sensitivity parameters of all aggregate-bitumen combinations

Aggregate	Bitumen			
	B1			
	ER <sub>1</sub>	ER <sub>2</sub>	ER <sub>3</sub>	ER <sub>4</sub>
	$\left  \frac{W_{BA}}{W_{BWA}} \right $	$\left  \frac{W_{BA}}{W_{BWA}} \right  \times SSA$	$\left  \frac{W_{BA} - W_{BB}}{W_{BWA}} \right $	$\left  \frac{W_{BA} - W_{BB}}{W_{BWA}} \right  \times \sqrt{SSA}$
L1	3.49	0.60	1.69	0.70
L2	47.58	4.12	18.16	5.34
G1	0.75	0.29	0.29	0.18
G2	31.49	11.99	11.22	6.92
G3	1.56	0.69	0.78	0.52
Aggregate	B2			
	ER <sub>1</sub>	ER <sub>2</sub>	ER <sub>3</sub>	ER <sub>4</sub>
	$\left  \frac{W_{BA}}{W_{BWA}} \right $	$\left  \frac{W_{BA}}{W_{BWA}} \right  \times SSA$	$\left  \frac{W_{BA} - W_{BB}}{W_{BWA}} \right $	$\left  \frac{W_{BA} - W_{BB}}{W_{BWA}} \right  \times \sqrt{SSA}$
	L1	2.68	0.46	1.33
L2	69.36	6.00	28.86	8.49
G1	0.71	0.27	0.31	0.19
G2	53.95	20.54	20.83	12.85
G3	1.29	0.57	0.65	0.43
Threshold limit	0.75	0.50	0.50	0.35

Note: the parameters in red colour means the related aggregate-bitumen adhesion have poor moisture damage property.

## 4.6 Conclusions

This chapter reports findings from the investigation of the surface energy properties of bitumen and aggregates. Two surface free energy measurement methods, which are the Wilhelmy plate method and the dynamic vapour sorption (DVS) technique, are introduced and used to measure the surface free energy of bitumen and aggregate, respectively. The three-component surface free energy values are then used to calculate the work of adhesion/debonding values for different aggregate-bitumen combinations using standard thermodynamic theory under dry and wet conditions. Four moisture

sensitivity parameters are finally calculated using energy ratios of dry and wet conditions with the view of evaluating the moisture damage ranking of different aggregate-bitumen combinations.

Based on the results it can be concluded that bitumen properties, such as the penetration and complex modulus, control the bonding strength of aggregate-bitumen combinations in the absence of moisture as the work of adhesion is much higher than the work of cohesion. However, with the presence of moisture, bonding results tend to show negative values demonstrating the thermodynamic potential that drives moisture damage. The works of debonding result for bitumens are much higher than those for aggregate-bitumen combinations. This means in the presence of moisture, the failure mechanism tends to transform from cohesive to adhesive.

In terms of the moisture sensitivity parameters, only one aggregate G1 is defined to be moisture sensitive. Four parameters show similar moisture sensitivity ranking for the five aggregates considered. In terms of the same aggregate, B2 bitumen tends to have smaller moisture sensitivity parameters demonstrating its poor moisture damage properties in comparison with B1 bitumen. One thing should be mentioned that all four moisture sensitivity equations contain absolute value symbols. The definition of these four equations maybe based on the hypothesis that all work of debonding result in negative values. However, there are two aggregates used in this research that result in positive work of debonding values. It could be misleading if two aggregate-bitumen combinations result in positive and negative work of debonding but with the same magnitude. In reality, the positive work of debonding indicates better moisture resistance than the negative one. However, these four equations cannot recognise their difference, so, the reliability of these moisture sensitivity parameters should be compared with the mechanical tests in Chapter 8.

## References

1. Van Oss C.J., Chaudhury M.K. and Good R.J. Interfacial Lifshitz-van der Waals and polar interactions in macroscopic systems. *Chemical Review* 1988, 88(6): 927-941.
2. Adamson A.W. and Gast A.P. *Physical chemistry of surfaces* (6th edition). John Wiley & Sons, New York, 1997.
3. Ahmad N. Asphalt Mixture Moisture Sensitivity Evaluation using Surface Energy Parameters. PhD dissertation, University of Nottingham, 2011.
4. Cheng D. Surface Free Energy of Asphalt-Aggregate Systems and Performance Analysis of Asphalt Concrete Based on Surface Free Energy. PhD dissertation, Texas A&M University, College Station, 2002.
5. Erbil H.Y. *Surface Chemistry of Solid and Liquid Interfaces*, Blackwell Publishing, Oxford, 2006.
6. Ahmad N., Cui S., Blackman B.R.K., Taylor A.C., Kinloch A.J. and Airey G.D. Predicting Moisture Damage Performance of Asphalt Mixtures. Nottingham Transportation Engineering Centre Report, 2011, Report Number: 11091.
7. Bhasin A. Development of Methods to Quantify Bitumen-Aggregate Adhesion and Loss of Adhesion due to Water. PhD dissertation, Texas A&M University, USA. 2006.
8. Kwok D.Y. and Neumann A.W. Contact angle measurements and criteria for surface energetic interpretation. *Contact Angle Wettability and Adhesion*, 2003, 3: 117-159.
9. Hefer A.W. Adhesion in bitumen-aggregate systems and quantification of the effect of water on the adhesive bond. PhD dissertation, Texas A&M University, 2005.

10. Apeageyi A.K., Grenfell J. and Airey G.D. Moisture-induced strength degradation of aggregate–asphalt mastic bonds. *Road Materials and Pavement Design*, 2014, 15(1): 239-262.
11. Little D.N. and Bhasin A. Using surface energy measurements to select materials for asphalt pavement. NCHRP Project 9-37, Transportation Research Board, Washington DC, 2006.

# 5. Fracture energy - Peel test

## 5.1 Introduction

As previously mentioned in Chapter 2, moisture damage is a complicated mode of distress that leads to the loss of stiffness and structural strength of asphalt pavement finally resulting in the failure of the road structure. Normally, the presence of moisture in the pavement can result in the loss of cohesion within the bitumen film itself or the loss of interfacial adhesion between binder and the aggregates [1, 2]. So, the adhesive/cohesive fracture property of the aggregate-bitumen interface is a fundamental parameter in considering the moisture damage of asphalt mixture.

Since the adhesive/cohesive fracture property of aggregate-bitumen interface is considered as one of the main fundamental properties of asphalt pavement materials, it is of importance to select a practicable and reliable measurement to study the fracture properties of the aggregate-bitumen interface. The method should accurately reflect the adhesive/cohesive strength of the aggregate-bitumen interface and distinguish the influence of moisture. There are several methods and procedures that can be used to measure the adhesive/cohesive bond strength between aggregate and bitumen, such as double cantilever beam (DCB) test, tapered double cantilever beam (TDCB) test, impact wedge peel (IWP) test, scratching of thin film test and peel test [3]. The DCB, TDCB and scratching of thin film tests are considered unsuitable to measure bituminous materials because these three methods are based upon linear-elastic-fracture-mechanics (LEFM) for the deformation [3]. Most grades of bitumen undergo viscoelastic deformation during loading at room temperature. In terms of the IWP test, the application of the wedge to separate the interface cannot represent the moisture damage mechanisms of adhesive or cohesive failure meaning it cannot be used for this study.

However, with the peel test, it is possible to calculate the adhesive fracture energy of the aggregate-bitumen interface even if elastic-plastic deformation occurs in the peel arm. In addition, the peel test is a widely used method to characterise the fracture properties of flexible laminates. So, the peel test was selected in this research. The

adhesive/cohesive fracture energy could be calculated from the measured peel force representing the crack resistance of the aggregate-bitumen interface or the bitumen film.

## 5.2 Theory of fracture energy

Fracture energy is defined as the energy required to open a unit area of crack surface. During the peel test, the raw data achieved will be the tensile force. In order to determine the fracture energy ( $G_c$ ) of aggregate-bitumen combinations, there are three energy functions, including the stored strain energy in the peel arm, the energy dissipated during tensile deformation of the peel arm and the energy dissipated due to bending of the peel arm that must be considered and removed from the total input energy [4]. Based on this case, the fracture energy was derived from an energy-balance argument as follows:

$$G_c = \frac{1}{b} \left( \frac{dU_{ext}}{da} - \frac{dU_s}{da} - \frac{dU_{dt}}{da} - \frac{dU_{db}}{da} \right) \quad (5-1)$$

where  $dU_{ext}$  is the external work applied,  $dU_s$  is the stored strain energy in the peel arm,  $dU_{dt}$  is the dissipated energy of the peel arm during deformation, and  $dU_{db}$  is the dissipated energy of the peel arm during bending.

The external work can be determined via the following equation:

$$dU_{ext} = Pda(1 + \varepsilon_a - \cos\theta) \quad (5-2)$$

where  $P$  is the tensile load applied during the test,  $\varepsilon_a$  is the tensile strain of the peel arm, and  $\theta$  is the applied peel angle.

The stored strain and dissipated energy of the peel arm can be obtained as:

$$d(U_s + U_{dt}) = bhda \int_0^{\varepsilon_a} \sigma \cdot d\varepsilon \quad (5-3)$$

where  $h$  is the thickness of the peel arm,  $b$  is the width of the peel arm,  $\sigma$  is the tensile stress of the peel arm at a specific tensile strain  $\varepsilon$ .

If assuming the tensile stiffness of the peel arm is infinite ( $\varepsilon_a = 0$ ) and bending stiffness is zero, the external work can be simplified as:

$$G_c^{\infty E} = \frac{P}{b}(1 - \cos\theta) \quad (5-4)$$

If considering the tensile deformation of the peel arm but assuming the peel arm bending is only elastic, the following equation could be obtained:

$$G_c^{eb} = \frac{P}{b}(1 + \varepsilon_a - \cos\theta) - h \int_0^{\varepsilon_a} \sigma \cdot d\varepsilon \quad (5-5)$$

For an elastic material, the maximum elastic energy ( $G_{max}^e$ ) which can be stored in the peel arm is given by:

$$G_{max}^e = \frac{1}{2}(\sigma\varepsilon_y h) = \frac{1}{2}(E\varepsilon_y^2 h) \quad (5-6)$$

where  $\varepsilon_y$  is the yield strain of the peel arm, and  $E$  is the Young's modulus of the peel arm.

However, if taking the plastic or viscoelastic bending of the peel arm into account, the fracture energy value is given by:

$$G_c = \frac{P}{b}(1 + \varepsilon_a - \cos\theta) - h \int_0^{\varepsilon_a} \sigma \cdot d\varepsilon - G_{db} \quad (5-7)$$

where  $G_{db}$  is the energy dissipated in the peel arm during bending. By substituting Equation 5-5, the following equation is achieved:

$$G_c = G_c^{eb} - G_{db} \quad (5-8)$$

In order to determine the fracture energy, the value of  $G_{db}$  needs to be determined as the value of  $G_c^{eb}$  can be easily achieved according to Equation 5-5.

With the view of evaluating the dissipated energy during bending, the deformation process of the peel arm is illustrated as shown in Figure 5-1. During testing, a steady section of peel arm is loaded rapidly to reach the maximum bending and results in crack propagation, as shown at 'A'. Then, as the crack grows, the section is remote from the crack point and unloads due to the straightening of the peel arm, as 'C'. The total energy dissipated during the loading and unloading process is the area [OABC] as shown in Figure 5-1. So:

$$G_{db} = \frac{Area[OABC]}{b} = \frac{A_a}{b} \quad (5-9)$$

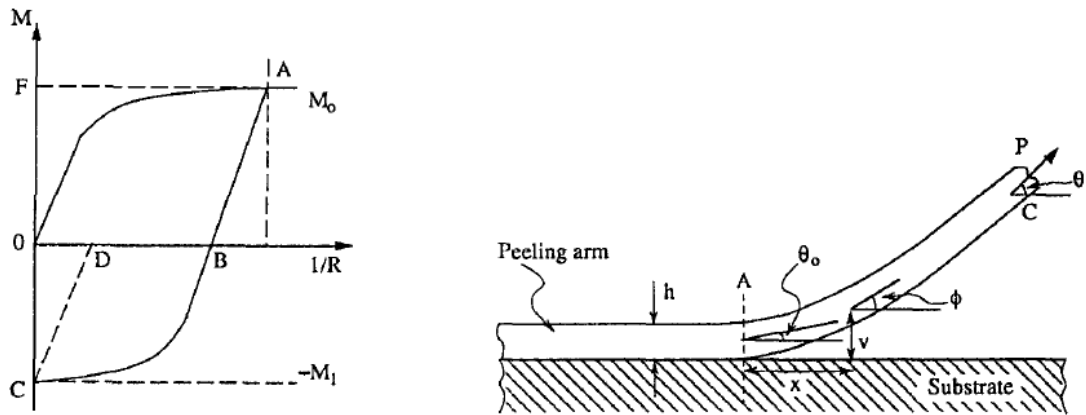


Figure 5-1 Deformation process of the peel arm. (a) deformation process of the peel arm. (b) large-displacement beam-theory model of the peel test [4].

The deformation process described in Figure 5-1a was then modelled according to the large displacement beam theory as shown in Figure 5-1b. The detailed scheme for modelling the deformation process can be seen in [4]. In addition, the elastic-plastic property of the peel arm has been modelled by fitting the stress-strain curve of the peel arm according to a bilinear model, as shown in Figure 5-2. Three parameters, which are Young's modulus  $E$ , plastic yield strain  $\epsilon_y$  and work-hardening parameter  $\alpha$ , were determined and will be used for the fracture energy calculation. Based on the deformation process modelling, the peel test could be derived for three different cases.

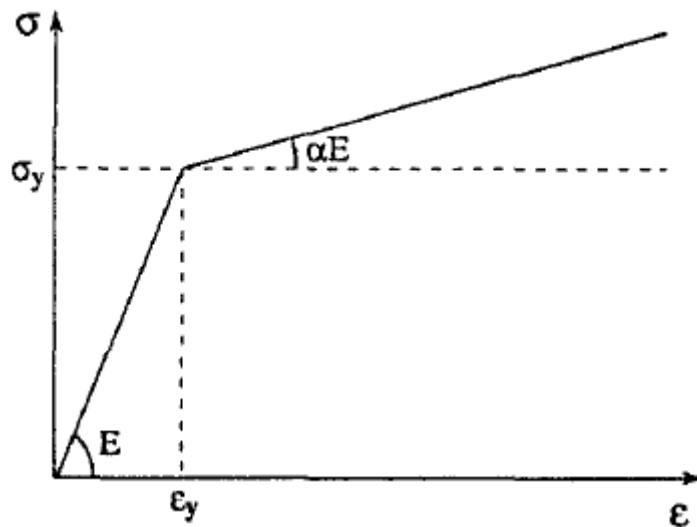


Figure 5-2 Schematic of the bilinear model for the stress-strain curve [4].

The first case is only elastic deformation involved during both loading and unloading process with  $0 < k_o < a$ , and is described as:

$$\frac{G_{db}}{G_{max}^e} = 0 \quad (5-10)$$

$$\frac{G_c^{\infty E}}{G_{max}^e} = \frac{(1 - \cos\theta)}{[1 - \cos(\theta - \theta_0)]} \cdot \frac{k_0^2}{3} \quad (5-11)$$

where  $\theta_0$  is the slope of the peel arm at the peel front and  $\theta$  is the applied peel angle.

The second case is the loading process being plastic deformation and the unloading process is elastic deformation, with  $1 < k_0 < 2(1 - \alpha)/(1 - 2\alpha)$  or  $\alpha \gg 0.5$ , then:

$$\frac{G_{db}}{G_{max}^e} = (1 - \alpha) \left[ \frac{k_0^2}{3} + \frac{2(1-\alpha)^2}{3k_0} - 1 \right] \quad (5-12)$$

$$\frac{G_c^{\infty E}}{G_{max}^e} = \frac{(1 - \cos\theta)}{[1 - \cos(\theta - \theta_0)]} \cdot \frac{k_0^2}{3} \quad (5-13)$$

The third case is plastic deformation involved in both loading and unloading process, with  $k_0 > 2(1 - \alpha)/(1 - 2\alpha)$  and  $\alpha < 0.5$ , resulting in:

$$\frac{G_{db}}{G_{max}^e} = f_1(k_0) \quad (5-14)$$

$$\frac{G_c^{\infty E}}{G_{max}^e} = \frac{(1 - \cos\theta)}{[1 - \cos(\theta - \theta_0)]} \cdot f_2(k_0) \quad (5-15)$$

where

$$f_1(k_0) = \frac{4}{3} \alpha (1 - \alpha)^2 k_0^2 + 2(1 - \alpha)^2 (1 - 2\alpha) k_0 + \frac{2(1-\alpha)}{3(1-2\alpha)k_0} [1 + 4(1 - \alpha)^3] - (1 - \alpha)[1 + 4(1 - \alpha)^2] \quad (5-16)$$

$$f_2(k_0) = \frac{1}{3} \alpha [1 + 4(1 - \alpha)^2] k_0^2 + 2(1 - \alpha)^2 (1 - 2\alpha) k_0 + \frac{8}{3} \frac{(1-\alpha)^4}{(1-2\alpha)k_0} - 4(1 - \alpha)^3 \quad (5-17)$$

The parameter  $k_0$  is:

$$k_0 = \frac{R_1}{R_0} \quad (5-18)$$

where  $R_0$  is the actual radius of curvature at the peel front and  $R_1$  is the radius of curvature at the onset of plastic yielding.

By modelling the root rotation of the peel arm at the peel front, the following relationship can be achieved:

$$\theta_0 = \frac{1}{3}(4\varepsilon_y) \cdot k_0 \quad (5-19)$$

With the view of evaluating the energy dissipated during bending  $G_{ab}$ , the values of  $G_c^{\infty E}$  and  $G_{max}^e$  should be calculated using Equations 5-4 and 5-6, respectively. Secondly, the work hardening parameter  $\alpha$  was determined by fitting the stress-strain curve of the peel arm material. Also, the initial  $k_0$  was estimated by combining ‘case 2’ or ‘case 3’ together with Equation 5-19. Then the achieved  $k_0$  and  $\alpha$  was iterated to determine which case was satisfied. Finally, the value of  $G_{ab}$  was calculated by using the satisfied case. The adhesive fracture energy result could be calculated using Equation 5-8.

### **5.3 Experimental procedure of peel test**

In this research, aggregate substrates were used for fixed arms which were bonded with the aluminium flexible peel arm using bitumen as the adhesive. During testing, the peel arm is peeled apart from the fixed aggregate substrate and the peel force is recorded for fracture energy calculation. Before testing, specimens with aggregate substrate and peel arm bonded by bitumen need to be prepared.

#### **5.3.1 Sample preparation**

For peel testing, the specimen should be rectangular, with the rigid aggregate and the flexible peel arm adhered along most of the length. The rigid aggregate should be thick enough to withstand the expected tensile force. The flexible peel arm should have a very good adhesion to the bitumen, in this way the fracture during the test does not take place at the interface between the peel arm and the bitumen. In this research, an aluminium alloy (Alu 1050A) with a thickness of 0.2mm was selected as the flexible peel arm. According to previous research [5], the overall dimensions of the aggregate substrates used in this research were selected as 200 mm × 20 mm × 10 mm. But because the length of the peel area is only 100 mm, 50 mm extra length of substrate is

enough to make sure the specimen is well fixed with the linear bearing. So, in this research, the length of the substrate was decreased to 150 mm and the results showed that it was reasonable.

Aggregate plates were first prepared by wet cutting stone boulders using a diamond-edged blade saw. Then, the aggregate plates were trimmed to a substrate with the size of 150 mm long and 20 mm wide. In this case, only big stone boulders could be used for the substrate preparation. The substrates were then polished with sand paper (P800, 21.8  $\mu\text{m}$ ) to make sure the surface is visibly flat with no saw marks. Then, the polished slices were cleaned using distilled water and dried at room temperature for at least 24 hours.

The aggregate substrates with dimensions of 150 mm  $\times$  20 mm  $\times$  10 mm were prepared as previously described. They were then bonded to the aluminum peel arm using bitumen as the adhesive layer. The thickness of the bitumen adhesive layer is controlled by placing five wire spacers on the aggregate which results in a film thickness the same as the diameter of the wire. The sample preparation consists of the following steps [6]:

1. Surface pre-treatment. Aggregate substrate was ground using sand paper to get a smooth surface. The ground substrate and peel arm are then wiped gently using a damp paper towel to remove any dust.
2. Pre-heating the aggregate and the bitumen. The aggregate and peel arm are then placed in an oven at 150  $^{\circ}\text{C}$  for 1 hour. Bitumen is preheated to 150  $^{\circ}\text{C}$  for 1 hour prior to making the joint.
3. Placing the sharp crack initiator. A release film polytetrafluoroethylene (PTFE) of dimensions 20 mm  $\times$  12 mm  $\times$  75  $\mu\text{m}$  is placed on the aggregate surface at one end.
4. Five wire spacers with a length of 20 mm are placed on the aggregate. The diameter of the wire controls the thickness of the bitumen (adhesive) layer.
5. The liquid bitumen is applied (at 150  $^{\circ}\text{C}$ ) evenly along the surface of the aggregate.

6. The preheated aluminium peel arm (of length 50 mm longer than the aggregate substrate and of thickness 0.2 mm) is placed on the top of the bitumen layer.
7. Gentle pressure is applied on top of the joint to control the thickness of the bitumen layer. The pressure should be uniformly distributed over the bond area. The bonded specimen is then cooled at ambient temperature overnight. The excess bitumen at the edges of the specimen should be trimmed with a heated knife.
8. All specimens were stored at room temperature ready for further testing.

### 5.3.2 Fracture energy evaluation

A universal testing machine (UTM) which can supply a constant rate of grip separation was used to measure the tensile force during the peel test. The sample was attached to a linear bearing to get a highly accurate and smooth motion during testing. The linear bearing is then attached to the universal testing machine. During the test, the free end of the peel arm was bent to an applied peel angle of 90 ° and this angle is maintained by the linear bearing system, as shown in Figure 5-3. According to Equation 5-20, the displacement velocity of the cross-head of the universal testing machine was equivalent to the fracture displacement velocity when the peel angle is 90 °.

$$R = \dot{C} / (1 - \cos\theta) \quad (5-20)$$

where,  $R$  is the peel rate (mm/min),  $\dot{C}$  is the crosshead displacement rate (mm/min) and  $\theta$  is the peel angle (degree).

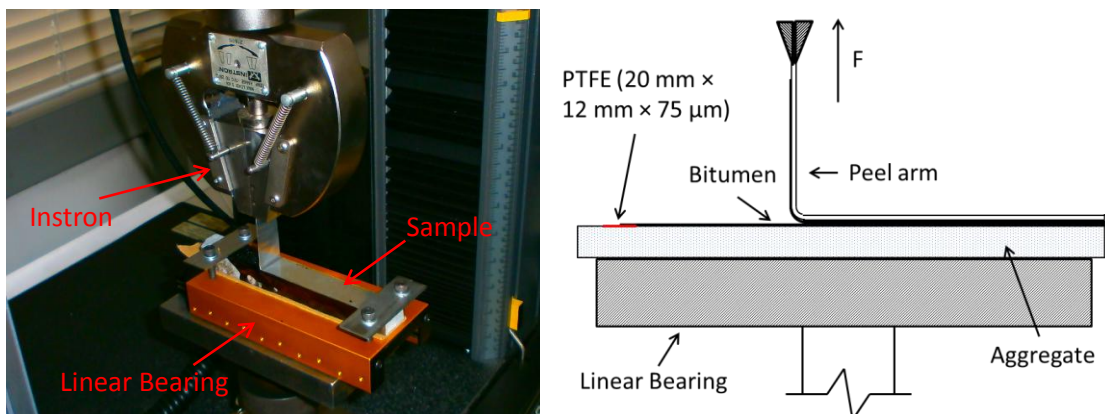


Figure 5-3 Details of peel test equipment

A peel speed of 10 mm/min was used in this test. The tensile force was recorded during the fracture development so as to calculate the fracture energy in the next step. The fracture energy,  $G_a$ , is considered to be a geometry-independent parameter which reflects (a) the energy to break the interfacial bonding forces and (b) the energy dissipated locally ahead of the peel front in the plastic or viscoelastic zone. The input energy to the peel test needs to be resolved into the various deformation energies; elastic, plastic and adhesive fracture energy [4]. The adhesive fracture energy  $G_c$  can be derived as follows:

$$G_c = \frac{1}{b} \left( \frac{dU_{ext}}{da} - \frac{dU_s}{da} - \frac{dU_{dt}}{da} - \frac{dU_{db}}{da} \right) \quad (5-21)$$

where  $dU_{ext}$  is the external work,  $dU_s$  is the stored strain energy in the peel arm,  $dU_{dt}$  is the energy dissipated during tensile deformation of the peel arm,  $dU_{db}$  is the energy dissipated during bending of the peel arm near the peel front, and  $b$  is the width of the peel arm (mm) and  $da$  is the differential of fracture area.

In order to calculate the plastic deformation energy associated with the peel arm, it is first necessary to have knowledge of the tensile stress-strain characteristics of the peel arm material. So, the aluminium peel arm with the same width as used in the sample preparation was subjected to tensile testing at the same cross-head speed (10 mm/min).

### 5.3.3 IC Peel software introduction

In order to calculate the fracture energy of aggregate-bitumen bonds more easily, software known as 'ICPeel' was developed at Imperial College London based on the fracture theories as introduced in Section 5.2 [7]. The software is free to download from the Imperial College London website. To determine the fracture energy, several parameters need to be inputted into the ICPeel software and the fracture energy is calculated automatically.

The software provides two types of methods to analyse the fracture energy which are a linear-elastic stiffness approach and the limiting maximum stress approach. The linear-elastic stiffness approach is a more standard option using only fracture energy  $G_c$  to characterise the fracture property. To conduct this calculation, the input cell 'Maximum

Stress' should be blank. The limiting maximum stress approach is a method which focuses on cohesive zone analysis describing the fracture process by two parameters, the fracture energy  $G_c$  and the maximum stress for the damage zone  $\sigma_{max}$ . To conduct this analysis, it is necessary to define the value of  $\sigma_{max}$  precisely and the value needs to be inputted in the 'Maximum Stress' cell. In this research, the bitumen film thickness is very thin. Though there were cohesive failures occurring in the dry condition, it is impossible to obtain the maximum stress for the damage zone as the amount of area of bitumen involved at a specific point is unknown. In addition, adhesive failures were found after moisture conditioning and the limiting maximum stress approach is not suitable to analyse the adhesive zone. So, in this research, the linear-elastic stiffness approach was selected to characterise the fracture energy of aggregate-bitumen bonds and this correlates well with previous researchers [5].

Figure 5-4 shows the whole software interface including input parameters and output parameters. The input parameters were defined as follows:

$E$  is the Young's modulus of the peel arm material (GPa).

$\sigma_y$  is the yield stress of the peel arm (MPa).

$\varepsilon_y$  is the yield strain of the peel arm material (%).

$n$  is the power law of the peel arm material.

$\alpha$  is the bilinear parameter of the peel arm material.

$h$  is the thickness of the peel arm (mm).

$b$  is the width of the peel arm (mm).

$h_a$  is the thickness of adhesive layer (mm).

$E_a$  is the Young's modulus of the adhesive material (GPa).

$P$  is the average peel force (N).

$\theta$  is the peel angle (degree).

$\sigma_{max}$  is the maximum stress for the damage zone (MPa).

The first five parameters are related to the properties of the peel arm material. These parameters were obtained by fitting the stress-strain curve of the peel arm material according to a bi-linear or power law equation. The procedures for determining these parameters are introduced in the next section. The thickness and width of the peel arm are 0.2 mm and 20 mm in this research, respectively. The parameter  $h_a$  of the adhesive material is the film thickness of the bitumen used in this research. The  $E_a$  of the adhesive materials was obtained from the stress-strain curve of the bitumen and will be introduced in the next section. The peel force could be obtained from the tensile force-displacement curve and will be introduced later. The peel angle used in this research is  $90^\circ$ . The value of  $\sigma_{max}$  could be neglected as the linear-elastic stiffness approach was selected in this research.

After inputting the required parameters, there are two options to calculate the results. One option is calculates a single case by clicking the bottom 'Compute a single case' or pressing the keys 'Ctrl + A', as shown in Figure 5-4. Another option are calculate a series of cases by clicking the 'Compute a series of cases' bottom or pressing the keys 'Ctrl + Z'.

The output parameters are presented as follows:

$G_c$  is the adhesive fracture energy ( $\text{J/m}^2$ ).

$G_d$  is the plastic work in bending ( $\text{J/m}^2$ ).

$G_{tot}$  is the input energy correlated for stored strain energy and tensile dissipations on the peel arm ( $\text{J/m}^2$ ).

$G$  is the total input energy ( $\text{J/m}^2$ ).

Correction is the ratio of  $G_d/G$  (%).

$\sigma_{max(0)}$  is the calculated maximum stress for the damage zone (MPa).

$\theta_0$  is the root rotation (deg).

$k_0$  is the non-dimensional maximum curvature of the peel arm.

$R_0$  is the radius of curvature of the peel arm at the root (mm).

$\varepsilon_{max}$  is the maximum bending strain in the peel arm at the root (%).

The value of adhesive fracture energy will be used to evaluate the bonding between bitumen and aggregate before and after moisture damage.

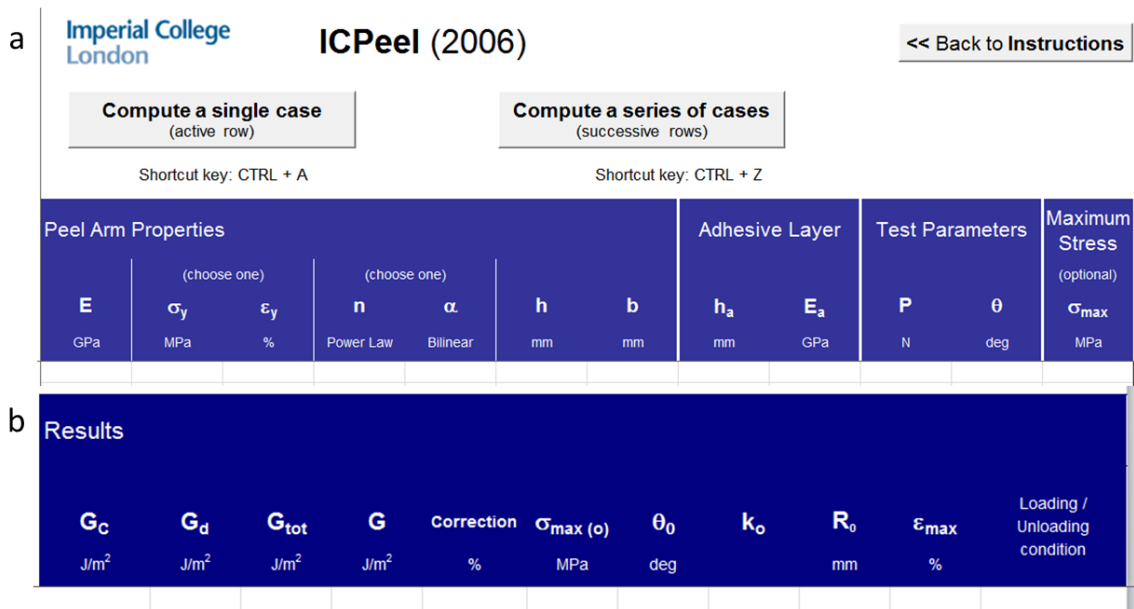


Figure 5-4 Interface of the ICPeel software [7]

## 5.4 Results

### 5.4.1 Parameters calculation

The objectives of measuring the tensile strength of the peel test specimen and the stress-strain properties of the peel arm are to calculate the fracture energy needed to break the aggregate-bitumen bonds apart. In order to calculate the fracture energy values, several parameters need to be determined so as to input them in the ICPeel software to calculate the fracture energy. As introduced in Section 5.3.3, there are five parameters related to the properties of the aluminium peel arm. The tensile stress-strain test of the peel arm was performed at a speed of 10 mm/min until fracture occurred. The tensile stress-strain curve is shown in Figure 5-5. In order to describe the elastic and plastic deformation of the peel arm, the stress-strain curve should be fitted according to a bi-linear or power law form [5]. The purpose of the bi-linear and power

law curve fits is to obtain a number of parameters which are used to calculate the fracture energy.

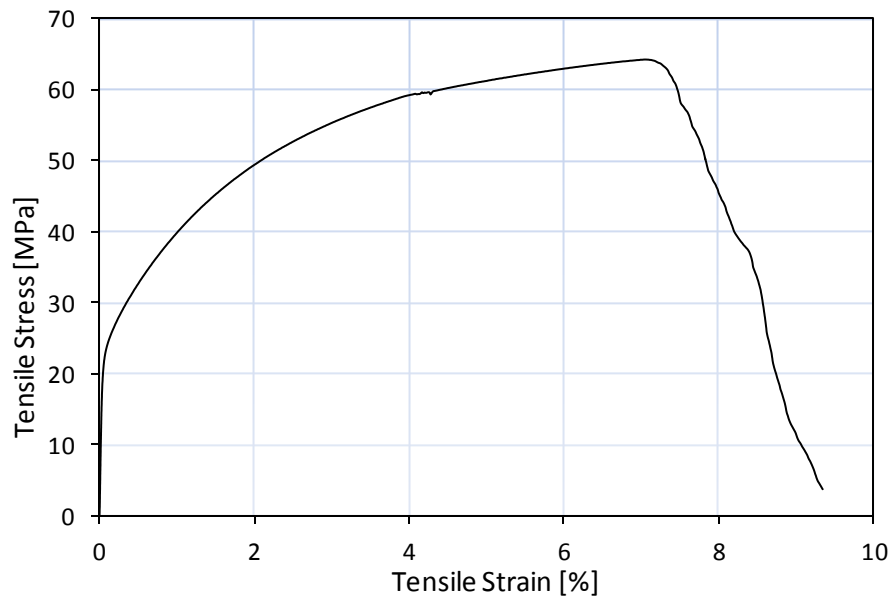


Figure 5-5 Stress-strain curve of peel arm test

When  $\varepsilon < \varepsilon_y$ ,

$$\sigma = E_1 \varepsilon \quad (5-22)$$

When  $\varepsilon > \varepsilon_y$ , according to the power law work hardening model:

$$\sigma = \sigma_y \left( \frac{\varepsilon}{\varepsilon_y} \right)^n \quad (5-23)$$

According to the bi-linear model:

$$\sigma = \sigma_y + \alpha E_1 (\varepsilon - \varepsilon_y) \quad (5-24)$$

where  $\sigma_y$  is the yield stress,  $\varepsilon_y$  is the yield strain,  $E_1$  is the elastic modulus of the peel arm,  $E_2$  is the plastic modulus of the peel arm,  $n$  is the work hardening coefficient of the peel arm, and  $\alpha$  is the ratio of plastic modulus to elastic modulus,  $E_2/E_1$ .

The measured stress-strain curve was modelled using the bi-linear and power law models as shown in Figures 5-6 and 5-7, respectively. From these two figures it can be seen that both models provide acceptable fit with high  $R^2$  values. Table 5-1 shows the parameters gained from the fitting process. It should be mentioned that the elastic

modulus of the peel arm obtained in this research (61 GPa) is lower in comparison with the existing literature with the value being around 70 GPa [5]. This measurement error may be because the stiffness of the UTM equipment is higher than the stiffness of the peel arm. During testing, a relatively lower tensile stress values obtained and finally results in lower elastic modulus when divided by the tensile strain.

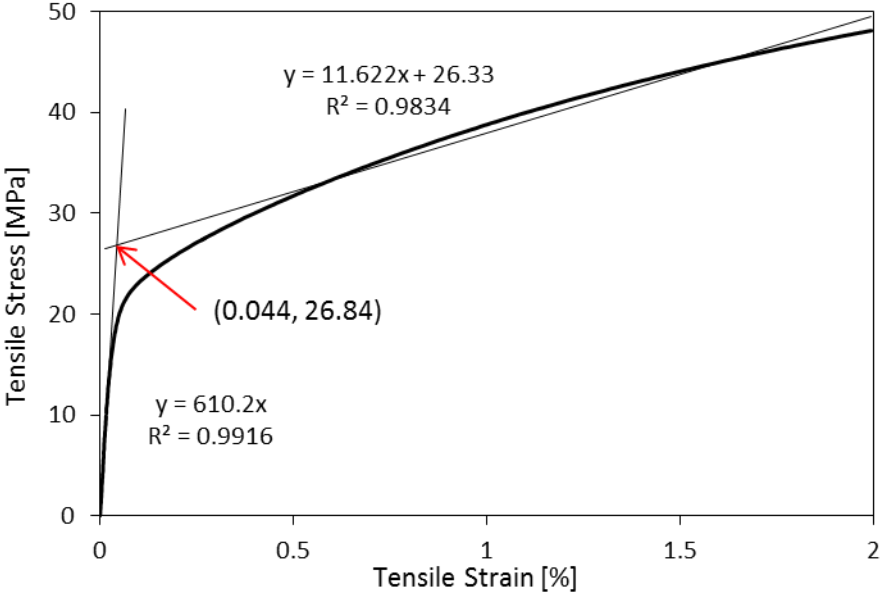


Figure 5-6. Tensile stress-strain curve fitted using bilinear model

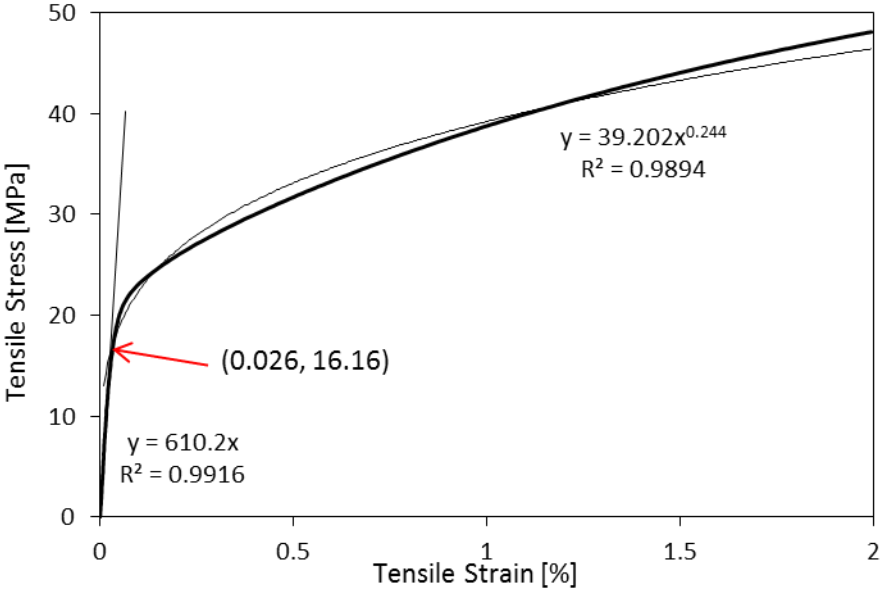


Figure 5-7 Tensile stress-strain curve fitted using power law model

Table 5-1 Plastic bending parameters of the peel arm

Model type	Parameters	Quantity
Bi-linear fit	Low strain modulus, $E_1$	61.0 GPa
	High strain modulus, $E_2$	1.16 GPa
	Yield strain, $\epsilon_y$	0.044 %
	$\alpha (E_2/E_1)$	0.019
	Yield stress, $\sigma_y$	26.84MPa
Power law fit	Low strain modulus, $E_1$	61.0 GPa
	Constant, n	0.244
	Yield strain, $\epsilon_y$	0.026 %
	Yield stress, $\sigma_y$	16.16 MPa

As shown in Section 5.3.3, the linear-elastic stiffness approach was selected in this research to characterise the fracture energy properties of aggregate-bitumen bonds. So, it is necessary to measure the Young's modulus of bitumen. The problem is that bitumen is a viscoelastic material; its Young's modulus can only be measured at extremely low temperature or high extension speed. However, the Young's modulus achieved cannot mirror the bitumen properties at experimental conditions (10 mm/min at 20 °C). So, the elastic modulus of the bitumen was selected to replace the Young's modulus.

To obtain the elastic modulus of the bitumen, the DSR results as shown in Chapter 3 were used. Bitumen binders are viscoelastic and behave with both viscous and elastic properties when deformation is applied. Furthermore, the viscoelastic properties of bitumen are also time-temperature dependent. This means that they behave like an elastic solid at low temperature or high deformation speed and like a viscous liquid at high temperature or low deformation speed. The experimental condition for the peel test is 10mm/min extension speed at the temperature of 20 °C. So, it is of importance to derive the shearing frequency of DSR test which could represent the 10 mm/min extension speed and then calculate the elastic modulus of bitumen at the specific frequency at 20 °C. The target strain  $\gamma_{max}$  can be defined as follows:

$$\gamma_{max} = \frac{\theta r}{h} \quad (5-25)$$

where  $\theta$  is the rotation angle (radians),  $r$  is the specimen radius (mm) and  $h$  is the specimen height (mm).

So, the maximum deformation ( $d_{max}$ ) of the specimen is:

$$d_{max} = h \cdot \gamma_{max} \quad (5-26)$$

The total deformation distance in one sinusoidal cycle is four times the maximum deformation. So, the deformation speed for the DSR specimen is:

$$S_d = 4 \cdot d_{max} \cdot f \cdot 60 \quad (5-27)$$

where  $S_d$  is the deformation speed of the DSR specimen (mm/min),  $f$  is the shearing frequency (Hz), 60 represents there are 60 seconds per minute.

As shown in Chapter 3, the specimen dimensions are 2 mm thick with a 4 mm radius, the target strain is 0.5%. By inputting these data into equations 5-26 and 5-27, the frequency which represents the speed of 10 mm/min is calculated as 4.17 Hz.

The relationship between frequency and elastic modulus of the two types of bitumen used in this research are plotted in Figures 5-8 and 5-9. By inputting the calculated frequency in the trend-line, the elastic modulus of these two types of bitumen was measured as 4.4 MPa and 3.8 MPa for 40/60 pen bitumen and 70/100 pen bitumen, respectively.

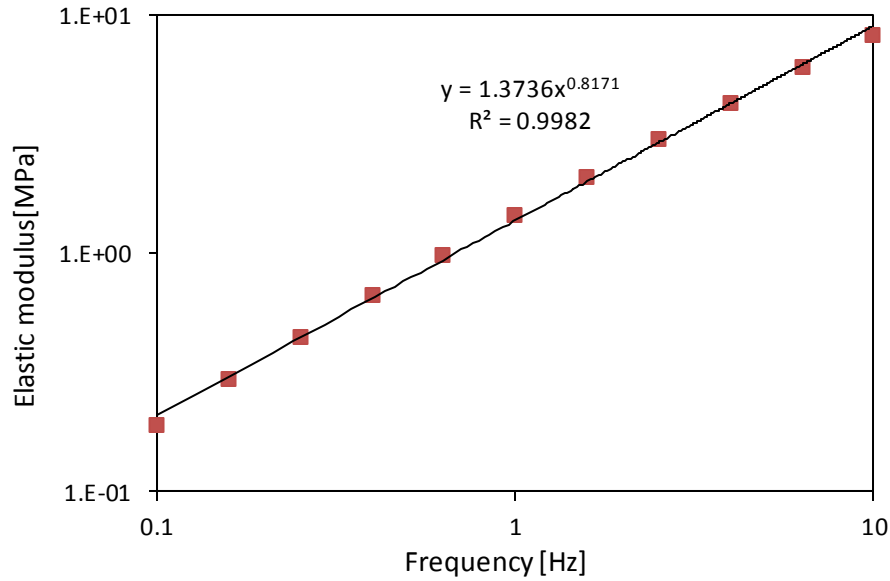


Figure 5-8 Relationship between elastic and frequency modulus of 40/60 pen bitumen

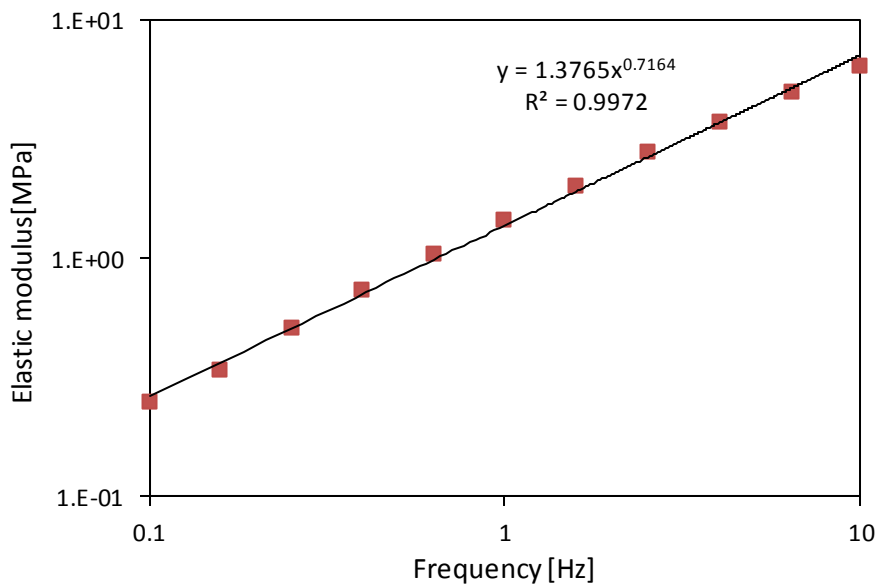


Figure 5-9 Relationship between elastic and frequency modulus of 70/100 pen bitumen

The specimens prepared as shown in Section 5.3.1 were subjected to the peel test. All peel tests were conducted at 20 °C with a speed of 10 mm/min, which is the same condition as for the peel arm stress-strain test. The tensile force was recorded by the Instron universal testing machine during testing and the tensile force versus displacement curve was plotted, as shown in Figure 5-10. It was observed that the tensile force remained at an approximately constant value after the initial stage. This means that the fracture experienced a steady propagation. Normally, at least 50 mm of constant crack propagation region will be defined with the average value of the tensile

force being calculated as shown in Figure 5-10. This average tensile force was used to calculate the values of the aggregate-bitumen fracture energy.

Four tests were performed on each aggregate-bitumen combination. The average force of each sample and the parameters achieved previously were entered into the Microsoft Excel macro IC Peel software to calculate the fracture energy [7]. Fracture energy results in terms of both the bi-linear model and power law model were calculated. For all tests, the fracture energy calculated according to the bi-linear model is slightly higher than that from the power law model, but the difference is less than 5%. Therefore it is possible to select either model to analyse the different bitumen-aggregate combinations. In this research, the power law model was employed for the analysis.

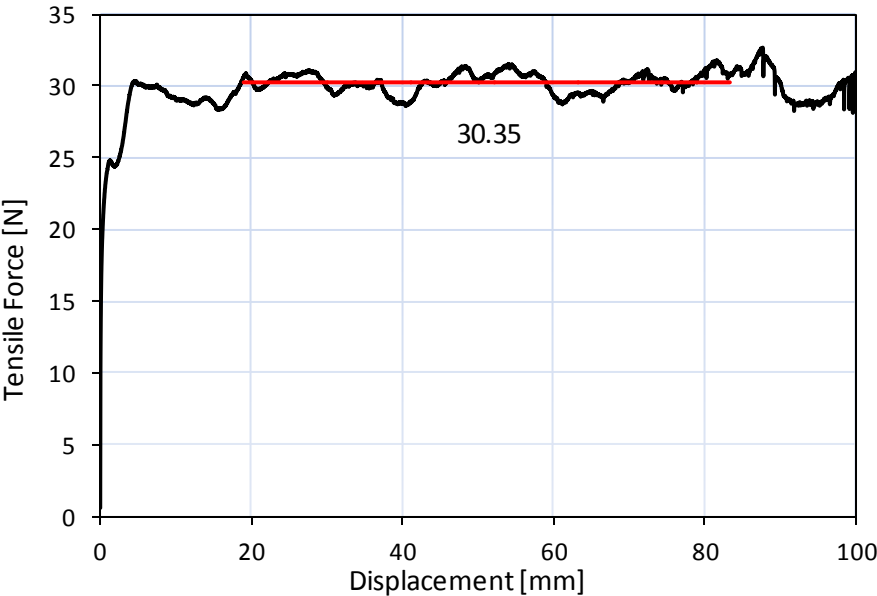


Figure 5-10 Measured tensile force-displacement curve for specimen prepared with 40/60 pen bitumen and L1 substrate with 0.25mm film thickness

**5.4.2 Influence of bitumen and aggregate in the dry condition**

The purpose of the peel test was to determine the fracture energy of the aggregate-bitumen bonds as a function of aggregate and bitumen type. Results are presented for four replicate tests performed on each aggregate-bitumen combination. The calculated average tensile force results of all specimens are shown in Table 5-2. The average force of each sample and the parameters described in Table 5-3 were entered into the Microsoft Excel macro IC Peel software to the calculate fracture energy. Table 5-4

shows three output parameters, which are fracture energy ( $G_c$ ), plastic work in bending ( $G_d$ ) and input energy ( $G_{tot}$ ), and their average values and test variability (standard deviation) of all specimens. The average values obtained for the energy associated with plastic bending in the peel arm ( $G_d$ ) were 465 J/m<sup>2</sup> and 331 J/m<sup>2</sup>, respectively for 40/60 pen bitumen and 70/100 pen bitumen. The standard deviation of fracture energy results suggest that the peel test has low variability (less than 10%) which compares quite well with the variability of  $\pm 9\%$  reported by Blackman et al. [5]. From Table 5-4, it can be seen that specimens prepared with the same bitumen have almost the same fracture energy in the dry condition, irrespective of which aggregate was used. The results suggest that in the dry state, cohesive failure controls the aggregate-bitumen bond and that the failure location is within the bitumen. These assertions agree with previous studies [8] related to dry aggregate-bitumen bonds. However, specimens prepared with B2 bitumen have significantly lower fracture energy than those with B1 bitumen. This is because B1 is stiffer than B2, so higher energy is needed to break it apart. This indicates that bitumen properties control the fracture energy in the dry condition.

Table 5-2 Tensile force results for all specimens in the dry condition

Bitumen	Aggregate	Tensile force (N)			
		1	2	3	4
B1 (40/60)	L1	29.8	26.9	28.2	30.4
	L2	29.0	29.5	29.0	27.1
	G1	30.6	28.7	30.4	28.7
	G2	33.3	27.7	28.5	28.5
B2 (70/100)	L1	15.4	15.3	15.4	14.6
	L2	14.6	17.4	14.9	13.8
	G1	16.3	13.9	15.1	15.4
	G2	16.2	14.3	16.4	15.3

Table 5-3 Relative parameters entered into the IC Peel software to calculate the fracture energy

Parameters	Quality
Young's modulus of the peel arm, $E$	69.0 GPa
Yield strain of the peel arm, $\epsilon_y$	0.044%
Bilinear parameter of the peel arm, $\alpha$	0.019
Thickness of the peel arm, $h$	0.2 mm
Width of the peel arm, $b$	20 mm
Thickness of adhesive layer, $h_a$	0.25 mm
Young's modulus of adhesive material, $E_a$	4.4 MPa for Ba bitumen
	3.8 MPa for B2 bitumen
Peel angle, $\theta$	90°

Table 5-4 Three output parameters of all specimens in the dry condition

Specimen	Energy (J/m <sup>2</sup> )	1	2	3	4	Average	SD
B1-L1	$G_c$	1020	898	953	1046	979	67.1
	$G_d$	470	447	458	474	462	12.1
	$G_{tot}$	1490	1345	1410	1520	1441	79.2
B1-L2	$G_c$	986	1008	986	906	972	44.8
	$G_d$	464	467	464	449	461	8.2
	$G_{tot}$	1450	1475	1450	1355	1433	53.0
B1-G1	$G_c$	1055	974	1046	974	1012	44.4
	$G_d$	476	461	474	461	468	7.7
	$G_{tot}$	1530	1435	1520	1435	1480	52.1
B1-G2	$G_c$	1171	931	965	965	1008	109.6
	$G_d$	494	454	460	460	467	18.5
	$G_{tot}$	1665	1385	1425	1425	1475	128.1
B2-L1	$G_c$	438	434	438	408	430	14.4
	$G_d$	332	331	332	322	329	4.9
	$G_{tot}$	770	765	770	730	759	19.3
B2-L2	$G_c$	408	476	457	416	439	32.5
	$G_d$	322	344	338	324	332	10.8
	$G_{tot}$	730	820	795	740	771	43.3
B2-G1	$G_c$	472	390	427	438	432	33.8
	$G_d$	343	315	328	332	330	11.5
	$G_{tot}$	815	705	755	770	761	45.3
B2-G2	$G_c$	468	397	476	434	444	36.0
	$G_d$	342	318	344	331	334	12.1
	$G_{tot}$	810	715	820	765	778	48.0

Note: B1 = 40/60 pen bitumen; B2 = 70/100 pen bitumen; L1 = limestone a; G1= granite 1; L2 = limestone 2; G2 = granite 2; SD = standard deviation.  $G_c$  = fracture energy (J/m<sup>2</sup>),  $G_d$  = plastic work in bending (J/m<sup>2</sup>), and  $G_{tot}$  = input energy (J/m<sup>2</sup>).

### 5.4.3 Influence of film thickness

With the purpose of characterising the influence of film thickness on fracture energy, the Peel Test was carried out with two bitumen types and L1 substrates with thicknesses from 0.2 mm to 0.9 mm in five steps: 0.2 mm, 0.25 mm, 0.38 mm, 0.5 mm, and 0.9 mm. The selection of one type of substrate is because the aggregate cannot influence the fracture energy as cohesive failure occurred in the dry condition. Figure 5-11 illustrates the change in fracture energy due to the increase of film thickness with the original fracture energy values showing in Appendix A. As the bitumen film thickness was increased, the fracture energy of these two types of bitumen experienced a steady increase as more energy was dissipated in the bulk of the bitumen binder. This could be attributed to the increased viscous flow of the base bitumen as the bitumen film becomes thicker. Furthermore, large differences in the magnitude of fracture energy were shown between these two types of bitumen. The fracture energy for B1 bitumen (40/60 pen) exceeded that of the B2 bitumen (70/100 pen) for every film thickness.

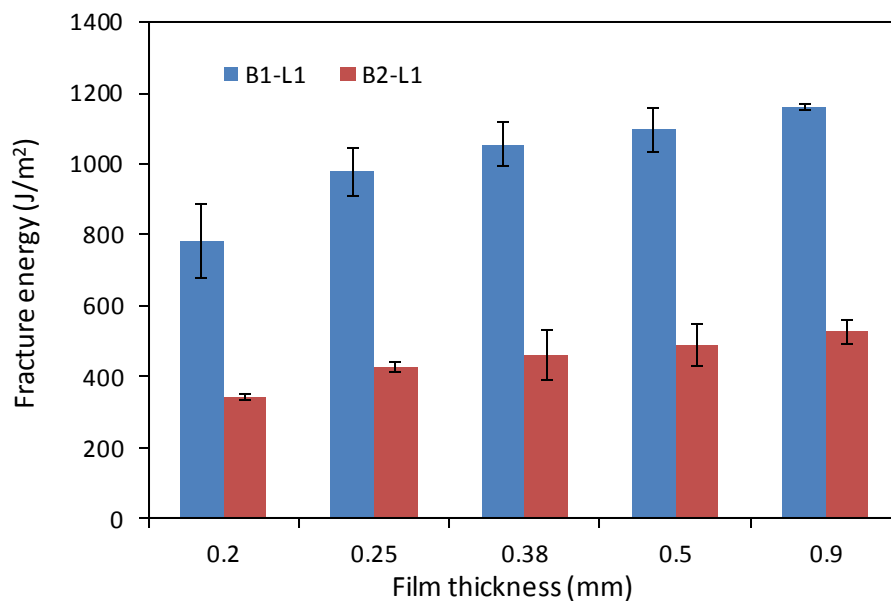


Figure 5-11 Fracture energy of bitumen-limestone specimens at different film thicknesses

If the fracture energy is divided by its film thickness, it gives the normalised toughness of each specimen. According to previous researchers [9], the normalised toughness is a better characterisation parameter than the energy per unit area for ductile thin films,

since there is no clearly defined area of fracture surface created in the ductile failure process [10]. Figure 5-11 presents the relationship between normalised toughness and film thickness. It was illustrated that the normalised toughness of these two types of bitumen decreased when the film thickness increased from 0.2 mm to 0.9 mm. In this film thickness region, the normalised toughness decreases with bitumen film thickness in a power law relationship. Fitting of the experimental data with a linear function produced coefficients of determination ( $R^2$ ) of 0.8741 and 0.8655 for the B1 bitumen and B2 bitumen, respectively. It can be seen that less energy was needed to fracture bitumen of unit volume when the film thickness increases from 0.2 mm to 0.9 mm.

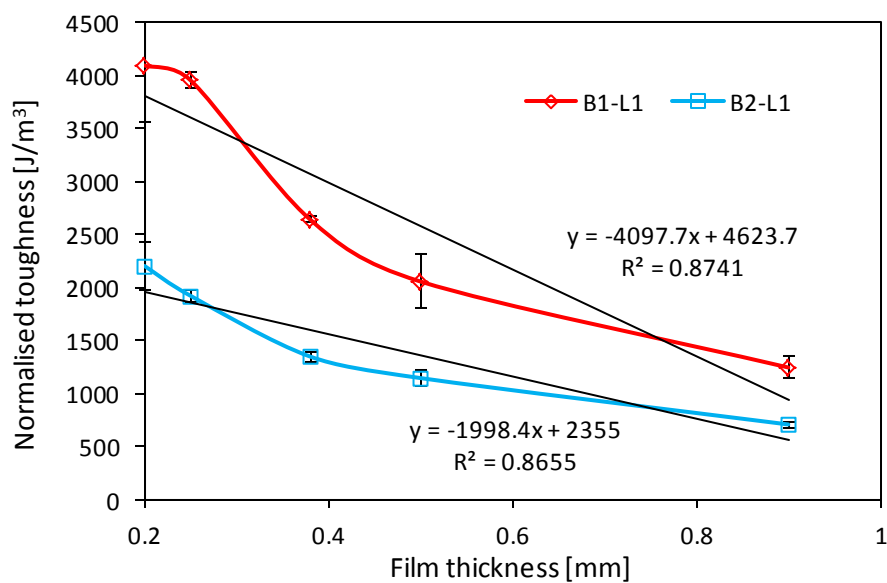


Figure 5-12 Relationship between normalised toughness and film thickness of bitumen

#### 5.4.4 Influence of moisture damage

To simulate the effect of moisture on the adhesion properties between bitumen and aggregate, the whole specimens were submersed in water at 20 °C for 7 days and 14 days. During the moisture conditioning stage, moisture could reach the aggregate-bitumen interface in three different ways: through the top and bottom aggregate, through the edge of the aggregate-bitumen interface and through the bitumen film. After moisture conditioning, specimens were removed from the water bath and then subjected to the peel test within a few hours. This conditioning method was considered to closely simulate the effect of moisture in an asphalt mixture.

In order to analyse the influence of bitumen on moisture damage for the same aggregate, the retained fracture energy of specimens after 7 days and 14 days moisture conditioning were calculated by dividing the conditioned fracture energy by the dry fracture energy, and the results are shown in Figure 5-13. The fracture energy values of all specimens after moisture conditioning are shown in Appendix B. After moisture conditioning, most of the specimens experienced a decrease in fracture energy, except for B1-L2 after 7 days conditioning. However, the specimens showed different fracture energy losses due to their different aggregate-bitumen combinations. For example, fracture energy losses in the samples containing G1 and L2 were the lowest for both bitumen types. The specimens prepared with G2 showed the highest fracture energy losses after moisture conditioning. It can be seen that, for the four aggregates used in this research, specimens containing the B1 bitumen showed slight higher percent retained fracture energy than those containing B2 bitumen. So, it can be concluded that the 40/60 pen bitumen used in this research has slightly better moisture durability in comparison with the 70/100 pen bitumen, based on the peel test. However, based on the results shown in Figures 5-13, it appears that the effect of bitumen on moisture sensitivity of aggregate-bitumen mixtures is minimal compared to the aggregate effects.

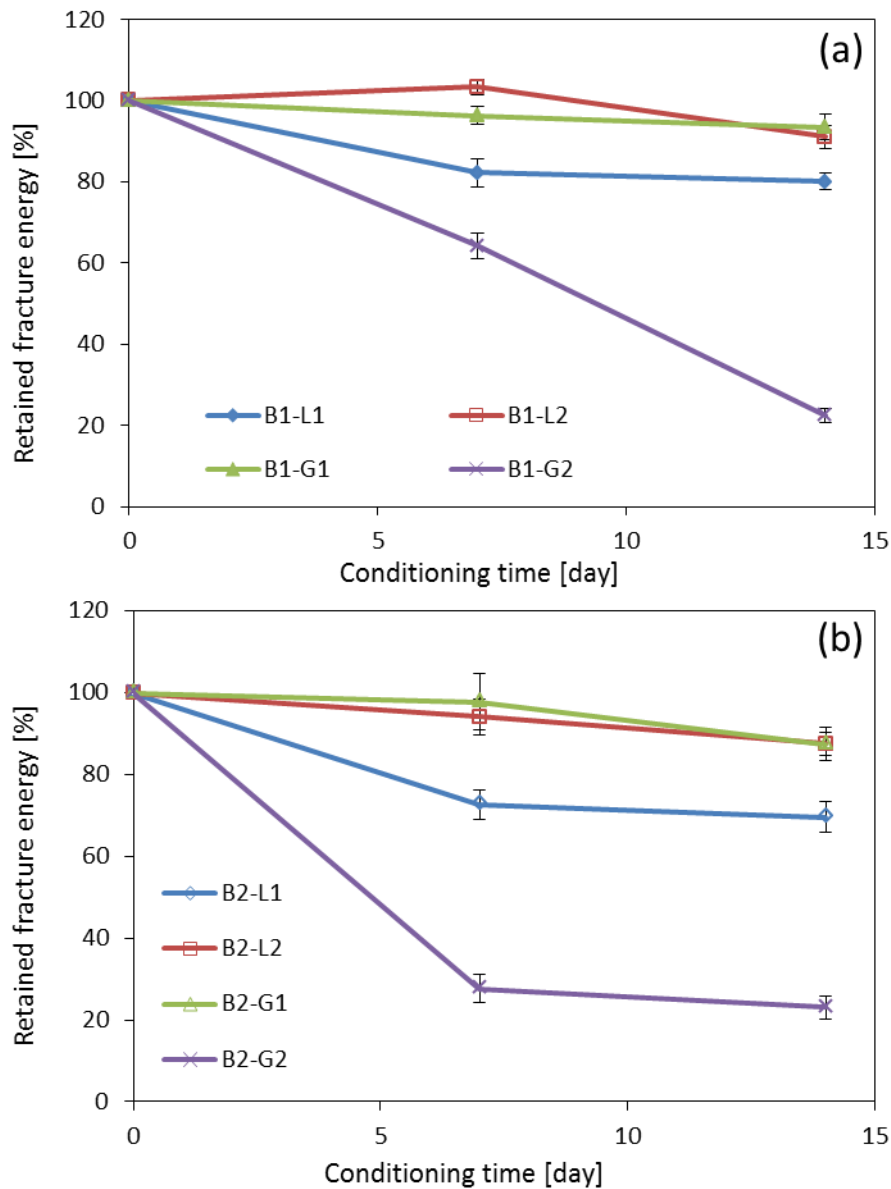


Figure 5-13 Effect of moisture conditioning time on retained fracture energy of different aggregate-bitumen combinations. (a) bitumen B1, (b) bitumen B2.

The failure surfaces of samples prepared with the four aggregate substrates (L1, L2, G1 and G2) and B1 bitumen before and after moisture condition are shown in Figure 5-14. Because B1 and B2 bitumen shown similar failure surface mode, only samples prepared with B1 bitumen were chosen to be analysed. Without moisture conditioning, all these four samples achieved cohesive failure within the bulk of the bitumen. That is why all aggregates show almost the same fracture energy in the dry condition. After moisture condition, the water could penetrate into the specimen and weaken the aggregate-bitumen interface. However, the four aggregates presented in Figure 5-14 show

different failure surfaces. Aggregates L2 and G1 have shown almost 100% cohesive failure even after 14 days moisture conditioning. The L1 aggregate results in an adhesive-cohesive mixed failure with a portion of bitumen still attached with aggregate. For G2 bitumen, adhesive failure occurred. The failure surfaces of these four aggregates could also be correlated with the retained fracture energy as shown in Figure 5-13(a). The cohesive failure surface for L2 and G1 aggregates correlate with the highest retained fracture energy. While the adhesive failure surface for G2 aggregate correlates with the lowest retained fracture energy.

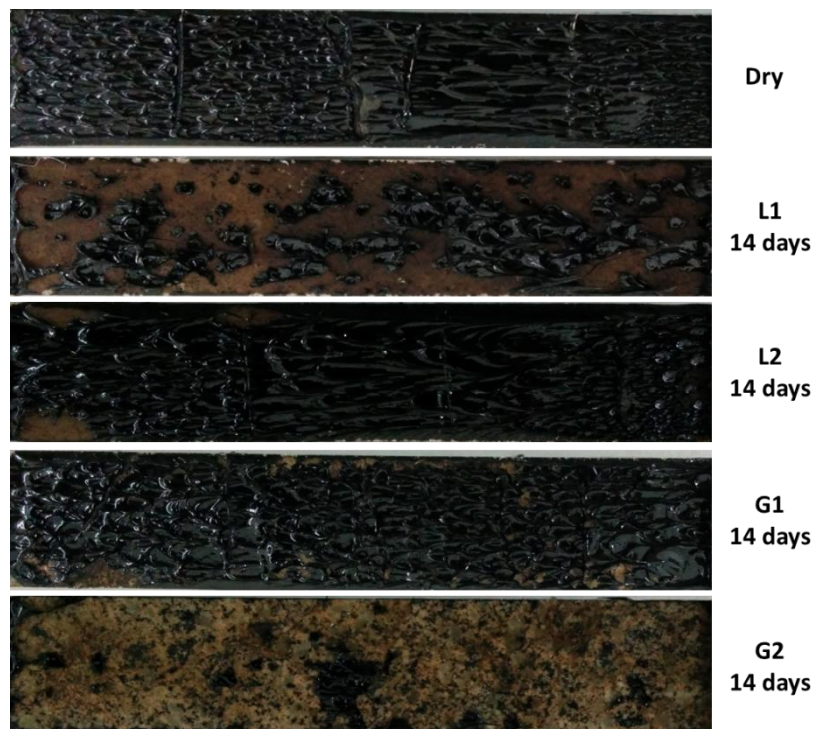


Figure 5-14 Failure surfaces of sample prepared with B1 bitumen in dry and after 14 days moisture condition

The results presented in Figure 5-13 show that the G1 and L2 aggregates have the highest retained fracture energy, with around 90% retained fracture energy after 14 days moisture conditioning. L1 aggregate has the middle retained fracture energy, with about 80% retained fracture energy for B1 bitumen compared with 70% for B2 bitumen. The lowest result belongs to G2 aggregate, with only 23% of fracture energy being retained after moisture conditioning for both types of bitumen.

The differences in moisture durability could be attributed to the mineral composition and water absorption of aggregates. As previously discussed in Chapter 3, there is a

strong correlation between certain aggregate minerals and aggregate moisture absorption. On this basis alone, it should be expected that degradation of bond strength in the presence of moisture should also be correlated to aggregate mineralogy. In an attempt to establish such a relationship, regression analysis was performed by using the retained fracture energy data (B1 bitumen 14 days) presented in Figure 5-13 and the mineralogical data presented in Figure 3-1. The regression followed the detailed procedure as shown in Chapter 3 and the obtained regression equation and relative parameters are shown in Equation 5-28.

The results support the assertion that moisture sensitivity of aggregate-bitumen bonds are influenced mainly by the aggregate mineralogy. The model in Equation 5-28 also shows the detrimental effects of certain minerals such as dolomite, clay and anorthite on moisture susceptibility. The signs of the model parameters in Equation 5-28 are revealing. For example, calcite and chlorite carry a positive signs suggesting positive correlation between mineral composition and moisture resistance. The results agree with general experience [11, 12]. Other minerals carry negative signs, this suggests these minerals are negatively correlated with moisture resistance and thus have detrimental effects on moisture damage resistance of asphalt mixtures. Previous studies like Horgnies et al. have identified albite, quartz, and k-feldspar as minerals with a detrimental effect on aggregate-bitumen bond [8]. The results of the current study provide evidence for extending the list of detrimental aggregate minerals to include dolomite, clay and anorthite as well as supporting the case of considering calcite as a moisture resistant mineral.

$$\begin{aligned}
 RS = & -0.143 + 0.929 * \textit{Calcite} - 4.230 * \textit{Dolomite} - 3.875 * \textit{Clay} - 1.670 * \\
 & \textit{Quartz} - 0.052 * \textit{Albite} - 0.173 * \textit{Anorthite} - 0.044 * \textit{Kfeldspar} + 4.025 * \\
 & \textit{Chlorite}
 \end{aligned}
 \tag{5-28}$$

where *RS* is the predicted retained fracture energy at 14 days (%); calcite is the amount of calcite mineral mass (%); dolomite is the amount of dolomite mineral mass (%); clay is the amount of clay minerals (%); quartz is the amount of quartz (%); albite is the amount of albite (%); anorthite is the amount of anorthite (%); kfeldspar is the amount of k-feldspar (%) and chlorite is the amount of chlorite (%).

## 5.5 Conclusions

This chapter focused on the fracture energy evaluation of aggregate-bitumen bonds using the peel test. A detailed introduction of the sample preparation and the ICPeel software utilisation were first presented. Several factors, such as bitumen hardness (penetration), mineralogical properties of aggregates, film thickness, and moisture conditioning were considered in this chapter to analyse their influence on the fracture energy of aggregate-bitumen bonds. The following major findings can be taken from this chapter.

The surface properties of aggregate cannot influence the fracture energies of specimens due to the cohesive failure regime experienced with the test at a temperature of 20 °C and a displacement rate of 10 mm/min under dry conditions. However, bitumen type dominates the magnitude of the fracture energy with stiffer bitumen resulting in a higher fracture energy value.

As film thickness increases, the fracture energy of the two types of bitumen experienced a steady increase. However, the normalized toughness decreased with increasing film thickness. Since the fracture energy and normalised toughness show film thickness dependency, it is of great importance to prepare specimens in which the bitumen film mirrors the bitumen film thickness of asphalt mixtures as closely as possible.

After moisture conditioning, most of the specimens experienced a decrease in fracture energy. Based on the materials considered, changing the binder grade from 40/60 pen to 70/100 pen produced a decrease in moisture durability for most aggregates. Strong correlations were also found between mineral compositions and moisture sensitivity with dolomite, clay and quartz having strong negative influence while calcite and chlorite showed positive effect on moisture sensitivity. Previous studies have identified various mineral phases like albite, quartz, and k-feldspar, as detrimental in terms of moisture sensitivity. The current study extended this list of detrimental aggregate minerals to include dolomite, clay and anorthite while supporting the case of calcite and chlorite as moisture resistant minerals.

## References

1. Airey G.D. and Choi Y.K. State of the Art Report on Moisture Sensitivity Test Methods for Bituminous Pavement Materials. *Road Materials and Pavement Design*, 2002, 3(4): 355-372.
2. Liu Y. Apeageyi A K, Ahmad N, Grenfell J and Airey G D. Examination of moisture sensitivity of aggregate–bitumen bonding strength using loose asphalt mixture and physico-chemical surface energy property tests. *International Journal of Pavement Engineering*, 2014, 15(7): 657-670.
3. BS7991. Determination of the mode I adhesive fracture energy,  $G_{IC}$ , of structural adhesives using the double cantilever beam (DCB) and tapered double cantilever beam (TDCB) specimens, BSI: London 2001.
4. Kinloch A.J., Lau C.C. and Williams J.G. The peeling of flexible laminates, *International Journal of Fracture*, 66: 45-70, 1994.
5. Blackman B.R.K., Cui S., Kinloch A.J. and Taylor A.C. The development of a novel test method to assess the durability of asphalt road-pavement materials. *International Journal of Adhesion and Adhesives*, 2013; 42: 1-10.
6. Ahmad N., Cui S., Blackman B.R.K., Taylor A.C., Kinloch A.J. and Airey G.D. Predicting Moisture Damage Performance of Asphalt Mixtures. Nottingham Transportation Engineering Centre Report, 2011, Report Number: 11091.
7. IC Peel software, <http://www3.imperial.ac.uk/meadhesion/testprotocols/peel>, Imperial College London. Accessed 14 March 2013.
8. Apeageyi A.K., Grenfell J.R.A. and Airey G.D. Moisture-induced strength degradation of aggregate–asphalt mastic bonds. *Road Materials and Pavement Design*, 2014, 15(1): 239-262.
9. Portillo O. Fracture mechanics of bitumen and asphalt mixes. PhD dissertation, Cambridge University, 2009.

10. Harvey J.A.F. and Cebon D. Failure Mechanism in Viscoelastic Films. *Journal of Materials Science*, 2003, 38: 1021-1032.
11. Airey G.D., Collop A.C., Zoorob S.E. and Elliott R.C. The influence of aggregate, filler and bitumen on asphalt mixture moisture damage. *Construction and Building Materials*, 2008, 22(9): 2015-2024.
12. Grenfell J., Ahmad N., Liu Y., Apegyei A.K., Large D. and Airey G.D. Assessing asphalt mixture moisture susceptibility through intrinsic adhesion, bitumen stripping and mechanical damage. *Road Materials and Pavement Design*, 2014, 15(1): 131-152.

# **6. Tensile strength - PATTI test and Pull-off test**

## **6.1 Introduction**

As presented in Chapter 5, fracture energy was used to characterise the adhesive/cohesive property of the aggregate-bitumen interface. This parameter represents the energy required to open a unit area of crack surface and proved to be sensitive to aggregate-bitumen bonding before and after moisture damage. Apart from this, there is another parameter named tensile strength that could also be used to evaluate the aggregate-bitumen bonding under different conditions. The tensile strength is defined as the maximum stress that a material can withstand while being stretched or pulled before failing or breaking.

Two established tests, namely the Pneumatic Adhesion Tensile Testing Instrument (PATTI) test and the pull-off test were used in this section to evaluate the tensile strength of aggregate-bitumen bonding. By performing the tensile strength tests under different conditions, these two methods were modified based on the experimental facilities in the Nottingham Transportation Engineering Centre (NTEC).

The objectives of this chapter are to evaluate the tensile strength of aggregate-bitumen bonds due to the influence of different conditions, such as temperature and moisture damage. The influence of each factor is determined by analysing available test results statistically. The results achieved from this chapter will also be compared with other bench mark results to evaluate the reliability and feasibility of these two modified tensile strength tests.

## **6.2 Pneumatic Adhesion Tensile Testing Instrument (PATTI) test**

The Pneumatic Adhesion Tensile Testing Instrument (PATTI) test was first developed by the National Institute of Standards and Technology (NIST) as a standard method

(ASTM D4541) used for paints and coatings [1]. Towards the end of the 1990s, this portable method attracted research attention to evaluate the mechanical strength of aggregate-bitumen adhesive joints [2]. Since then, the PATTI test has been used by many researchers for evaluating the adhesion of asphalt materials and the moisture susceptibility of asphalt binders [3, 4].

The specimen used for the PATTI test is assembled by using an aggregate substrate and a steel pull-stub using bitumen as the adhesive. Aggregate plates were first prepared by wet cutting stone boulders using a diamond-edged blade saw. The slices were then sand paper (P800, 21.8  $\mu\text{m}$ ) ground to make sure the surface is flat. Then, the ground slices were cleaned using distilled water and dried at room temperature for at least 24 hours. In order to get a well bonded specimen, the aggregate surface and the pull-stub should be wiped carefully using a damp paper towel to remove any dust. After that, the aggregate and pull-stub are placed in an oven and heated to a temperature of 70  $^{\circ}\text{C}$  for one hour. The bitumen must be heated to 150  $^{\circ}\text{C}$  for 1 hour to allow it to be fluid enough to coat the aggregate plate. The liquid bitumen is then poured onto a prepared aggregate plate (with dimensions of 100 mm  $\times$  100 mm  $\times$  20 mm) which is pressed immediately by a metal pull-stub to establish a good aggregate-bitumen bond. In this process the film thickness of bitumen was controlled by four raised edges on the pull-stub to make sure all specimens have a 0.8 mm bitumen film thickness, as shown in Figure 6-1(a). Finally, the excess bitumen at the edge of the pull-stub should be removed by using a heated palette knife. The prepared specimen for PATTI test is shown in Figure 6-1(b).

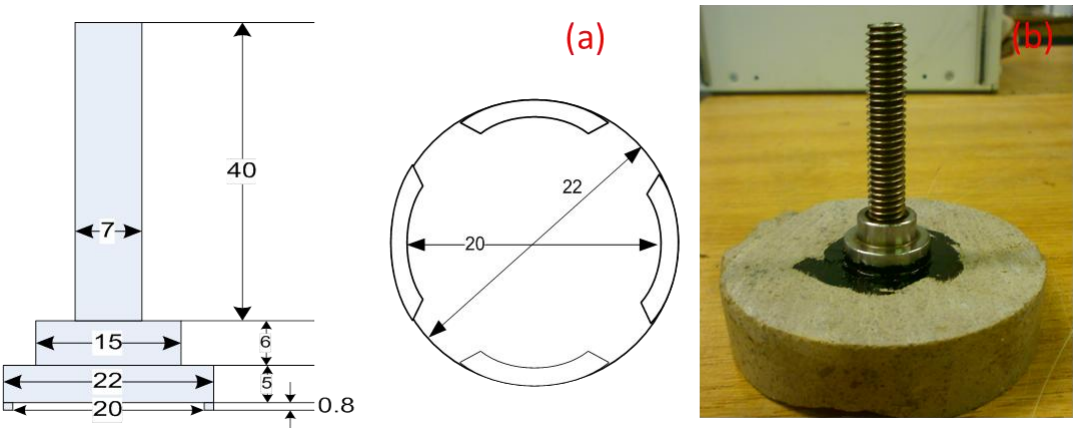


Figure 6-1 Pull-stub in profile and bottom views (a) and the prepared specimen (b)

The PATTI equipment used in this research is made up of four main parts, which are the pressure release part, analysis software, piston and reaction plate, and camera, as shown in Figure 6-2. Figure 6-3 shows a cross-sectional schematic of the setup of the PATTI with the piston attached to a pull-stub which in turn is attached by means of the bitumen coating to the aggregate substrate. During testing, a constant air pressure generated from the CO<sub>2</sub> pressure tank is transmitted to the piston which is placed over the pull stub and screwed onto the reaction plate. It should be mentioned that the speed of air release is controlled manually. The air pressure induces an airtight seal formed between the piston gasket and the aggregate surface. A constant rate of pulling pressure, which is set in the pressure control panel, is applied to the bonded specimen. The test generates data in the form of tensile pressure versus testing time which is recorded by the data acquisition system. After the test, the failure surface of the specimen can be recorded by using the camera to distinguish between cohesive and adhesive failure. The maximum tensile pressure to separate the bitumen from the substrate is captured by the software. This pressure is then converted to its pull-off tensile strength, as expressed in the following equation:

$$POTS = \frac{(BP \times A_g) - C}{A_{ps}} \quad (6-1)$$

where, *POTS* is the pull-off tensile strength (kPa), *BP* is air pressure (kPa), *A<sub>g</sub>* is the contact area of gasket with the reaction plate (mm<sup>2</sup>), *C* is the piston constant and *A<sub>ps</sub>* is the area of pull-stub (mm<sup>2</sup>).

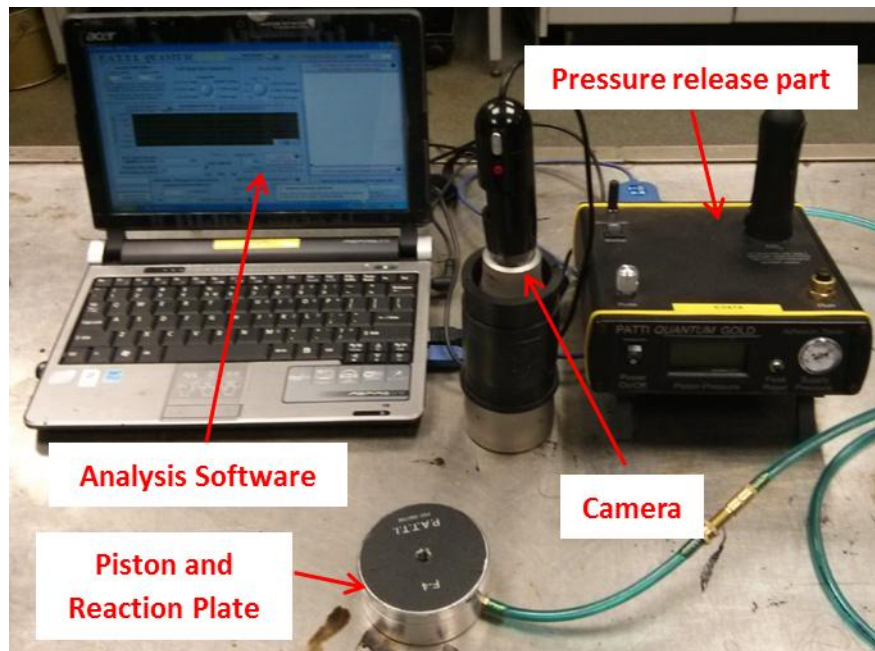


Figure 6-2 Equipment associated with PATTI test

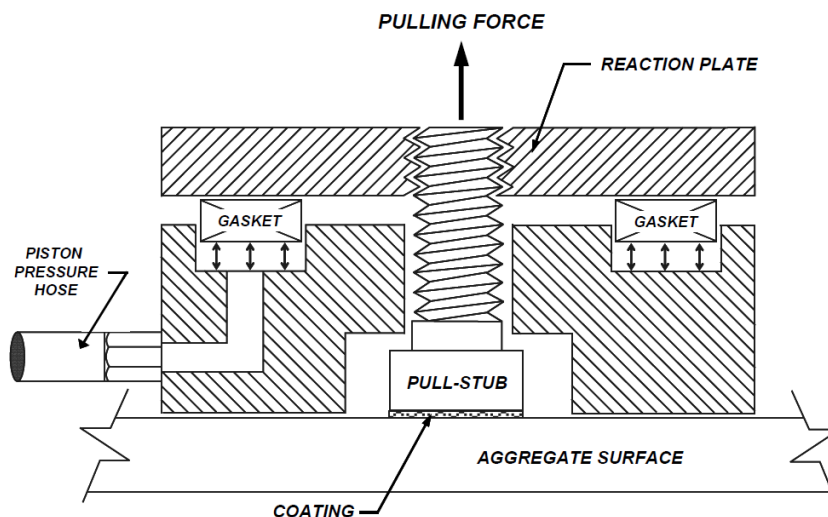


Figure 6-3 Cross-section view of piston attached to pull-stub [5]

As a portable adhesion tester, the PATTI equipment has no temperature control system to maintain the specimen temperature during testing. So, the testing temperature is usually the environmental temperature when testing is performed. Because bitumen is a visco-elastic material, its properties are very sensitive to the temperature change. When performing the PATTI test without strict temperature control, the variation of temperature may influence the tensile strength values and mislead the final conclusion.

In this research, the PATTI equipment and an environmental chamber were assembled together to evaluate the tensile strength under well controlled temperatures, as shown in

Figure 6-4. The reaction plate was placed inside the environmental chamber connected with the pressure release unit by placing the pressure air pipe through a hole with the diameter of 50 mm placed on the broadside of the environmental chamber. A rubber plug with the same dimensions as the hole was used to block the hole to maintain the inside temperature. The environmental chamber could accurately control the temperature in the range of  $-10\text{ }^{\circ}\text{C}$  -  $40\text{ }^{\circ}\text{C}$  with the precision of  $\pm 0.1\text{ }^{\circ}\text{C}$ . Specimens were first conditioned in the environmental chamber for 3 hours at the test temperature to get a homogeneous temperature distribution. Before testing, one conditioned specimen was installed on the piston and reaction plate followed by 1 hour of conditioning. During testing, the PATTI equipment was controlled from outside of the chamber to release a constant rate of pulling pressure to detach the specimen and record the maximum tensile pressure.

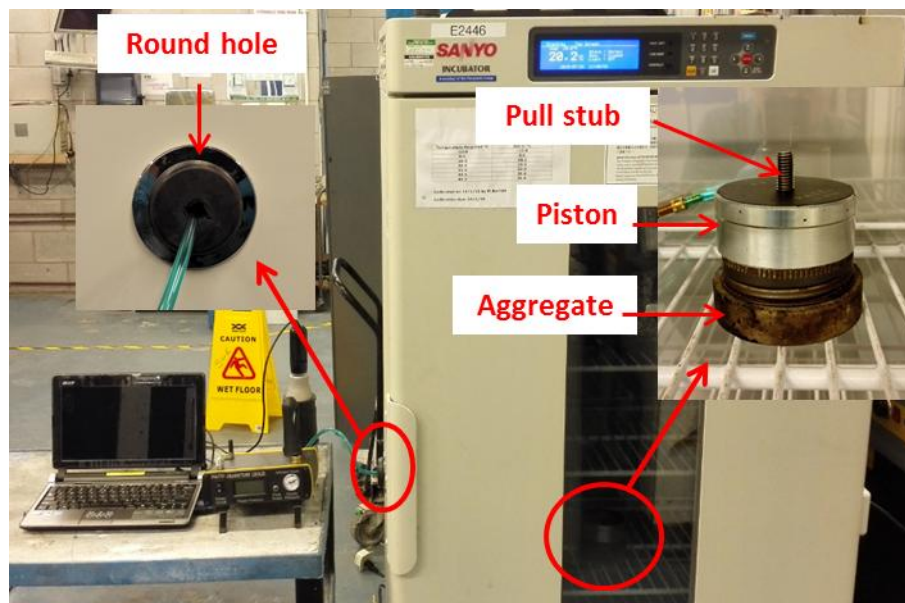


Figure 6-4 The PATTI equipment connected with environmental chamber to control temperature

### 6.3 Pull-off test

An adhesion evaluation method based on the pull-off test is considered to be a simple, practical and reliable approach in characterising the bond strength between the adhesive materials and the substrate, especially in terms of the procedures for specimen preparation and testing. In pavement engineering research, the pull-off test is usually

conducted to evaluate the tensile strength necessary to detach the aggregate-bitumen bonds under different conditions. According to previous research, the size of contact area and the thickness of adhesive materials affect the adhesive bond strength based on the pull-off test [6]. The contact area of the adhesive material is very easy to control by changing the diameter of the substrates. However, the thickness of the adhesive material is difficult to control. By specifying the film thickness of bitumen, the volume-density calculation method was performed to convert the film thickness to bitumen weight [7]. The film thickness could also be controlled by using the thickness of a metal block or spacers [4]. Though these methods theoretically control the film thickness, their shortcomings should not be neglected. For the volume-density calculation method, it is inevitable that there is a small amount of bitumen released out so that influences the thickness. Furthermore, by pouring the bitumen onto substrates, there is no guarantee that the bitumen and substrates can achieve full coating. In terms of the block or spacer method, it seems very difficult to control the film thickness to a very thin level.

This research presents the development of a new pull-off test. The innovation of this test is the ability to accurately control bitumen film thickness using a modified dynamic shear rheometer. The test uses small aggregate substrates that permit realistic moisture conditioning and simplified custom-made direct tension fixtures that can be easily mounted on an Instron universal testing machine. The pull-off test set-up has been successfully used in the past to evaluate aggregate-bitumen mastic bonds [8]. The test set-up consists of three main parts: a moisture conditioning step designed to ensure characteristic moisture diffusion into the aggregate-bitumen interface, accurate determination of bitumen film thickness using a modified dynamic shear rheometer and direct tension fixtures mounted on an Instron universal testing machine. The capability to vary loading rate, accurately control film thickness and ensure moisture diffusion to the aggregate-bitumen interface are an important improvement over most existing pull-off tests.

Figure 6-5 shows the whole procedure in terms of sample preparation and pull-off test. For sample preparation, boulders of each aggregate were first drilled using a coring tool to get aggregate cylinders with 25 mm diameter. A trimming saw was used to cut the aggregate cylinders into discs with 5mm thickness. To obtain a relatively constant

surface roughness, both surfaces of the aggregate discs were polished using a rotary polishing machine with the fine sand paper (P4000, 5  $\mu\text{m}$ ). All discs were cleaned in an ultrasound cleaning machine for 15min and dried in an oven at a temperature of 40  $^{\circ}\text{C}$  for 24 hours. The finished polished aggregate substrate is shown in Figure 6-5A.

Two aluminum specimen holding plates (Figure 6-5B) were specially designed and fabricated to fit in a standard DSR (Gemini DSR). The plates had dimensions (diameter and thickness) which were similar to a DSR. They differ from a DSR top and bottom plate in terms of the provision of sample holders (2 mm tall rings with 3 screen pins, Figure 6-5B).

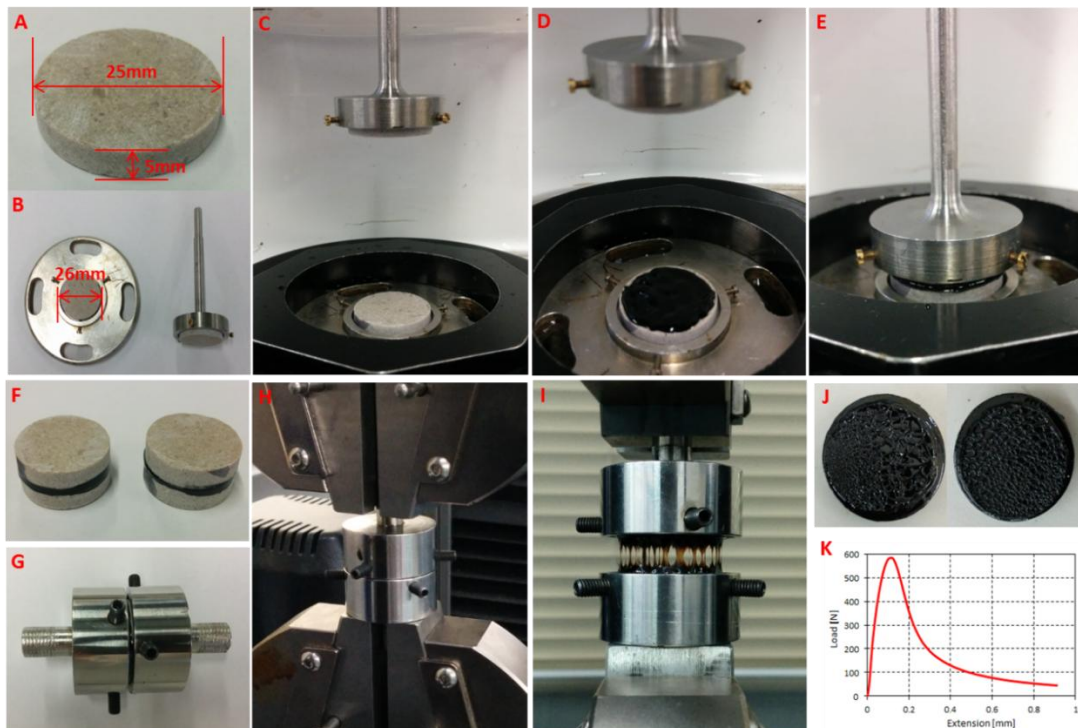


Figure 6-5 Sample preparation and pull off test procedures

With a view to precisely controlling the film thickness of the bitumen, two modified fixtures were designed to clamp the discs (Figure 6-5B) and then fixed into the DSR machine (Figure 6-5C). Firstly, the gap between the upper and lower surfaces should be set to zero and these two surfaces should be parallel. After establishing the zero gap and ensuring that the discs are parallel, a small amount of hot bitumen was placed on the lower aggregate surface (Figure 6-5D) and then pressed with the upper aggregate to achieve the required bitumen film thickness (Figure 6-5E), with a gap resolution of 1  $\mu\text{m}$ . In order to simulate the real bitumen film thickness in asphalt mixtures, the bitumen

film thickness was controlled at 20  $\mu\text{m}$ . The sample was removed from the DSR after about 15 minutes of cooling and then the excess asphalt binder removed by means of a heated pallet knife, as shown in Figure 6-5F.

Before the pull off test, the prepared sample was first fixed to two direct tension fixtures with three screws on each, as shown in Figure 6-5G. These two fixtures were then installed on the Instron machine (Figure 6-5H). During the test, an extension speed of 10 mm/min and a temperature of 20  $^{\circ}\text{C}$  were applied to break the interface (Figure 6-5I). After testing, the failure surfaces of each sample were photographed with a camera (Figure 6-5J) and the pull force was recorded by the Instron machine (Figure 6-5K). At least four repeat tests were made for each aggregate-bitumen combination. The results were used to calculate the tensile strength. Tensile strength was computed as the ratio of the peak load divided by the cross-sectional area of the bitumen film, as shown in Equation 6-2:

$$TS = \frac{F}{\pi r^2} \quad (6-2)$$

where  $TS$  is tensile strength (Pa),  $F$  is the peak tensile force (N) and  $r$  is the radius of aggregate disc (m).

## **6.4 Results for PATTI test**

### **6.4.1 PATTI cohesive and adhesive bond strength measurements in dry condition**

In order to characterise the influence of temperature on the bond strength, the PATTI test was performed at six temperatures from -10  $^{\circ}\text{C}$  to 40  $^{\circ}\text{C}$  at 10  $^{\circ}\text{C}$  intervals. Samples and the reaction plate were conditioned in an environmental chamber for 3 hours to get a homogeneous temperature distribution. During the test, a constant rate of air pressure was applied to get repeatable results. Less than 40 seconds was needed to complete one test.

#### 6.4.1.1 Influence of temperature and bitumen type

Figure 6-6 shows examples of the applied pressure (tensile strength) versus time at different temperatures for samples prepared with B1 (40/60 pen) bitumen and G1 substrate. It can be seen that the increase of applied pressure versus time at different temperatures is almost identical, confirming the successful application of a constant rate of pulling pressure for these tests. The specimen response is characterised by the linear increase in pressure (tensile stress) until the pressure exceeds the cohesive strength of the bitumen or the adhesive strength of the aggregate-bitumen system and suddenly decreases to zero. Failure can be taken to occur at the peak pressure (tensile stress) and is defined as the pull-off tensile strength.

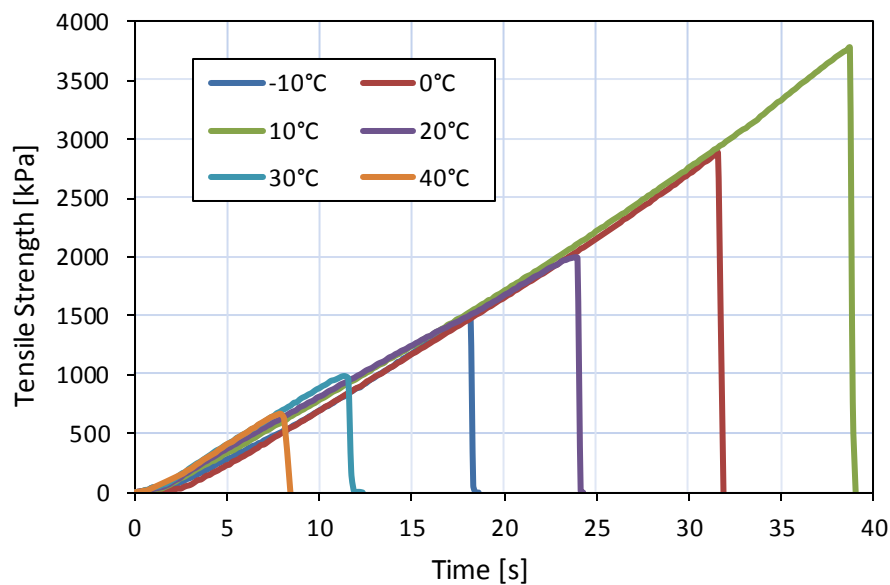


Figure 6-6 PATTI tensile strength versus loading time (B1 + G1).

Four tests (similar to those shown in Figure 6-6) were performed for two bitumens with G1 and L1 substrates at each temperature and the average tensile strength versus temperature curves, as well as the error bars which represent the standard deviation of the original data, are shown in Figure 6-7. From this figure it can be seen that in the temperature range from -10 °C to 10 °C, the tensile strength of all four combinations of bitumen and aggregates shows an increasing trend from between 1500 kPa and 2500 kPa to between 2500 kPa and 3500 kPa. However, as the temperature exceeds 10 °C, all the specimens experienced a steady decline in terms of tensile strength with values dropping to only about 500 kPa at 40 °C. It should be pointed out that the lowest

temperature does not correspond to the highest tensile strength. This phenomenon is in agreement with the relationship found for tensile strength versus bitumen stiffness modulus as shown in Figure 6-8 [9]. The tensile strength in Figure 6-8 was achieved from direct tension tests with a speed of 50 mm/min using cylindrical samples. These results show an equivalent behaviour where very high stiffness modulus (low temperatures) results in lower tensile strength [10].

As expected based on previous studies [11], samples prepared with B1 (40/60 pen) bitumen have a higher tensile strength than those prepared with B2 (70/100 pen) bitumen from 0 °C to 40 °C. It can therefore be concluded that bitumen with low penetration and high softening point can develop a stronger bond with aggregate under dry conditions.

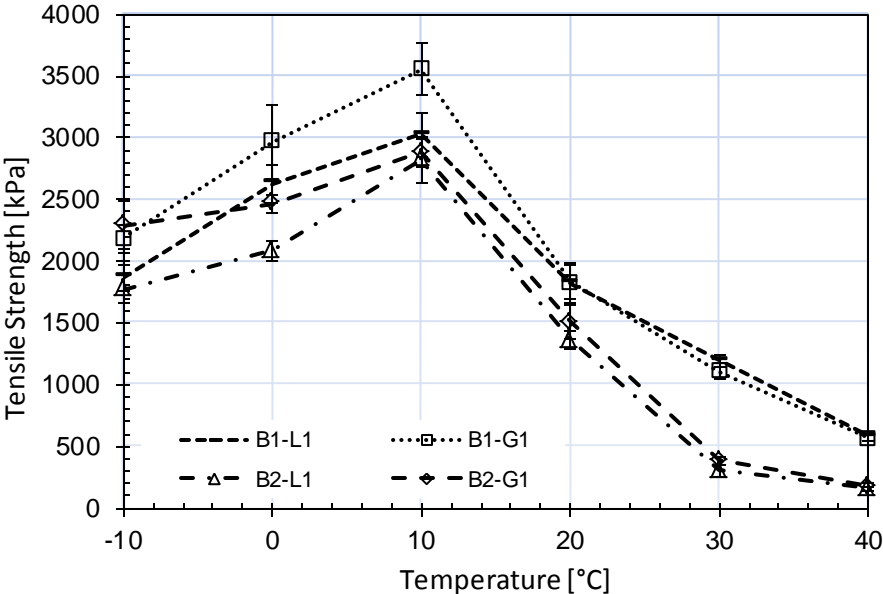


Figure 6-7 PATTI tensile strengths from PATTI test at different temperatures

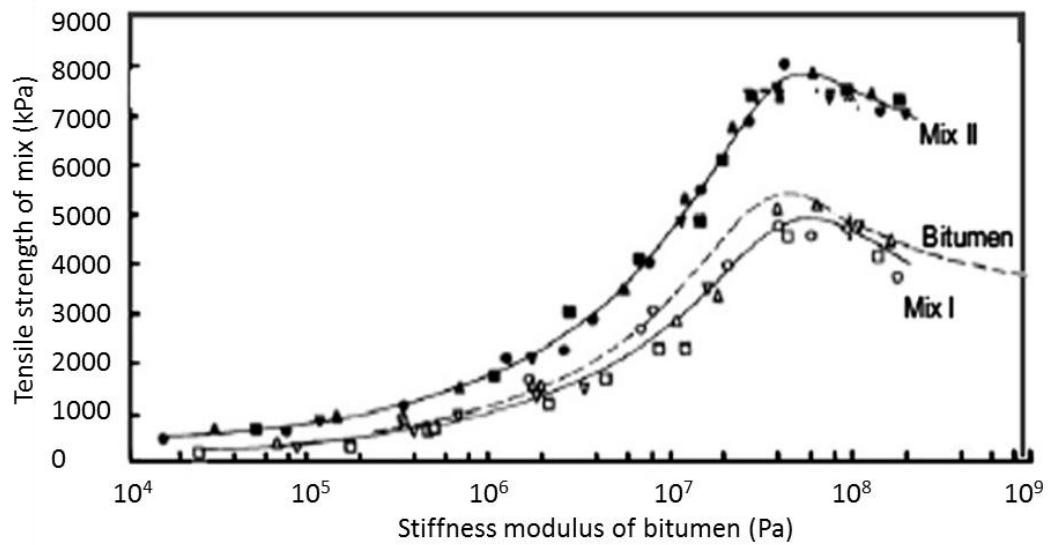


Figure 6-8 Bitumen tensile strength versus stiffness modulus reported by Heukelom and Wijga [9].

#### 6.4.1.2 Influence of Aggregate Type

In the temperature range from  $-10\text{ }^{\circ}\text{C}$  to  $10\text{ }^{\circ}\text{C}$ , as shown in Figure 6-7, tensile strengths for B1-G1 combination are over 10% higher when compared with those prepared with L1 aggregate. For B2 (70/100 pen) bitumen, this phenomenon only occurred at  $-10\text{ }^{\circ}\text{C}$  and  $0\text{ }^{\circ}\text{C}$  due to the lower brittle to ductile transition temperature associated with the softer bitumen. A digital image of the failure surfaces at the end of the PATTI test were captured using the equipment's integrated camera for all the aggregate-bitumen combinations at all six test temperatures. Images of the failure pattern for the B1 (40/60 pen) bitumen with G1 substrate are shown in Figure 6-9. The specimens prepared with B2 (70/100 pen) bitumen show similar failure surfaces, so only failure surfaces of B1 bitumen were selected for analysis. From Figure 6-9 (a-c) it can be seen that failure surfaces from  $-10\text{ }^{\circ}\text{C}$  to  $10\text{ }^{\circ}\text{C}$  exhibit cohesive-adhesive mix mode failure with the red areas are recognised as the adhesive failure.

Based on the photographs obtained, the adhesive proportions of the specimens were analysed by the Image-J software. The percentage of adhesive section of each specimen was calculated by identifying the grayscale with results being 30% for  $-10\text{ }^{\circ}\text{C}$ , 23% for  $0\text{ }^{\circ}\text{C}$  and 18% for  $10\text{ }^{\circ}\text{C}$ . This implies that the cohesive strength of bitumen is stronger

than the adhesive strength of the aggregate-bitumen interface. It also means that the tensile strength when adhesive failure occurs is influenced by the mineral properties of the aggregate. As G1 contains more Si and Al, which can form strong chemical bonds with carboxylic acids and sulfoxides in bitumen under dry conditions, the tensile strengths for the two granite-bitumen combinations were greater than the two limestone-bitumen combinations. This meant that at -10 °C, the two types of bitumen (40/60 pen and the softer 70/100 pen) tended to have the same tensile strength with the same aggregate.

With temperature increase, the two aggregates seem to give the same tensile strength. This is due to the failure mechanism show cohesive failure as shown in Figure 6-9(d-f). The adhesive strength at the bitumen-aggregate interface exceeds the bitumen cohesive strength at temperatures of 20 °C and higher. In this region, the mineral properties of the aggregate cannot influence the tensile fracture strength results.

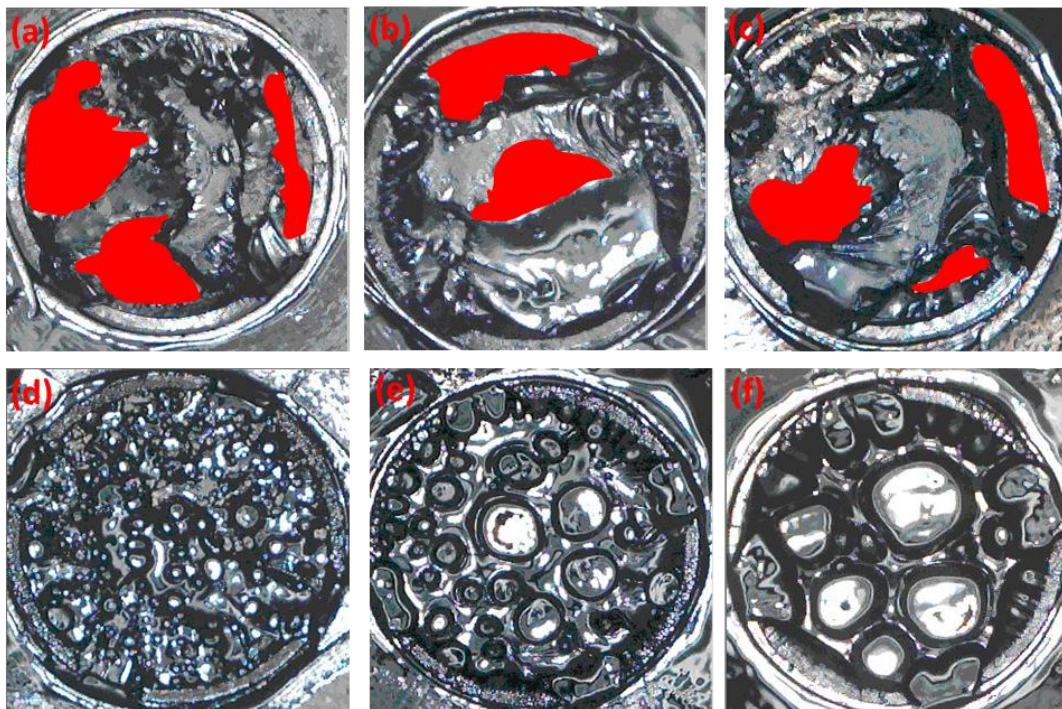


Figure 6-9 Failure surfaces of B1 bitumen with G1 aggregate samples at different temperatures: (a) -10 °C, (b) 0 °C, (c) 10 °C, (d) 20 °C, (e) 30 °C (f) 40 °C. The red area showed the adhesive failure.

### **6.4.1.3 Failure surface analysis**

From -10 °C to 10 °C, as shown in Figure 6-9 for the B1 (40/60 pen) bitumen with G1 substrate, the failure surfaces are flat and shiny and their texture is smooth. In addition, there is no evidence of voiding being observed in these specimens. Within this temperature region, the B1 (40/60 pen) bitumen can be considered to behave in a brittle manner. As bitumen, aggregate and the steel stub have different Poisson's ratios and Young's moduli, when load is applied to the specimen, it is impossible to get the same tensile stress everywhere, as the stress distribution is non-uniform. Also, during sample preparation, it is hard to get ideal adhesion without any physical defect around the edge, especially at the aggregate-bitumen interface. The faults existing around the film edge play an important role as stress concentrators. During the test, the stress which is applied to the specimen is focused on these faults to cause the fracture to start at these points. At the same time with temperature decrease, the bitumen becomes harder and more likely to experience a brittle-type failure mode. This brittle failure, together with the shift from cohesive to adhesive failure, results in a decrease in the tensile fracture strength as the temperature decreases from 10 °C to -10 °C.

When the temperature is over 20 °C, several round voids exist on the failure surfaces. With increasing temperature, the size of the voids increase but the quantity (number) of voids decreases. This is because the bitumen transforms from brittle behaviour to ductile behaviour as the temperature increases. The void formation can be explained by the flow and voiding failure mechanisms for ductile failure of bitumen films [12]. At low aspect ratios  $A = D/h$  (film diameter  $D$  and thickness  $h$ ), no voiding is observed and the material flows over the central area of the specimen. If the specimen has high aspect ratio but very low strain rate, voids are formed during the fracture process but they do not leave visible evidence on the final surface. When samples have aspect ratios in the range of 8-100, voids nucleate and coalesce. In this test, the aspect ratio of the sample is over 25, so all failures behave with this voiding mechanism at high temperatures. For samples at 20 °C, voids are visible but do not fully coalesce on the failure surface because the binder viscosity is still relatively high at this temperature. With temperature increase, binder viscosity decreases gradually so that it can flow more easily and small voids combine into bigger voids.

## 6.4.2 Cohesive and adhesive bond strength measurements after moisture damage

For each aggregate-bitumen combination, four specimens were tested to get their average result to compare with other conditions. Through this test, the tensile strength can be measured and an image of the failure surface taken. The average tensile strength results before moisture conditioning are shown in Table 6-1, while the original data are shown in Appendix C. In the dry condition, specimens prepared with B1 bitumen showed higher tensile strength than those prepared with B2 bitumen. In addition, the aggregate type did not influence the tensile strength when used with the same bitumen. The phenomenon in the dry condition correlates well with the peel test results.

Table 6-1 Dry tensile strength (kPa) of aggregate-bitumen bonds in the dry state at 20 °C (PATTI).

Sample ID	Mean $\pm$ SD (kPa)			
	L1	L2	G1	G2
B1	1820 $\pm$ 209	1805 $\pm$ 95	1831 $\pm$ 138	1840 $\pm$ 161
B2	1359 $\pm$ 71	1495 $\pm$ 45	1504 $\pm$ 185	1486 $\pm$ 117

Note: B1 = 40/60 pen bitumen; B2 = 70/100 pen bitumen; L1 = limestone 1; L2 = limestone 2; G1= granite 1; G2 = granite 2; SD = standard deviation

The differences in moisture sensitivity for different aggregate-bitumen combinations could be explained by the remaining percentage of bond strength after moisture conditioning which was achieved by dividing the conditioned bonding strength by the dry bonding strength, as shown in Figure 6-10. The bonding strength values of all specimens before and after moisture conditioning are shown in Appendix C. From this figure it is clear that all samples experienced a decline in their retained bonding strength after moisture conditioning. However, the declining rates of bonding strength are different for different bitumen aggregate combinations. In terms of the B1 bitumen, as shown in Figure 6-10a, specimens prepared with G1 and L2 aggregates have the highest retained strength with the results being 69% and 68%, respectively, after 14 days of moisture conditioning. This means that G1 and L2 aggregates have good moisture resistance. However, G2 aggregate shows the lowest retained strength with 47% of the tensile strength retained which means poor moisture resistance. Specimens

prepared with B2 bitumen (Figure 6-10b) showed the same ranking, with G1 and L2 aggregates having the best resistance to moisture-induced damage, while G2 aggregate shows the worst moisture resistance. The trend in terms of the retained tensile strength correlates well with the retained fracture energy results as shown in Chapter 5.

Figure 6-11 shows the failure surface of specimens before and after moisture conditioning. In dry conditions, all specimens show a cohesive failure surface. This phenomenon explains why all aggregates have almost the same tensile strength in the dry condition, as shown in Table 6-1. After moisture conditioning, the failure surfaces tend to change to adhesive due to the impact of moisture. It can be seen that the B1-L2 and B1-G1 specimens retained the highest percentage of cohesive failure section, followed by B1-L1 specimen. The B1-G2 specimen retained the lowest retained cohesive surface. Furthermore, some relationship was found between the retained tensile strength and failure surface with more cohesive surface resulting in higher retained tensile strength. Taking G1 and G2 for instance, specimens prepared with G1 aggregate have more cohesive failure area in comparison with G2 aggregate. So, higher retained tensile strength results were formed for specimens with G1 aggregate rather than G2 aggregate. It can be concluded that the failure surface can reflect the retained tensile strength with higher cohesive percentage resulting higher retained tensile strength.

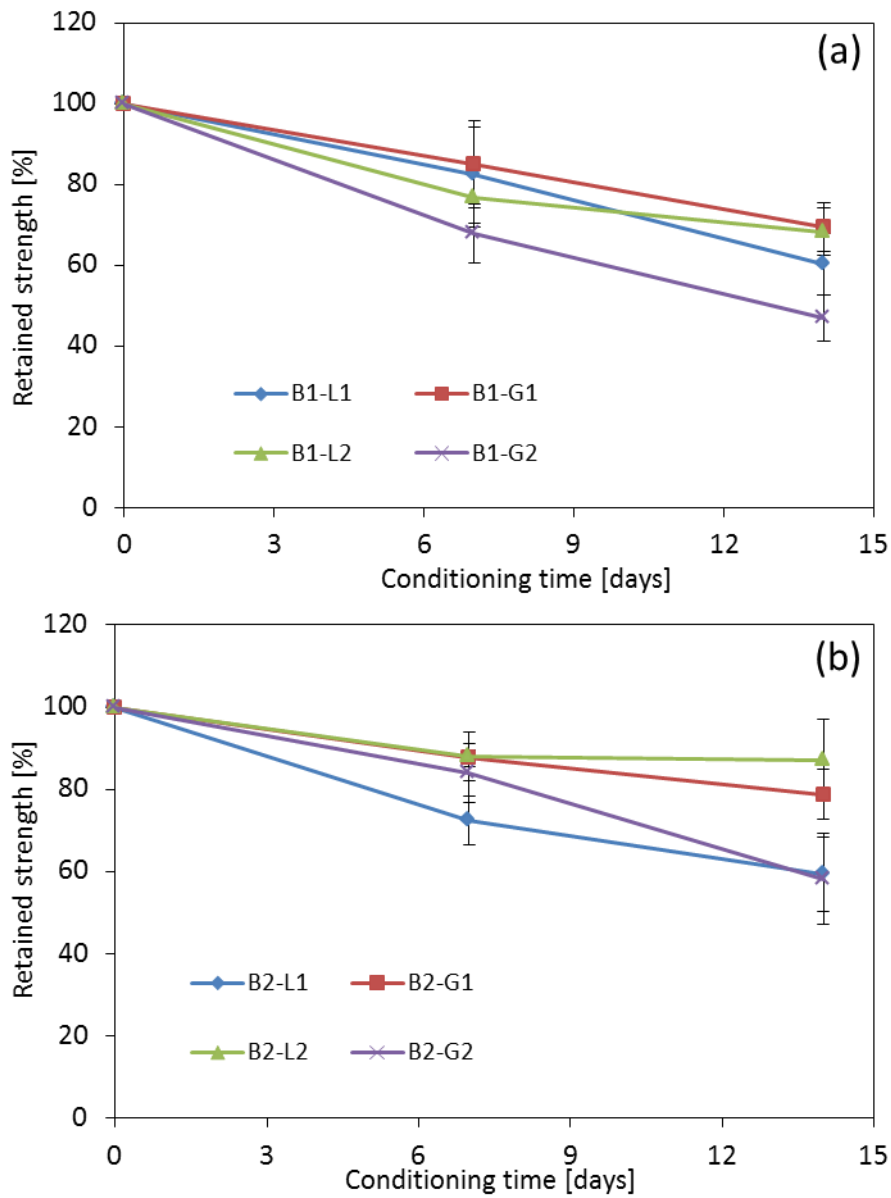


Figure 6-10 Retained bonding strength obtained from the PATTI test after moisture conditioning showing the effect of aggregate type on moisture sensitivity of aggregate-bitumen bonds at 20 °C: (a) bitumen B1, (b) bitumen B2.

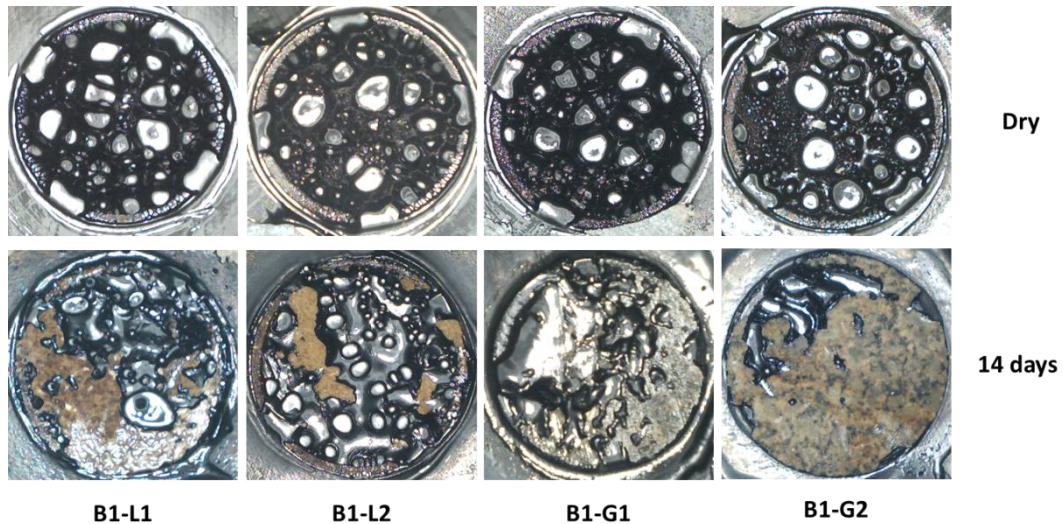


Figure 6-11 Sample failure surfaces for dry and moisture-conditioned aggregate-bitumen bonds tested in the PATTI test. Note: moisture conditioning time for all specimens in this Figure is 14 days.

## 6.5 Results for Pull-off test

All pull-off tests were performed at a temperature of 20 °C with the same extension speed as the peel test (10 mm/min). In order to simulate the real bitumen film thickness in asphalt mixtures, the bitumen film thickness was controlled at 20 μm. During the pull-off test, because the L1 aggregate is very soft, the fixtures could not mount the specimens properly. So, the samples prepared with L1 aggregate tended to break in the aggregate rather than the bitumen film or aggregate-bitumen interface. An alternative method to mount L1 specimens into the fixtures will need to be designed in the future. So, only specimens prepared with G1, L2 and G2 achieved reliable results.

### 6.5.1 Influence of aggregate and bitumen on tensile strength in dry condition

Four replicate tests were performed on each aggregate-bitumen combination. The average tensile strength of each aggregate-bitumen bond in the dry condition was calculated using Equation 6-2. The results are depicted in Table 6-2 together with the test variability (standard deviation); the latter suggesting that the new pull-off test has low variability with a coefficient of variability ranging from about 5-16%. The original tensile strength of all specimens in the dry condition are shown in Appendix D. It can

be seen from Table 6-2 that samples prepared with bitumen B1 have higher tensile strength in comparison with bitumen B2. This phenomenon correlates well with the DSR results with shear complex modulus higher for B1 than B2, as shown in Chapter 2. In addition, this result also correlates with the peel test results and PATTI test results. It can be demonstrated that bitumen with higher shear complex modulus results in higher tensile strength. In terms of the same bitumen, samples prepared with different aggregates tend to yield similar tensile strength. This suggests that, in the dry condition, the tensile strength of samples is controlled mainly by the bitumen properties, aggregate effects appear minimal. One reason for this observation is that damage was mainly cohesive (i.e. within the bitumen) but not interfacial.

Table 6-2 Dry tensile strength (kPa) of aggregate-bitumen in the dry state at 20 °C (Pull-off test).

Sample ID	Mean $\pm$ SD (kPa)		
	L2	G1	G2
B1	1920 $\pm$ 103	1947 $\pm$ 199	1938 $\pm$ 259
B2	1425 $\pm$ 147	1386 $\pm$ 72	1413 $\pm$ 128

B1 = 40/60 pen bitumen; B2 = 70/100 pen bitumen; L2 = limestone 2; G1= granite 1; G2 = granite 2; SD = standard deviation

## 6.5.2 Influence of moisture damage on Pull-off test

Due to their much smaller dimensions, the moisture damage process for the pull-off test is faster than for the peel or PATTI tests. The specimen prepared with G2 aggregate separated at the bitumen-aggregate interface without loading after 14 days moisture conditioning thereby demonstrating that 14 days of conditioning time is too long to get comparable results with the PATTI test. In this part of the study, the conditioning times were shortened to 1 and 7 days.

### 6.5.2.1 Effect of moisture conditioning on loading behaviour

To simulate the effect of moisture on the stress-strain properties of the aggregate-bitumen combined samples, moisture conditioning was applied at 20 °C over periods of

1 day and 7 days. Figure 6-12 shows the influence of increasing moisture conditioning time on the load-displacement behaviour of samples prepared with bitumen B1 and the three aggregates. From this figure it can be seen that the tensile loads for all specimens decreased after moisture conditioning. In terms of the load-displacement curve, B1-L2 and B1-G2 with 1 day moisture conditioning experienced a sharp decrease once they reached the peak load, which is totally different from other specimens. This may be due to the short-term moisture conditioning for these two specimens hardening the bitumen and it having no chance to release during extension. Due to the lower moisture absorption of G1 aggregate as shown in Chapter 3, it is not easy for water to penetrate into the aggregate-bitumen interface and harden the bitumen so that the sharp decrease of tensile load does not appear in B1-G1.

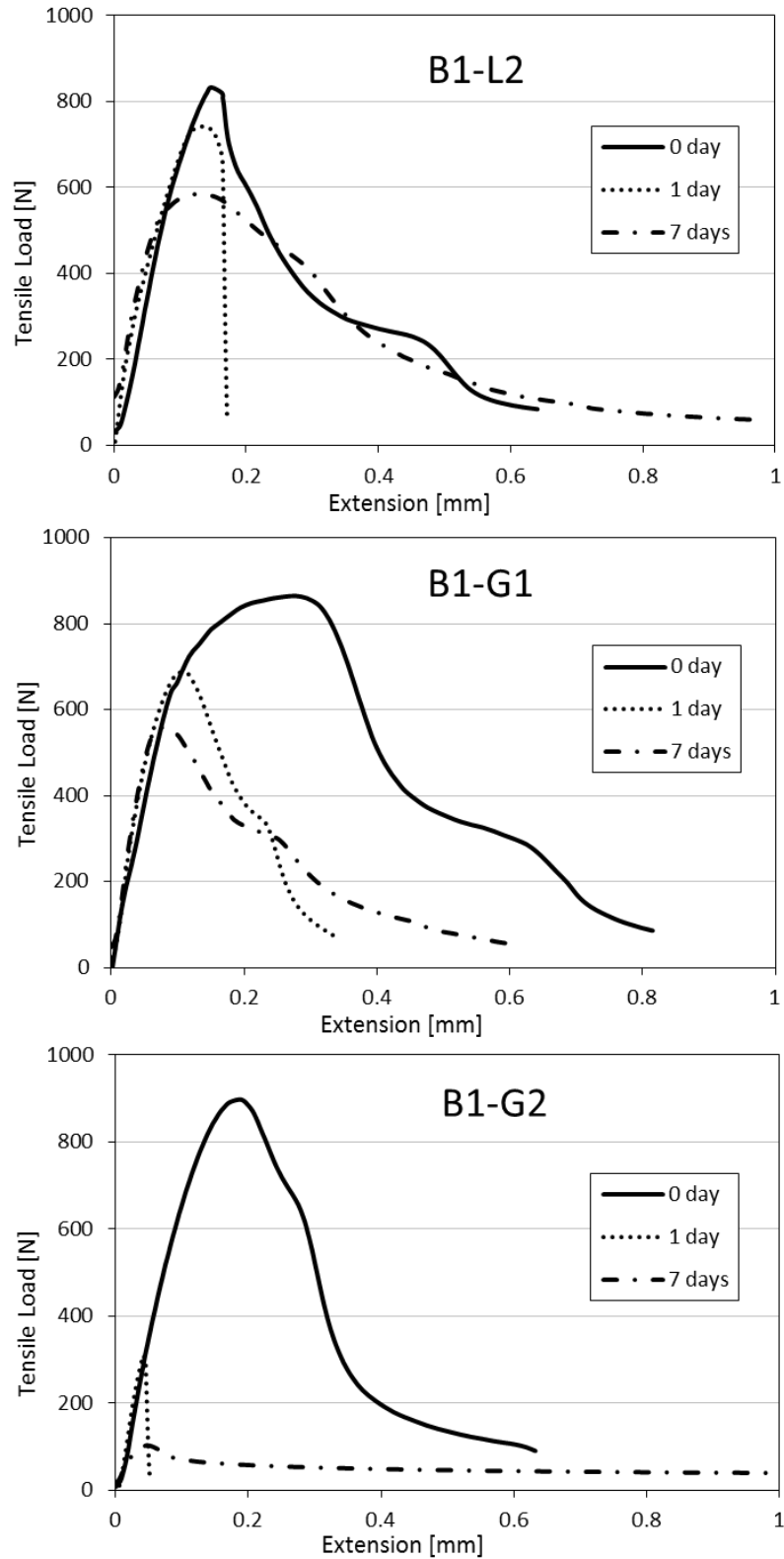


Figure 6-12 Effect of moisture on load-displacement behaviour of aggregate-bitumen combined samples before and after moisture conditioning. Samples were conditioned in water at 20 °C; loading rate was 10 mm/min (Pull-off test).

### **6.5.2.2 Effect of moisture on retained strength**

Retained strength, the ratio of bond strength after a given level of moisture conditioning to the dry bond strength, is a common measure of moisture sensitivity of asphalt mixtures. The higher the retained strength of an asphalt mixture, the better the moisture damage resistance of the bond. Figure 6-13 shows the effect of conditioning time on retained tensile strength of the aggregate-bitumen bond. The tensile strength values of all specimens before and after moisture damage are shown in Appendix D. From this Figure it can be seen that specimens which contain L2 or G1 aggregate show good moisture resistance with over 75% tensile strength retained after 7 days conditioning. On the contrary, the moisture effect was more pronounced in the specimens containing G2 aggregate where the strength decreased by over 80% and 40% for B1 and B2 bitumen, respectively. Aggregate L2 and G2 have similar moisture absorption properties, but they show obviously different moisture sensitivity. This result suggests moisture absorption alone is not an indicator of moisture damage, the mineralogy of the aggregate is also important. Another reason for the differences observed in L2 and G2 could be that because G2 contains a large amount of albite and quartz, the bonds formed with bitumen are quickly broken in the presence of water. The results showing better resistance to moisture-induced damage for specimens containing limestone rather than granite are in agreement with previous studies [13, 8]. However, although G1 is granite, but because of its lower moisture absorption, it is hard for water to diffuse through the aggregate into the aggregate-bitumen interface so there is no weakening of the bond. On this basis, it is reasonable to state that the moisture-induced damage of aggregate-bitumen bonds is not only controlled by the mineralogical composition but the moisture absorption of aggregate should also be considered. The differences in retained strengths between G1 and G2 could be attributed to higher moisture absorption of the latter. This result combined with the L2 results previously discussed leads one to conclude that for susceptible aggregates, the amount of moisture absorption is a significant factor.

In terms of the same aggregate, specimens prepared with B2 bitumen show slightly better resistance to moisture damage in comparison with B1. This is in contrast to previous studies with stiffer bitumen have better moisture resistance [14]. This may be due to the dimensions of the specimen used for pull-off test. During aggregate substrate

preparation, it is very hard to make sure all substrates get a thickness of 5 mm. The difference in the substrate thickness can influence the speed and amount of water delivered to the aggregate-bitumen interface and finally influence the moisture resistance. In addition, because the designed bitumen film thickness is very thin (20  $\mu\text{m}$ ), a little un-parallel of the top and bottom aggregate surfaces may obviously impact the consistency of the bitumen film thickness. The variation in the film thickness can directly influence the tensile load so as to affect the moisture resistance. However, more tests need to be done to confirm this conclusion.

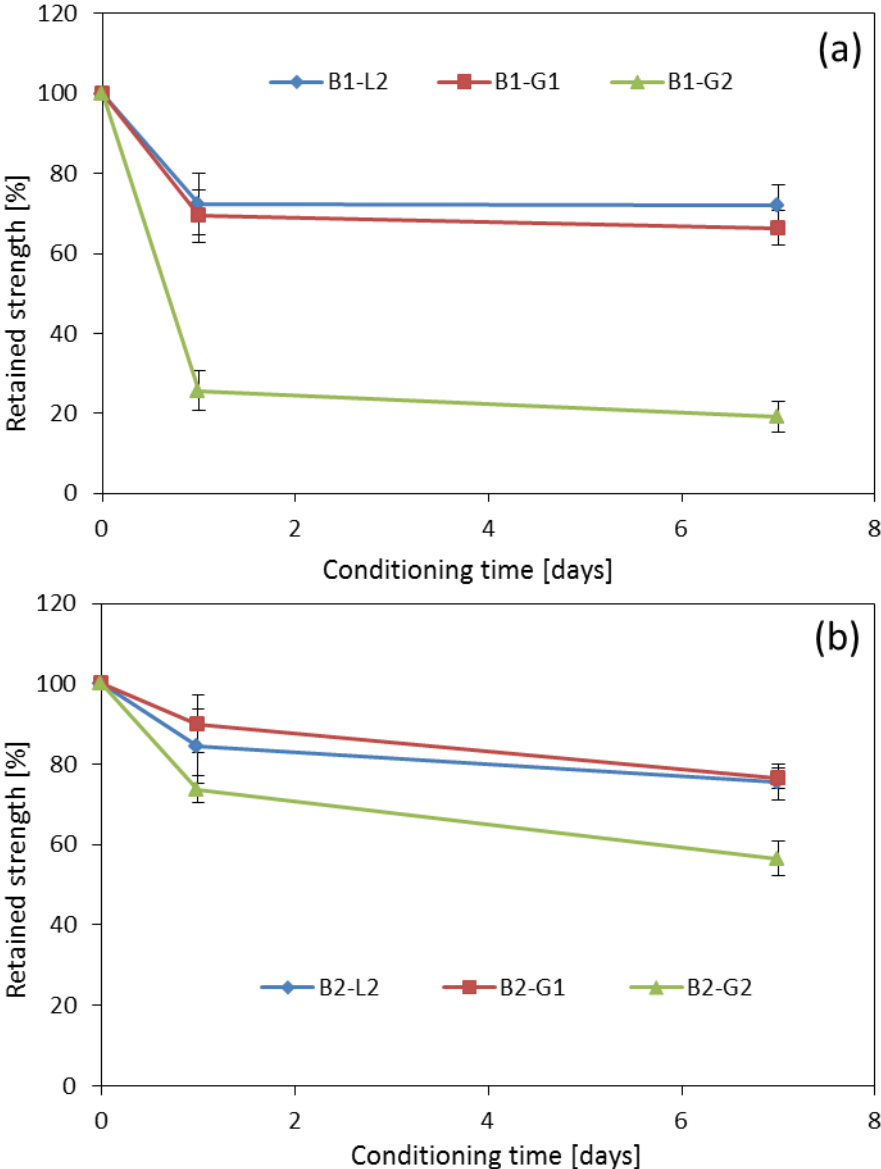


Figure 6-13 Effect of moisture conditioning time on tensile strength of different aggregate-bitumen combinations obtained from pull-off test. In general acidic

aggregate performed worse than basic aggregates. The combination of bitumen B1 with aggregate G2 performed worst: (a) bitumen B1, (b) bitumen B2.

### ***6.5.2.3 Moisture effects on failure type***

Figure 6-14 shows the effect of increasing conditioning time on the failure surface of aggregate-bitumen specimens. Without moisture conditioning, cohesive failure occurred in the bulk of the bitumen film. Under this condition, the tensile strength depends on the cohesive bond of the bitumen film. So, the same bitumen shows almost the same tensile strength, no matter which aggregate was used. After moisture conditioning, the water could penetrate into the specimen and weaken the aggregate-bitumen interface. The failure tends to transfer from cohesive to an adhesive-cohesive mix with the increase of conditioning time. It can be seen that specimens prepared with L2 retained the most cohesive failure, followed by G1 and specimens with G2 showed the least cohesive failure. Specimens with G2 aggregate even show totally adhesive failure after 7 days moisture conditioning. The results demonstrated that, with similar moisture absorption properties, limestone showed better resistance to moisture-induced damage than granite. The results show that the effect of aggregate is more dominant than the effect of bitumen type.



## 6.6 Conclusions

This chapter presents the findings from an investigation of the tensile strength of different aggregate-bitumen combinations in dry and after moisture damage conditions using an improved PATTI test and a pull-off test system. In this research, the improved PATTI test could accurately control the temperature from -10 °C to 40 °C while the pull-off test has the capability to accurately control the bitumen film thickness and loading rate. The influence of temperature on tensile strength of aggregate-bitumen was evaluated using the PATTI test with an environmental chamber to control the temperature. Tensile strength and retained tensile strength were used as measures of moisture sensitivity of the aggregate-bitumen bonds. The following conclusions were reached based on the results presented in this chapter.

The tensile strength of the bitumen film and the aggregate-bitumen interface measured with the PATTI test was shown to be sensitive to temperature. The failure pattern was shown to change from cohesive failure to mixed cohesive/adhesive failure as the test temperature decreased from 40 °C to -10 °C. At the same time, the bitumen failure behaviour changes from brittle to ductile as the temperature increases from -10 °C to 40 °C. These combined effects resulted in the maximum tensile fracture strength for the various bitumen-aggregate combinations occurring at approximately 10 °C.

In the dry state, for both tests (PATTI test and Pull-off test) at 20 °C, the loci of failure of all the aggregate-bitumen combinations were cohesive. The effect of bitumen grade was significant with samples prepared with B1 (40/60 pen) bitumen having higher tensile strength than those prepared with B2 (70/100) pen bitumen. The results suggest that the bitumen grade controls the aggregate-bitumen bond strength in the dry state to a higher extent than aggregate type.

The bond strength of the various aggregate-bitumen combinations measured with these two tensile strength tests was shown to be sensitive to moisture conditioning. The failure pattern was shown to change from cohesive to mixed cohesive/adhesive and even adhesive failure as the conditioning time extended. These two tests showed similar ranking in terms of moisture sensitivity but the pull-off test was found to be the most sensitive. The higher sensitivity of the pull-off test could be attributed to smaller

specimen geometry that allowed faster moisture diffusion into the aggregate-bitumen interface where damage is believed to be initiated.

Results suggest that the moisture damage of different aggregate-bitumen combinations could be explained by the moisture absorption and mineralogical compositions of aggregates. With the same moisture absorption, limestone tends to have better resistance to moisture damage than granite. Furthermore, in terms of similar mineralogical compositions, lower moisture absorption may result in better moisture resistance.

## References

1. Standard Test Method for Pull-off Strength of Coatings Using Portable Adhesion Testers. D4541. ASTM International, US. (<http://www.astm.org/Standards/D4541.htm>) [accessed 03.07.14].
2. Nguyen T., Byrd E., Bentz D. and Seiler J. Development of a Method for Measuring Water-Stripping Resistance of Asphalt/Siliceous Aggregate Mixtures. NCHRPID-002. National Cooperative Highway Research Program, Transportation Research Board, National Research Council, Washington DC, 1996.
3. Santagata F.A., Cardone F., Canestrari F. and Bahia H.U. Modified PATTI test for the characterization of adhesion and cohesion properties of asphalt binders. Sixth International Conference on Maintenance and Rehabilitation of Pavements and Technological Control (MAIREPAV6), 2009.
4. Kanitpong K. and Bahia H.U. Role of adhesion and thin film tackiness of asphalt binders in moisture damage of HMA. Journal of the Association of Asphalt Paving Technologists, 2003, 72: 611-642.
5. Santagata F.A., Cardone F., Canestrari F. and Bahia H.U. Modified PATTI Test for the Characterization of Adhesion and Cohesion Properties of Asphalt Binders, International Conference on Maintenance and Rehabilitation of Pavements and Technological Control, Sixth Proceedings, Turin, 2009.
6. Mohd Jakami F. Adhesion of asphalt mixtures. PhD dissertation, University of Nottingham, July 2012
7. Wood P.R. Rheology of asphalts and the relation to behaviour of paving mixtures. Highway Research Board Bulletin, 1958, 192: 20-25.
8. Apeageyi A.K, Grenfell J. and Airey G.D. Moisture-induced strength degradation of aggregate–asphalt mastic bonds. Road Materials and Pavement Design, 2014, 15(1): 239-262.

9. Heukelom W. and Wijga P. Bitumen testing: an introduction to the use of test methods at the Koninklijke/Shell-Laboratorium, Koninklijke/Shell-Laboratorium, Amsterdam, 1973.
10. Mo L.T., Huurman M., Wu S.P. and Molenaar A.A.A. Bitumen–stone adhesive zone damage model for the meso-mechanical mixture design of ravelling resistant porous asphalt concrete. *International Journal of Fatigue*, 2011, 33: 1490-1503.
11. Blackman B.R.K., Cui S., Kinloch A.J. and Taylor A.C. The development of a novel test method to assess the durability of asphalt road-pavement materials. *International Journal of Adhesion and Adhesives*, 2013, 42: 1-10.
12. Harvey J.A.F. and Cebon D. Failure Mechanism in Viscoelastic Films. *Journal Materials Science*, 2003, 38: 1021-1032.
13. Airey G.D. and Choi Y.K. State of the art report on moisture sensitivity test methods for bituminous pavement materials. *Road Materials and Pavement Design*, 2002, 3(4): 355-372.
14. Airey G.D., Collop A.C., Zoorob S.E. and Elliott R.C. The influence of aggregate, filler and bitumen on asphalt mixture moisture damage. *Construction and Building Materials* 2008, 22(9): 2015-2024.

# **7. Composite Substrate Peel Test (CSPT)**

## **7.1 Introduction**

As presented in Chapter 5, the peel test has been successfully used to evaluate the moisture sensitivity of different aggregate-bitumen combinations. The peel test is based on the fracture mechanics approach to measure the adhesive fracture energy of aggregate-bitumen joints tested in both the dry state and after being conditioned in moisture. When preparing the peel test specimen, a large flat aggregate surface with regular shape should be initially prepared. In this case, only large stone boulders (>200 mm) could be used for the substrate preparation. However, commonly used asphalt mixture aggregates are crushed coarse aggregates which are significantly smaller than stone boulders. So, a newly developed procedure to prepare a composite substrate using coarse aggregates was applied in this chapter. The innovation of this procedure is the ability to combine several coarse aggregates together and get a flat aggregate surface that can be easily used for the peel test. The objectives of this chapter are to describe the detailed procedures of the newly developed composite substrate peel test (CSPT) and evaluate the susceptibility of the aggregate-bitumen bonds to moisture damage based on the values obtained from the newly developed test as compared to the standard peel test. The reliability of the newly developed peel test was also evaluated using the standard peel tests.

## **7.2 Experimental program**

### **7.2.1 Substrate preparation**

For the peel testing used in Chapter 5, the specimens should be rectangular, with the rigid aggregate and the flexible peel arm adhered along most of the length. The rigid aggregate should be thick enough to withstand the expected tensile force. At the same time, the flexible peel arm should have good adhesion with bitumen to avoid fracture at the interface. In this research, an aluminium alloy with a thickness of 0.2 mm was

selected as a flexible peel arm. According to Chapter 5, the aggregate substrates were produced from aggregate boulders with the overall dimensions selected as 150 mm × 20 mm × 10 mm.

By preparing the aggregate substrates, the stone boulders were first wet-sawn to get aggregate slabs with a thickness of 10 mm. Then, the aggregate slabs were trimmed to a size of 150 mm long and 20 mm wide, as shown in Figure 7-1a. In this case, only big stone boulders (>200 mm) could be used for the substrate preparation. However, the commonly used asphalt mixture aggregate are crushed coarse aggregates (20 mm-32 mm) which are significantly smaller than stone boulders. So, it is necessary to design a new procedure to prepare an aggregate substrate by using easily accessible asphalt mixture coarse aggregates.

This research presents the development of a novel method to prepare a composite substrate using crushed coarse aggregates (Figure 7-1b) as a more practical replacement for the aggregate substrate prepared from boulders (Figure 7-1a). The innovation of this procedure is the ability to combine several coarse aggregates together and get a flat surface that can be used for the peel test.



Figure 7-1 Aggregate substrate and coarse aggregates: (a) substrate must be prepared from large boulders, while (b) coarse aggregates are readily available in most labs.

In order to combine the coarse aggregates together, a mould made up from five aluminium plates was designed and is shown in the schematic diagram in Figure 7-2. These five aluminium plates could be assembled together by using eight screws to produce inside dimensions of 150 mm × 20 mm × 50 mm.

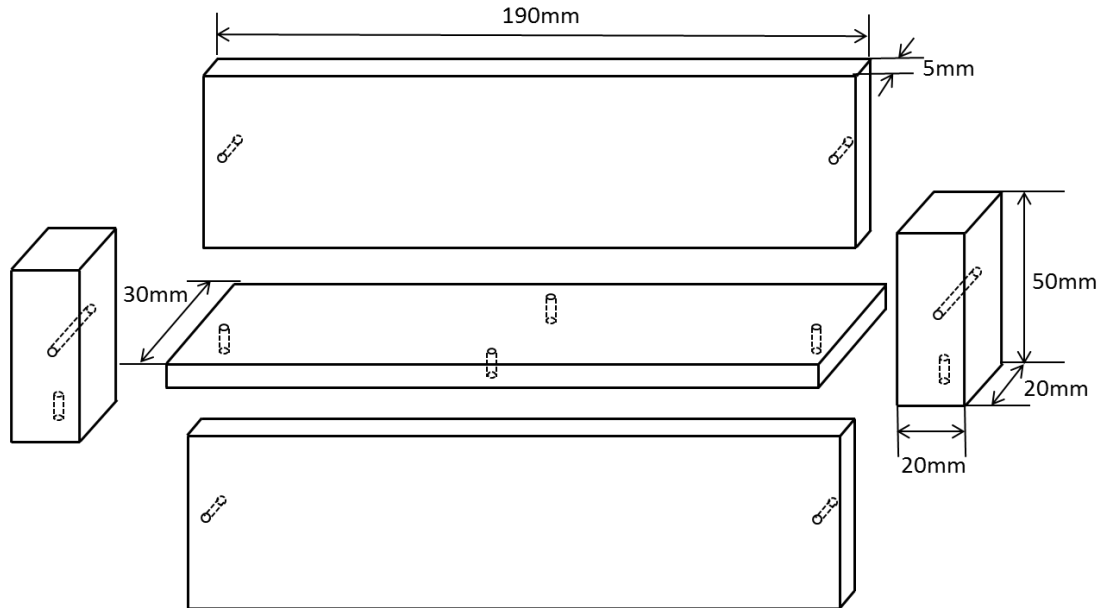


Figure 7-2 Schematic of the aluminium mould used for composite substrate preparation

Figure 7-3 shows the whole procedure in terms of substrate preparation using coarse aggregates. For the substrate preparation, graded or crushed rocks with sizes passing 50 mm and retained on 20 mm were first trimmed using a trimming saw (as shown in Figure 7-3a) to get an appropriately rectangular aggregate with one dimension being less than 20 mm. The trimmed coarse aggregates are shown in Figure 7-3b. The aluminium mould was then assembled and a release compound (Dow Corning DC4) used to grease the inside of the mould surface to avoid it sticking to the epoxy resin used in the next step, as shown in Figures 7-3c and d. An epoxy resin bonding material (Araldite 2000), as shown in Figure 7-3e was prepared by mixing the two components together according to the required proportions. The trimmed aggregates were assembled into the mould followed by filling the spaces in the mould with the epoxy resin as shown in Figure 7-3f. The assembled mould was stored at room temperature for 24 hours to allow the epoxy resin to cure. After 24 hours of curing, the mould was disassembled and the cured sample tipped out, as shown in Figure 7-3g. Finally, the cured sample was cut down the middle to get two substrates with a thickness no less than 10 mm, as shown in Figure 7-3h.

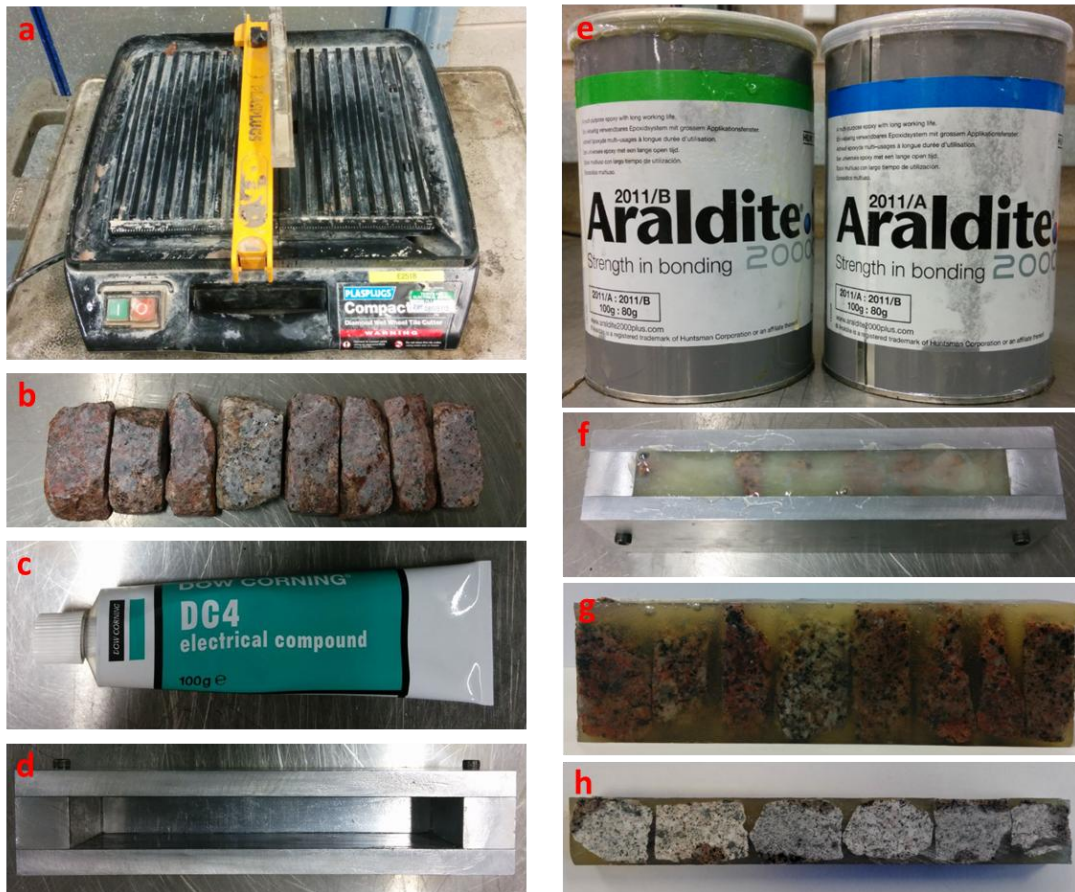


Figure 7-3 Procedures for aggregate substrate preparation: (a) trimming saw, (b) aggregates after trimming, (c) release compound, (d) assembled mould, (e) epoxy resin, (f) combine trimmed aggregates in the mould and fill the gaps with epoxy resin, (g) cured composite aggregate, (h) composite substrate used for peel test.

## 7.2.2 Adhesion specimen fabrication

The aggregate substrates, including the standard aggregate substrates and composite substrates using coarse aggregates, with dimensions of 150 mm × 20 mm × 10 mm were prepared as previously described. They were then bonded to the aluminium peel arm using bitumen as the adhesive layer. The thickness of the bitumen adhesive layer is controlled by placing five wire spacers on the aggregate and results in a 0.25 mm film thickness. The sample preparation consists of the following steps [1]:

1. Surface pre-treatment. Aggregate substrate was ground using sand paper to get a smooth surface. The ground substrate and peel arm are then gently wiped using a damp paper towel to remove any dust.

2. Pre-heating the aggregate and the bitumen. The aggregate and peel arm are then placed in an oven at 150 °C for 1 hour. Bitumen is preheated to 150 °C prior to making the joint.
3. Placing the sharp crack initiator. A release poly tetra fluoro ethylene (PTFE) film with dimensions of 20 mm × 12 mm × 75 μm is placed on the aggregate surface at one end.
4. Five wire spacers with a length of 20 mm are placed on the aggregate. The diameter of the wire controls the thickness of the bitumen (adhesive) layer.
5. The liquid bitumen is applied (at 150 °C) evenly along the surface of the aggregate.
6. The preheated aluminium peel arm (of length 50 mm longer than the aggregate substrate and of thickness 0.2 mm) is placed on the top of the bitumen layer.
7. Gentle pressure is applied on top of the joint to control the thickness of the bitumen layer. The pressure should be uniformly distributed over the bond area. The excess bitumen at the edges of the specimen was trimmed with a heated knife with the prepared specimens shown in Figure 7-4.
8. All specimens were stored at room temperature ready for further testing.



Figure 7-4 Prepared adhesion specimens used for peel test

### 7.2.3 Moisture conditioning

The prepared aggregate-bitumen adhesion specimens were tested in the dry condition or after moisture conditioning. Moisture was introduced into the aggregate-bitumen interface by submerging the completed specimens in deionized water at 20 °C for 7 days or 14 days, as shown in Figure 7-5. During the conditioning period, moisture could reach the aggregate-bitumen interface and directly attack the bond. The specimens should be tested within 1 hour after removing them from the water bath.



Figure 7-5 Moisture conditioning of adhesion specimens

### 7.2.4 Parameter evaluation

A universal testing machine (UTM) which can supply a constant rate of grip separation was used to measure the tensile force during the peel test. The sample was attached to a linear bearing to get a highly accurate and smooth motion. During testing, the free end of the peel arm was gripped by the UTM fixture and stretched up at a speed of 10 mm/min with the peel angle maintained at 90 °, as shown in Figure 7-6. The tensile force was recorded during the fracture development and the results used to calculate the fracture energy.

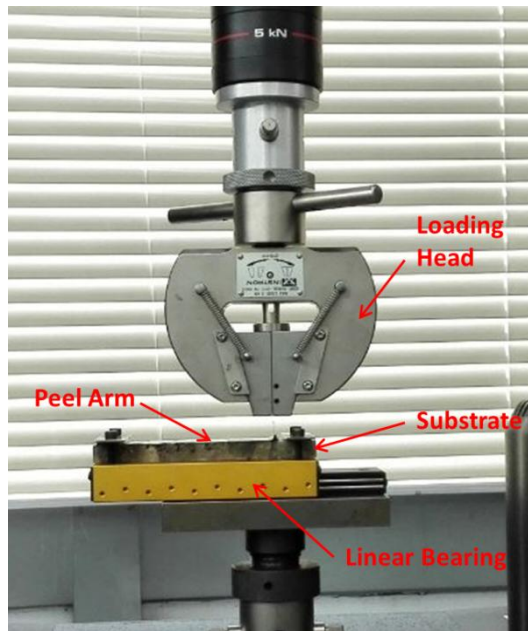


Figure 7-6 Details of peel test equipment

The achieved peel force was first used to calculate the uncorrected adhesive fracture energy, using equation 7-1 as follows:

$$G = \frac{P}{b}(1 - \cos \theta) \quad (7-1)$$

where  $P$  is the average peel force,  $b$  is the width of the adhesive surface and  $\theta$  is the applied peel angle ( $90^\circ$ ).

Then, the corrected fracture energy is obtained by removing the energy associated with the plastic bending of the peel arm:

$$G_A = G - G_p \quad (7-2)$$

where  $G_A$  is the corrected fracture energy and  $G_p$  is the energy associated with the plastic bending of the peel arm.

In order to calculate the fracture energy of the aggregate-bitumen bond, the mechanical properties of the aluminium peel arm were first determined using the same tensile speed as the peel test. In order to describe the elastic and plastic deformation of the peel arm, the stress-strain curve should be fitted with a bi-linear or power law equation. The purpose of the bi-linear and power law curve fits is to get a number of parameters which are used to calculate the fracture energy. The following parameters of the bi-

linear model (Eq. 7-3) for the peel arm were used for the plastic corrections as described in the following equation:

$$\sigma = \sigma_y + \alpha E_1(\varepsilon - \varepsilon_y) \quad (7-3)$$

where  $\sigma_y$  is yield stress and  $\varepsilon_y$  is the yield strain,  $E_1$  is the elastic modulus of the peel arm,  $E_2$  is the plastic modulus of the peel arm and  $\alpha$  is the ratio of plastic modulus to elastic modulus,  $E_2/E_1$ .

The measured stress-strain curve was modelled using the bi-linear model and the parameters gained from the fitting process are shown in Table 7-1. The value of corrected fracture energy was then calculated using large displacement beam theory.

Table 7-1 Plastic bending parameters of the peel arm based on bi-linear model fit

Parameters	Quantity
Low strain modulus, $E_1$	61.0 GPa
High strain modulus, $E_2$	1.16 GPa
Yield strain, $\varepsilon_y$	0.044 %
$\alpha$ ( $E_2/E_1$ )	0.019
Yield stress, $\sigma_y$	26.84MPa

## 7.3 Results

### 7.3.1 Fracture energy calculation for CSPT

The purpose of the peel test was to determine the fracture energy of aggregate-bitumen bonds as a function of material type and moisture conditioning time. Results are presented for four replicate tests performed on each aggregate-bitumen combination. The tensile force was recorded by the UTM during testing and the tensile load versus displacement curve was plotted. For the standard peel test, the tensile force tends to remain at an approximately constant value after the initial stage. Normally, around 50 mm of constant crack propagation region will be selected for the average tensile force calculation and this procedure has been presented in Chapter 5.

In terms of the newly designed CSPT, the method to calculate the average tensile force shows some differences in comparison with the standard peel test. One type of specimen (G2) was selected to illustrate this point, as shown in Figure 7-7. In the dry condition, as shown in Figure 7-7a, the tensile force values were constant with the development of the fracture. This means that the average tensile force could be calculated using the same approach as the standard peel test. After moisture conditioning, the tensile force is not constant and three obvious fluctuations occurred with the crack propagation, as shown in Figure 7-7b. In this condition, the tensile force results in fluctuations need to be removed and the retained values were used to calculate the average tensile force. The choice was set based on the peak heights with the values which over half of each peak values were not involved in the calculation. As shown in Figure 7-7b, the values over the vertical red lines were removed. In addition, the results at the beginning of the curve were removed. The average force of each sample and the parameters in Table 7-1 were entered into the Microsoft excel macro IC Peel software to calculate the fracture energy values [2].

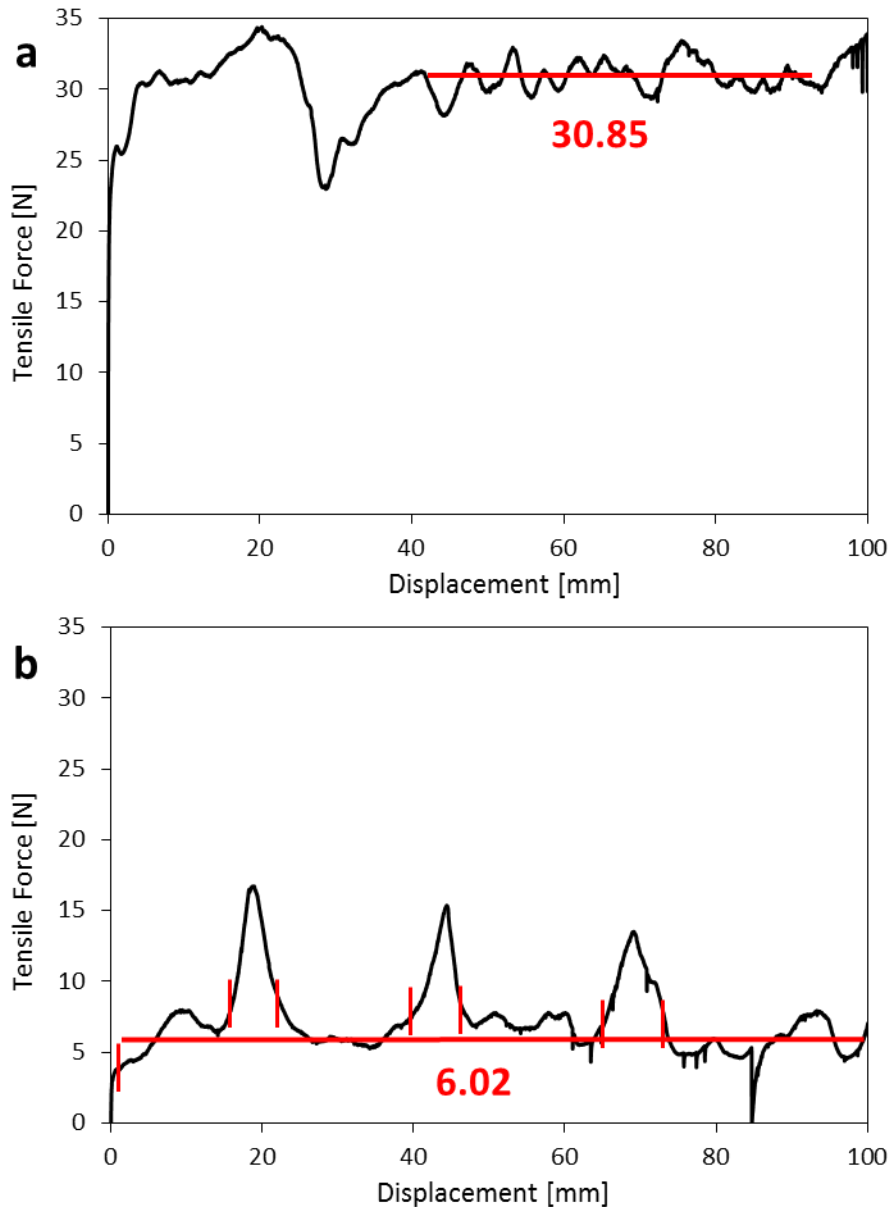


Figure 7-7 Measured tensile load-displacement curve of: (a) B1-G2 in dry condition using CSPT and (b) B1-G2 after 14 days conditioning using CSPT. The three fluctuations presented in Figure 7-7b is because the epoxy resin segments between two aggregates result in high bond strength with bitumen even after moisture conditioning.

### 7.3.2 Fracture energy in dry condition

Specimens prepared with B1 bitumen and five coarse aggregates (L1, L2, G1, G2 and G3) were subjected to the CSPT. The aggregates were first combined together using epoxy resin and the self-designed mould followed by preparing the peel test specimen, as shown in Sections 7.2.1 and 7.2.2. The tensile load and fracture energy of specimens

before and after moisture damage were evaluated based on the procedures in Sections 7.2.4 and 7.3.1.

Table 7-2 shows the average fracture energy and test variability (standard deviation) of specimens before moisture conditioning with results being achieved from the newly designed CSPT. The standard deviation suggests the test has low variability. From this Table it can be seen that all specimens have almost the same fracture energy in the dry condition, irrespective of which aggregate was used. Without moisture conditioning, a cohesive failure occurred within the bulk of the bitumen, as shown in Figure 7-8. The fracture energy depended on the cohesive bond in the bulk of the bitumen layer. This is why all aggregates show almost the same fracture energy in the dry condition.

Table 7-2 Dry fracture energy ( $J/m^2$ ) of aggregate-bitumen bonds in the dry state at 20 °C using the newly designed composite substrate peel test.

Methods	Fracture Energy Mean $\pm$ 1 SD ( $J/m^2$ )				
	B1-L1	B1-L2	B1-G1	B1-G2	B1-G3
CSPT	992 $\pm$ 9.4	987 $\pm$ 26.3	1003 $\pm$ 6.7	982 $\pm$ 7.8	983 $\pm$ 7.3

Note: SD = standard deviation



Figure 7-8 Failure surface of specimens prepared with G2 coarse aggregates in dry condition

### 7.3.3 Failure behavior after moisture conditioning

To simulate the effect of moisture on the bonding properties between bitumen and aggregate, the whole specimens were submersed in water at 20 °C for 7 days and 14 days. During that time, moisture is able to reach the aggregate-bitumen interface in three different ways: through the top and bottom of the aggregate, through the edge of aggregate-bitumen interface and through the bitumen film. After moisture conditioning,

specimens were removed from the water bath and then subjected to the peel test within 1 hour.

In this research, the loading behavior and failure surface of two granite samples were selected for detailed analysis, as shown in Figure 7-9. It can be seen that these samples showed different loading behavior and failure surfaces due to different moisture sensitivity of the aggregates. The sample prepared with G1 aggregate showed mainly cohesive failure surface with adhesive failure occurring at both edges of the specimen after 14 days of moisture conditioning with the tensile load not decreasing significantly in comparison with the tensile load in Figure 7-7a. In contrast, the failure surface of G2 is nearly completely adhesive and the tensile load decreased significantly. There are also three obvious fluctuations (peaks) due to the cohesive failure over the epoxy resin segments between two adjacent aggregates. From this Figure it can be seen that the peel force accurately reflects the failure mode which demonstrates that the composite substrate could be used for fracture energy evaluation. It should be mentioned that there is small amount of cohesive failure occurred on the edges of the substrate because the epoxy resin occupied the aggregate place, as shown in Figure 7-9. The small amount of cohesive failure may slightly influence the final result. So, in the future, the aggregate need to be carefully trimmed to slice off the edges to make sure the width of the aggregate is exactly 20mm.

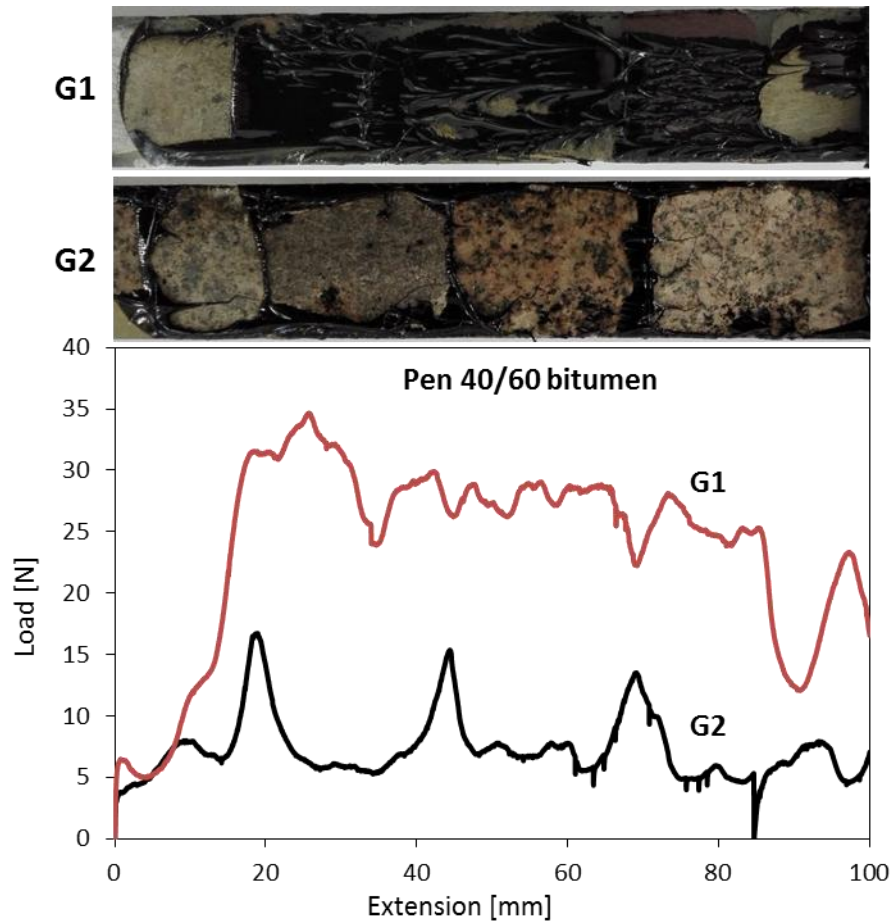


Figure 7-9 Failure surfaces and loading behavior of two specimens (B1-G1 and B1-G2) after 14 days of moisture conditioning using the CSPT

With the aim of directly comparing the measurements made with the CSPT and the standard peel test as introduced in Chapter 5, the loading behavior of G1 and G2 specimen obtained from these two tests were plotted in Figure 7-10. From this figure it can be seen that when using the same aggregate, these two different tests show similar loading results thus demonstrating that the newly developed CSPT could obtain similar loading behavior as determined with the standard peel test.

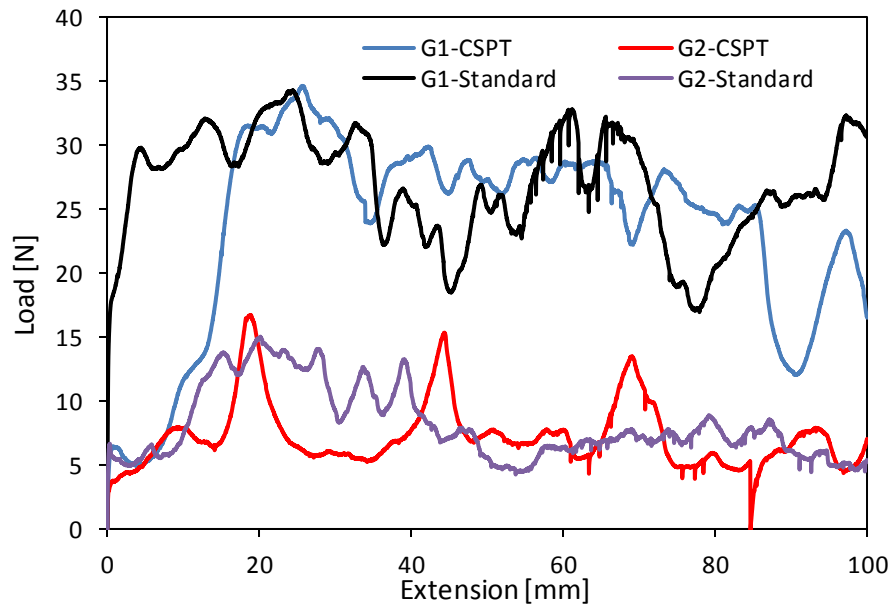


Figure 7-10 Loading behavior of two samples (B1-G1 and B1-G2) after 14 days of moisture conditioning obtained using both standard peel test and CSPT

### 7.3.4 Retained fracture energy

The effect of moisture on the bond strength could be captured using a single retained fracture energy percentage as a more elegant and unified way of characterising aggregate-bitumen bond strength. In general, the larger the magnitude of retained fracture energy of a joint, the greater the resistance to failure from applied loading after moisture conditioning. The retained fracture energy of specimens after 7 days and 14 days moisture conditioning were calculated by dividing the conditioned fracture energy by the dry fracture energy, and the results are shown in Figure 7-11. The fracture energy results of all specimens before and after moisture conditioning are shown in Appendix E. As the materials used in CSPT are coarse aggregates used in actual asphalt mixture field applications, the results are much more reliable in terms of identifying a ‘good’ versus ‘bad’ moisture resistant mixture.

As shown in Figure 7-11, one effect of moisture on the aggregate-bitumen interface is the reduction in fracture energy with different aggregates showing different values. The significant difference in retained fracture energy results could be explained by the water absorption properties and mineralogical composition of aggregates. For G1 aggregate, the dominant mineral phases, albite and quartz, are considered to be sensitive to

moisture damage. However, because of its lower moisture absorption (0.13%), it is hard for water to diffuse through the aggregate into the aggregate-bitumen interface to weaken the bond. The other granite aggregate G2 with higher moisture absorption values had the lowest retained fracture energy. This is not surprising as G2 aggregate has had a long history of very poor moisture damage performance in the field [3]. Aggregate G3 shows the lowest retained fracture energy demonstrating its susceptibility to moisture damage. One thing that should be mentioned is that the retained fracture energy of B1-G3 is higher than B1-G2 after 7 days of moisture conditioning but the sequence was exchanged after 14 days conditioning. This could be due to the moisture absorption of G3 being lower than G2, with 7 days conditioning not letting the moisture fully reach the aggregate-bitumen interface. Once the moisture attacked the interface, the adhesion between aggregate and bitumen deteriorated quickly.

In terms of the limestone aggregates (L1 and L2), both showed good moisture resistance due to their dominant mineral phase (calcite) which can form a stable bond with bitumen even in the presence of water. The slightly lower result of L1 could be attributing to its higher water absorption (2.21%) in comparison with L2 (0.46%). On this basis, it is reasonable to state that the moisture sensitivity of aggregate-bitumen bonds is not only controlled by the mineralogical compositions but the moisture absorption of the aggregate should also be considered.

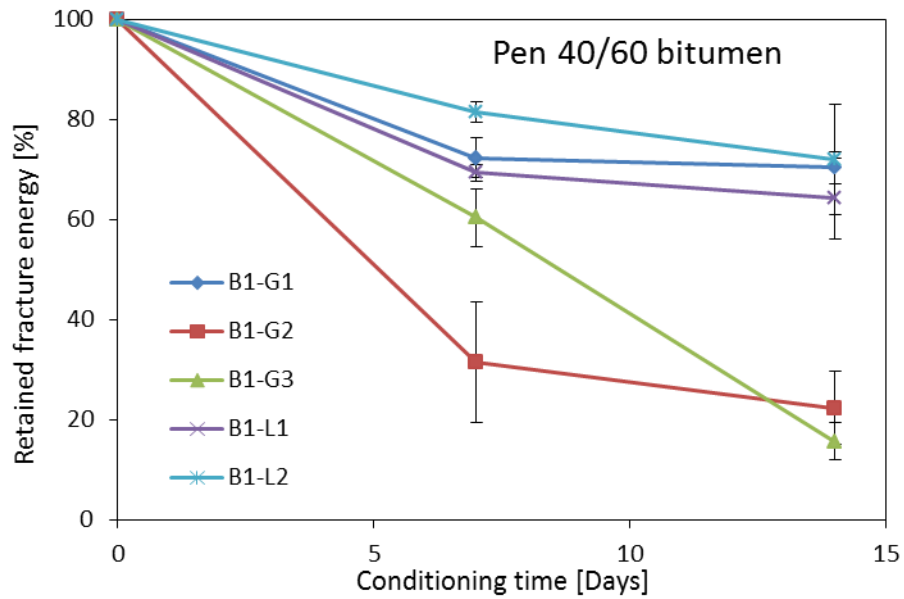


Figure 7-11 Retained fracture energy with respect to moisture damage achieved from CSPT

#### 7.4 Correlation between CSPT and standard peel test

As the CSPT is a newly designed method to characterise the moisture susceptibility of the aggregate-bitumen bond using coarse aggregate, the relationship between the CSPT and the standard peel test was evaluated by plotting the retained fracture energies from the two tests against each other. It should be mentioned that as there is no G3 aggregate boulder to prepare specimens for the standard peel test, only four specimens (B1-L1, B1-L2, B1-G1 and B1-G2) were selected in this section. Figure 7-12 shows the plot depicting the relationship between retained fracture energy, including 7 days and 14 days moisture conditioning, obtained from the CSPT and those from the standard peel test. It can be seen that the eight results are all located on one trend line demonstrating that the CSPT and the standard peel test give almost the same evaluation in terms of the moisture susceptibility of different aggregate-bitumen systems. It should be noted that in general the CSPT results are lower in comparison with the standard peel test. The results suggest that the newly developed CSPT is reliable in term of moisture damage evaluation and provides a more practical means of assessing the moisture damage performance of aggregate-bitumen systems using actual asphalt mixture coarse aggregates rather than large aggregate boulders.

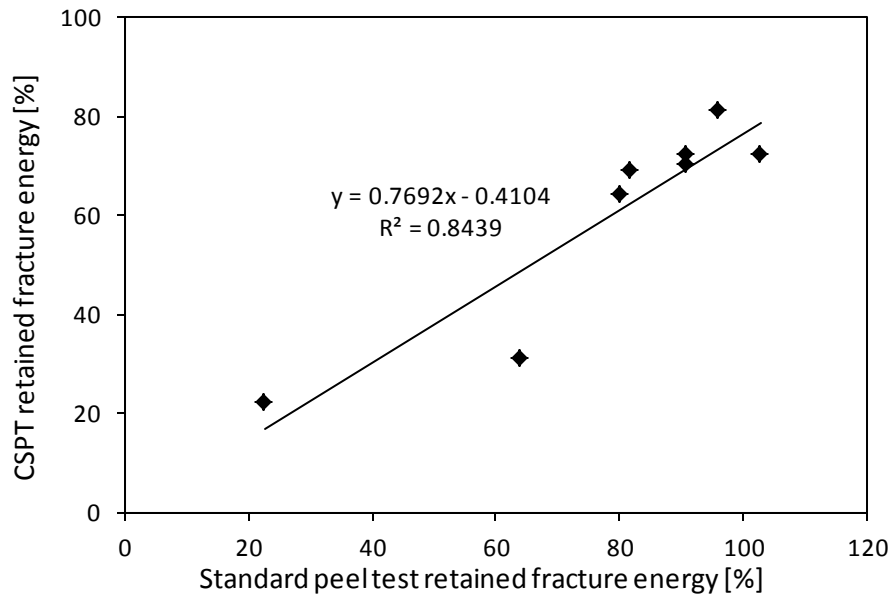


Figure 7-12 Plots of standard peel test retained fracture energy and CSPT retained fracture energy of specimens prepared with B1 bitumen showing good agreement between these two tests

## 7.5 Conclusions

This chapter presented the development of a reliable procedure to prepare peel test specimens using commonly used asphalt mixture coarse aggregates and evaluated the moisture sensitivity of different aggregate-bitumen combinations. The following conclusions were deduced based on the results presented in this chapter.

The newly designed procedure was found to be practicable to combine several coarse aggregates together and get a flat aggregate surface. The CSPT could correctly evaluate the fracture energy of aggregate-bitumen bonds in both dry conditions and after moisture damage.

Based on the CSPT, the aggregate properties do not influence the bonding strength of aggregate-bitumen combinations in the absence of moisture when the dominant failure mechanism is cohesive. Under these dry conditions the samples from both the CSPT and the peel test showed similar fracture energy values.

The magnitude of the fracture energy in the presence of water was found to be aggregate type dependent rather than bitumen dependent with failure being adhesive in nature. The tests demonstrated that the physico-chemical properties of the aggregates play a fundamental and significant role in the development of the moisture damage performance of aggregate-bitumen bonds.

The retained fracture energy results were shown to be sensitive to moisture conditioning and the moisture resistance could be explained by the moisture absorption and mineralogical compositions of the aggregates. Limestone tends to have better resistance to moisture damage than granite with the same moisture absorption. Furthermore, in terms of similar mineralogical compositions, lower moisture absorption may result in better moisture resistance.

The newly developed CSPT was found to be effective in characterising the moisture resistance of the aggregate-bitumen bond. The fracture energy accurately correlated with the failure mechanisms. The newly developed CSPT and the standard peel test showed the same ranking in terms of the moisture damage evaluation demonstrating that the CSPT is a reliable and feasible design to assess the moisture damage performance of aggregate-bitumen systems.

## References

1. Ahmad N., Cui S., Blackman B.R.K., Taylor A.C., Kinloch A.J. and Airey G.D. Predicting Moisture Damage Performance of Asphalt Mixtures. Nottingham Transportation Engineering Centre Report 2011, Report Number: 11091.
2. IC Peel software. <http://www3.imperial.ac.uk/meadhesion/testprotocols/peel>. Imperial College London. Accessed 14 March 2013.
3. Airey G.D., Collop A.C., Zoorob S.E. and Elliott R.C. The influence of aggregate, filler and bitumen on asphalt mixture moisture damage. *Construction and Building Materials* 2008, 22(9): 2015-2024.

## 8. Correlation between different tests

### 8.1 Introduction

One of the main objectives of this research is to understand the influence of several fundamental properties of pavement materials on the moisture damage of different aggregate-bitumen combinations. By evaluating the aggregate-bitumen adhesion and its deterioration in the presence of moisture (liquid or vapour), different methods had been used in this research with the results being presented in previous chapters. In Chapter 4, the surface energy properties of aggregates and bitumen used in this research were measured and the moisture sensitivity parameters of all aggregate-bitumen combinations were also calculated. In addition, the deterioration of aggregate-bitumen bonds was evaluated through three established mechanical tests (standard peel test, Pneumatic Adhesion Tensile Testing Instrument (PATTI) test and pull-off test) and one newly developed test (the composite substrate peel test (CSPT)). However, the correlations between the adhesion performance in both dry and wet conditions from these different techniques are not really understood.

The aim of this chapter is to combine the surface energy results with the mechanical property results in order to study the correlation between the moisture sensitivity parameters obtained from the different methods and evaluate the reliability of each technique in terms of moisture damage assessment. Firstly, the work of adhesion, fracture energy and tensile strength values obtained from different methods in the dry condition are correlated and compared. Secondly, retained fracture energy and retained tensile strength obtained from the mechanical techniques after moisture damage are correlated between each other. Finally, the moisture factor values obtained from mechanical techniques are compared with the moisture sensitivity assessment parameters so as to evaluate the reliability of each method.

## 8.2 Correlations of different tests in dry conditions

The bonding properties of different aggregate-bitumen combinations obtained from different techniques were first compared in this section with the results shown in Table 8-1. From this table it can be seen that there are two parameters, which are work of cohesion in the bitumen film and work of adhesion at the aggregate-bitumen interface, obtained from the surface energy tests with the work of adhesion values significantly higher than the cohesion values. This phenomenon theoretically demonstrated that the failure of asphalt mixtures is cohesive rather than adhesive in dry conditions and the aggregate-bitumen bonds tend to obtain similar results by using the same bitumen.

From the mechanical tests it can be seen that for the same bitumen, different samples obtained similar fracture energy or tensile strength values irrespective of which aggregate was used. This finding firstly confirmed the theoretical demonstration deduced from the surface energy test. In terms of the mechanical tests, the standard peel test and the newly developed CSPT showed similar fracture energy values demonstrating the good correlation of these two tests. In addition, the PATTI test and the pull-off test also obtained similar tensile strength values for the same aggregate-bitumen combination.

Based on the data presented in Table 8-1, it can be concluded that the techniques used in this research, including surface energy testing, established mechanical tests and the newly developed test, can be used to assess the bonding properties of the aggregate-bitumen interface in dry conditions.

Table 8-1 Aggregate-bitumen bonding values in dry condition

Sample	Surface energy test	Surface energy test	Peel test	CSPT	PATTI	Pull-off test
	$W_{11}$ (mJ/m <sup>2</sup> )	$W_{12}$ (mJ/m <sup>2</sup> )	$G_c$ (J/m <sup>2</sup> )	$G_c$ (J/m <sup>2</sup> )	POTS (kPa)	TS (kPa)
B1-L1	76.19	147.42	979	992	1820	-
B1-L2	76.19	123.22	972	987	1805	1920
B1-G1	76.19	125.28	1012	1003	1831	1947
B1-G2	76.19	118.39	1008	982	1840	1938
B1-G3	76.19	152.30	-	983	-	-
B2-L1	67.24	132.95	430	-	1359	-
B2-L2	67.24	115.14	439	-	1495	1425
B2-G1	67.24	118.59	432	-	1504	1386
B2-G2	67.24	109.52	444	-	1486	1413
B2-G3	67.24	136.70	-	-	-	-

Note:  $W_{11}$  = work of cohesion result for bitumen,  $W_{12}$  = work of adhesion result for bitumen-aggregate combinations,  $G_c$  = fracture energy (J/m<sup>2</sup>), POTS = pull-off tensile strength (kPa) and TS = tensile strength (kPa).

## 8.3 Correlations of different mechanical tests after moisture damage

### 8.3.1 Sensitivity of different mechanical tests on moisture damage

There are four mechanical tests, including the standard peel test, PATTI test, pull-off test and the newly developed CSPT, which have been used in this research to assess the moisture sensitivity of different aggregate-bitumen combinations. The moisture sensitivity of different aggregate-bitumen combinations was evaluated based on the retained fracture energy or retained tensile strength values after moisture conditioning with larger values suggesting better moisture resistance properties. However, these four tests were performed individually so that the relationship and correlations of these tests are less well understood. So, it seems important to evaluate the correlations of these tests and to characterise the reliability of each individual test. As the reliability of the

standard peel test had been proved in previous publications [1, 2, 3], this test is used as a benchmark in this section.

As the CSPT is a newly developed method to characterise the moisture susceptibility of the aggregate-bitumen bonds using coarse aggregates, the relationship between the CSPT and the standard peel test was first evaluated by plotting the retained fracture energies obtained from Chapters 5 and 7 against each other. It should be mentioned that there were no G3 aggregate boulders to prepare specimens used for the standard peel test, so only four specimens (B1-L1, B1-L2, B1-G1 and B1-G2) were selected for comparison in this section. Figure 8-1 shows the plot depicting the relationship between retained fracture energy, including both 7 days and 14 days moisture conditioning, obtained from the CSPT and those from the standard peel test. It can be seen that the eight results are all located on one trend line demonstrating that the CSPT and the standard peel test give almost the same evaluation in terms of moisture susceptibility of different aggregate-bitumen systems. It should be noted that in general the CSPT results are lower in comparison with the standard peel test. The results suggest that the newly developed CSPT is reliable in terms of moisture damage evaluation and provides a more practical means of assessing the moisture damage performance of aggregate-bitumen systems using actual asphalt mixture coarse aggregates rather than large aggregate boulders.

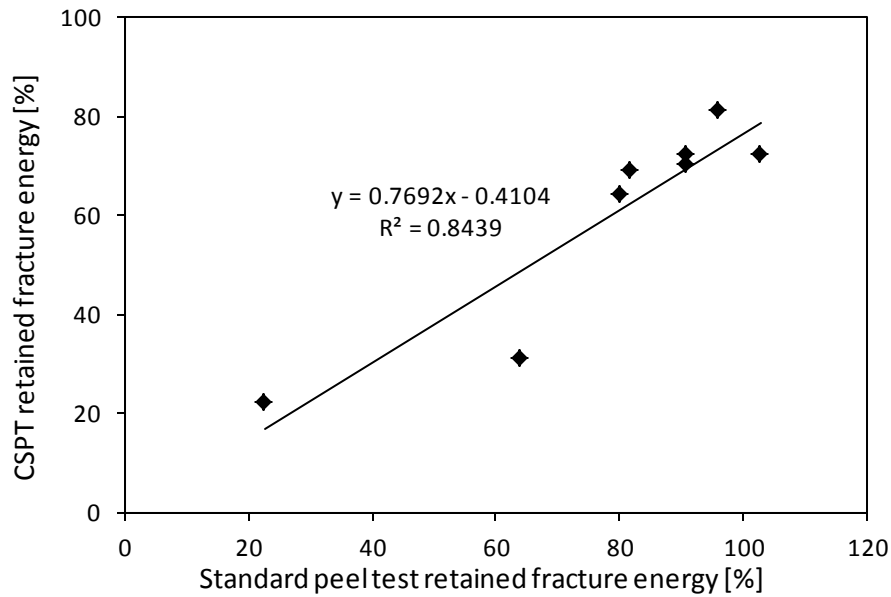


Figure 8-1 Plots of CSPT retained fracture energy and standard peel test retained fracture energy of specimens prepared with B1 bitumen showing good agreement between these two tests

The relationship between the standard peel test and the PATTI test was also quantified by combining the retained fracture energy and retained tensile strength from these two tests together. The retained fracture energy values and retained tensile strength values of specimens prepared with all aggregate-bitumen combinations presented in Chapters 5 and 6 were selected to compare with each other. Figure 8-2 shows the relationship between the retained fracture energy and the retained tensile strength obtained after 7 days and 14 days of moisture conditioning. From this Figure it can be seen that most of the results, except specimen B2-G2 after 7 days conditioning, were located on one trend line with higher retained fracture energy correlating with higher retained tensile strength. This demonstrated that the PATTI test is able to identify the moisture sensitivity of different aggregate-bitumen systems and obtain a similar ranking as the standard peel test. It should be mentioned that the values of retained tensile strength are only located in the region of 40% - 90% meaning the differences between each other are not really significant. So, the sensitivity of the PATTI test for moisture damage evaluation appears lower than for the standard peel test.

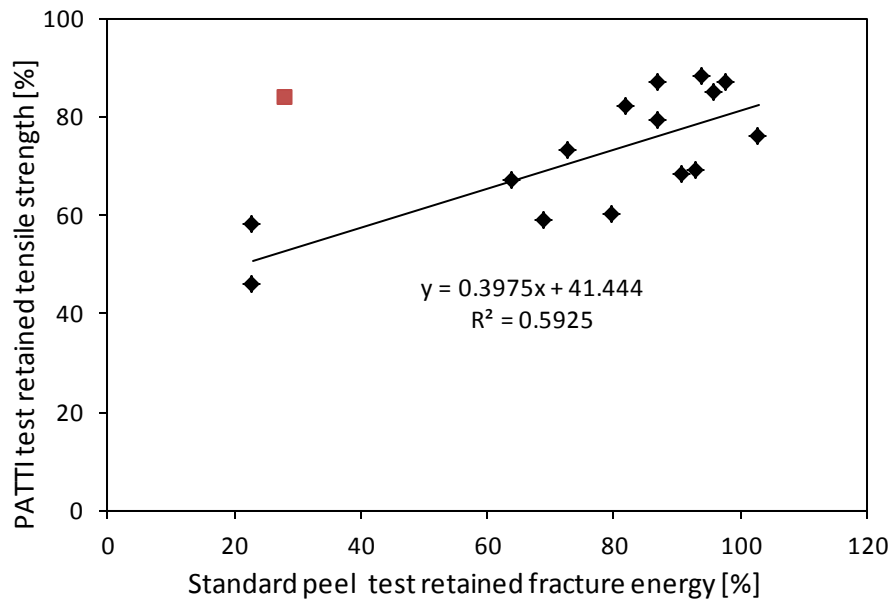


Figure 8-2 Plots of retained fracture energy and retained tensile strength obtained from the standard peel test and PATTI test showing good agreement between these two tests.

Note: The data in red colour (B2-G2 after 7 days conditioning) is far away the trend line.

As the specimens used for the pull-off test were moisture conditioned for 1 day and 7 days while those for standard peel test were conditioned for 7 days and 14 days, it seems difficult to correlate all the results with each other. So, for evaluating the correlation between the pull-off test and the standard peel test, only the results after 7 days moisture conditioning were selected to be analysed. A comparison of the standard peel test retained fracture energy versus the pull-off test retained tensile strength is provided in Figure 8-3. In this Figure, all specimens prepared with B1 and B2 are plotted together and there is one parameter (in the red colour) located far away the trend line. This demonstrated that these two tests obtained contrast results in the moisture sensitivity for this specimen. For other five specimens, the results are all located near the trend line meaning the good correlation of these two tests. It can be concluded that these two tests tend to results in similar moisture sensitivity values for most of the specimens. The contrast result may be because the specimen used for pull-off test is very small. Factors such as the substrate thickness and the bitumen film thickness cannot be well controlled and these factors may finally influence the moisture sensitivity results.

In summary, when taking the standard peel test as a benchmark, the other three mechanical tests, including the newly developed CSPT, the PATTI test and the pull-off test are all considered as being reliable in terms of evaluating the moisture sensitivity of different aggregate-bitumen systems. The newly developed CSPT showed the best correlation with the standard peel test. Though the pull-off results correlate well with the standard peel test for most of the specimens, the contrast results obtained from these two tests should not be neglected.

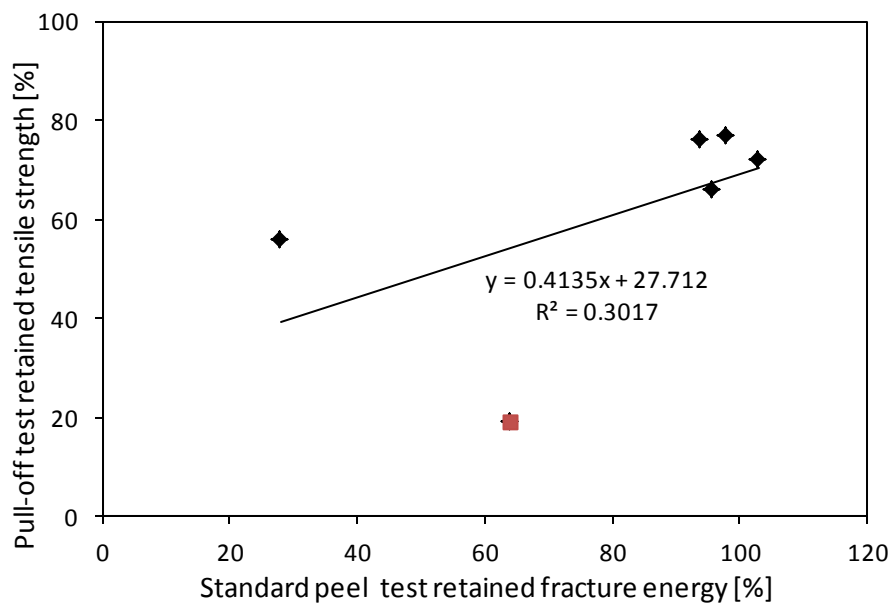


Figure 8-3 Plots of retained fracture energy and retained tensile strength obtained from standard peel test and pull-off test. Note: The data in red colour (B1-G2 after 7 days conditioning) is far away the trend line.

### 8.3.2 Correlations between different tests in terms of failure surface

All four methods used in this research can be considered as tensile in nature. The major differences are in terms of specimen geometry and loading rate. Apart from the retained fracture energy and retained tensile strength, the failure surface of the aggregate-bitumen systems after moisture conditioning can also be used to evaluate the correlation between different tests. The failure surfaces of B1-G2 samples obtained from all four tests before and after moisture conditioning are shown in Figure 8-4. Without moisture conditioning, a cohesive failure occurred within the bulk of the bitumen, as shown in Figure 8-4. The fracture energy and tensile strength depended on

the cohesive bond in the bulk bitumen layer. That is why all aggregates show almost the same fracture energy and tensile strength in the dry condition. After moisture conditioning, water penetrated into the specimen and weakened the aggregate-bitumen interface. The failure surfaces of all specimens tend to transform from cohesive to adhesive. However, less time was needed for the pull-off test (7 days) to achieve adhesive failure in comparison with the other three tests (14 days). This phenomenon also supports the assertion that the pull-off test is the most sensitive test to measure the moisture sensitivity of aggregate-bitumen combinations.

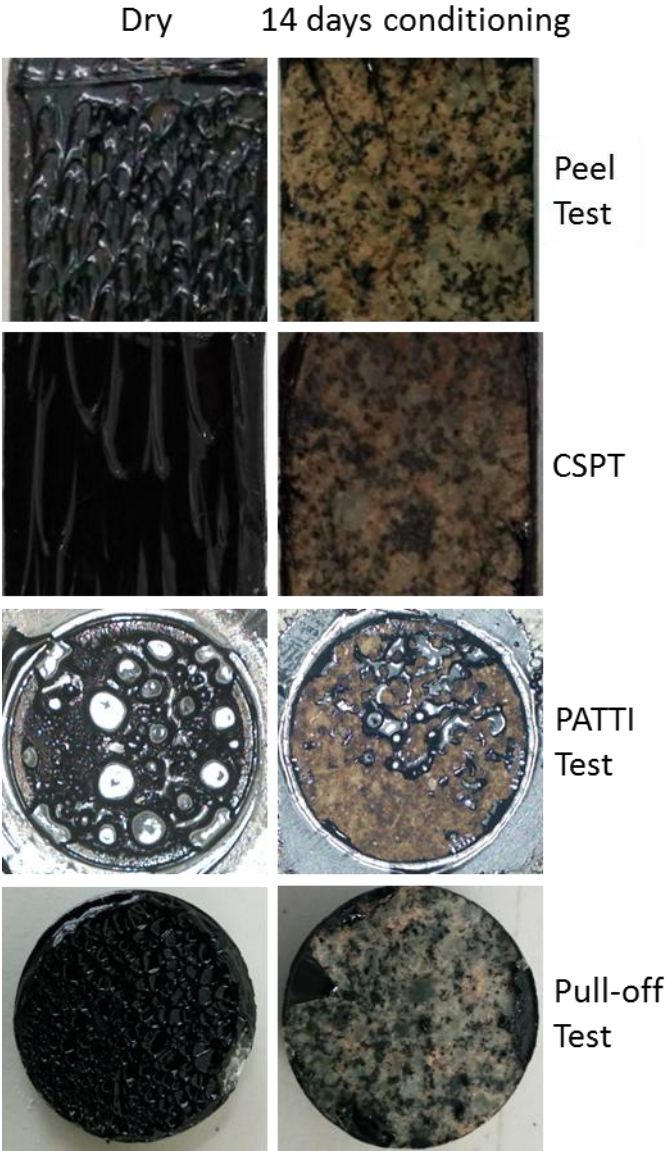


Figure 8-4 Failure surfaces of B1-G2 specimens before and after moisture conditioning obtained from the standard peel test, the newly developed peel test, the PATTI test and the pull-off test. Note: specimens of the standard peel test, CSPT and PATTI test were

moisture conditioned for 14 days, while the pull-off specimen was moisture conditioned for 7 days.

## **8.4 Correlation between surface energy test and mechanical test**

As presented in Chapter 4, four parameters were calculated based on the work of adhesion and debonding to compare the moisture sensitivity of different aggregate-bitumen systems with higher values representing better resistance to moisture damage. As the four moisture sensitivity parameters showed the same ranking in terms of the moisture sensitivity for the aggregate-bitumen systems considered in this research, only one parameter ( $ER_4$ ) was selected to correlate with the mechanical tests. As shown in Section 8.3, the four mechanical tests used in this research showed the same ranking in terms of the moisture sensitivity of different aggregate-bitumen combinations and these four tests are all recognised as reliable techniques to assess the moisture sensitivity of asphalt mixtures. In this case, any of the mechanical tests can be selected to be compared with the surface energy test. The retained fracture energy after 14 days moisture conditioning obtained from the newly developed CSPT and the standard peel test were selected to be correlated with the moisture sensitivity parameter calculated based on the surface energy results.

A comparison of the CSPT retained fracture energy versus the moisture sensitivity parameter  $ER_4$  obtained from the surface energy testing is provided in Figure 8-5. From this figure it can be seen that these two tests showed different ranking in terms of the moisture sensitivity with no correlation being found between these two tests. For instance, B1-G1 is considered to have good moisture resistance properties based on the CSPT and the other three mechanical tests. However, the B1-G1 combination has the lowest moisture sensitivity parameter value demonstrating its susceptibility to moisture damage. In addition, B1-G2 also yields misleading results because these two tests showed significantly different moisture resistance properties.

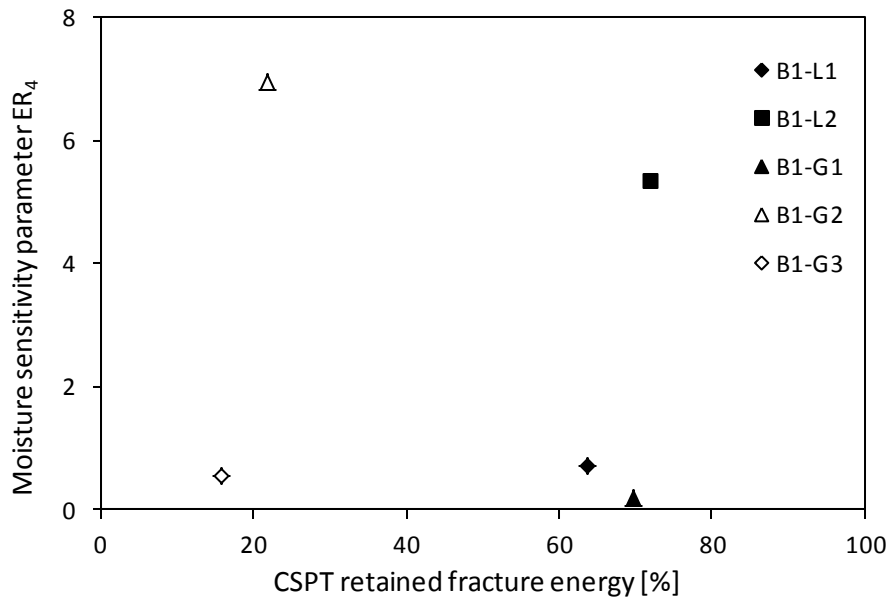


Figure 8-5 Plots of retained fracture energy and moisture sensitivity parameter obtained from CSPT and surface energy test

Figure 8-6 shows a plot depicting the relationship between the standard peel test retained fracture energy and the moisture sensitivity parameter  $ER_4$  obtained from the surface energy test. In all cases, a higher value of the parameter suggests better resistance to moisture damage. The results in this figure also show that these two tests obtained different moisture sensitivity ranking. In terms of the moisture sensitivity evaluation, the surface energy test cannot correlate with the mechanical peel test. Other two mechanical tests, PATTI test and pull-off test also show the same trend with no correlation with the surface energy test in terms of moisture sensitivity evaluation. It can be concluded that, based on the aggregates considered in this research, the surface energy-based method cannot correlate with the mechanical tests in terms of the moisture sensitivity evaluation of different aggregate-bitumen systems.

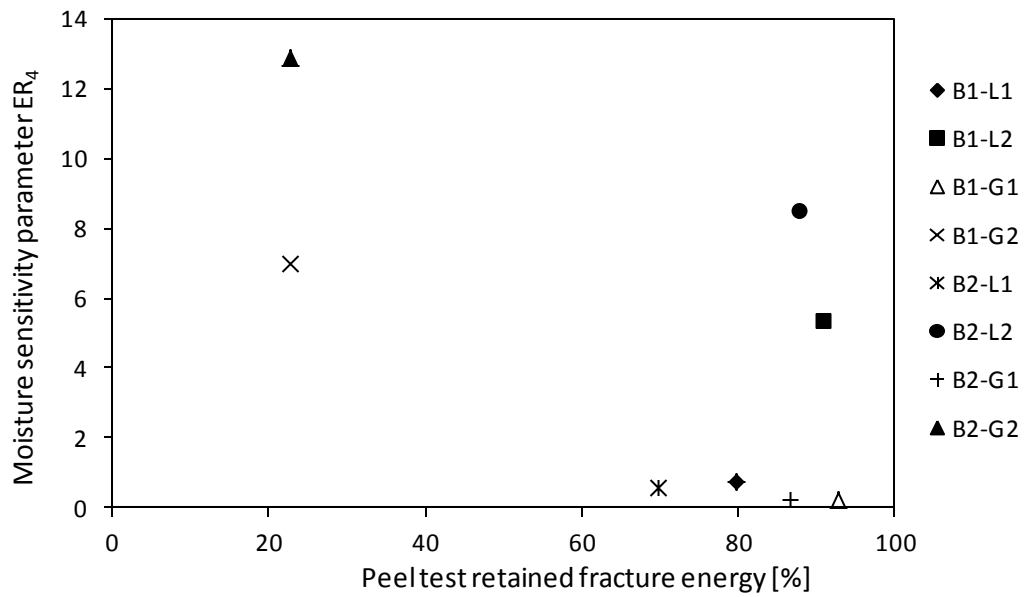


Figure 8-6 Plots of retained fracture energy and moisture sensitivity parameter obtained from standard peel test and surface energy test

The finding in this section seems cannot correlate with previous researchers. In Bhasin's research [4], the moisture sensitivity parameters obtained from the surface energy tests showed the same results as the dynamic creep test, as shown in Figure 8-7. In addition, Ahmad also found that the results from the surface energy tests and the SATS test generally follow the same trend, but there are still discrepancies which are not clearly explainable [5]. The different result in this research could be attributed to the following reasons. Firstly, the development of moisture sensitivity parameters were based on the aggregates that are commonly used in US, the aggregates from UK quarries may result in different trend. In addition, bitumen specimens used for the DCA test were actually aged due to the contact with air. So, the surface energy results of bitumen maybe different from those used for mechanical tests. Furthermore, the surface energy tests were performed at room temperature while the specimens used for mechanical tests were prepared at much higher temperatures. The surface energy results obtained at room temperature maybe cannot reflect the material properties at high temperatures so as to result in different trends in terms of moisture sensitivity evaluation.

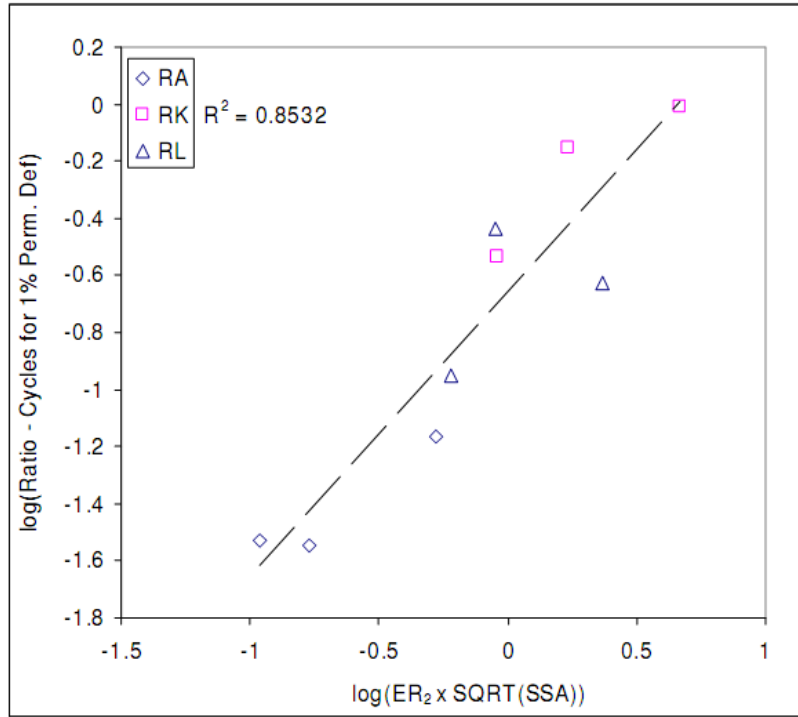


Figure 8-7 Moisture sensitivity parameter ER4 versus Wet to Dry Ratio of Fatigue Life [4]

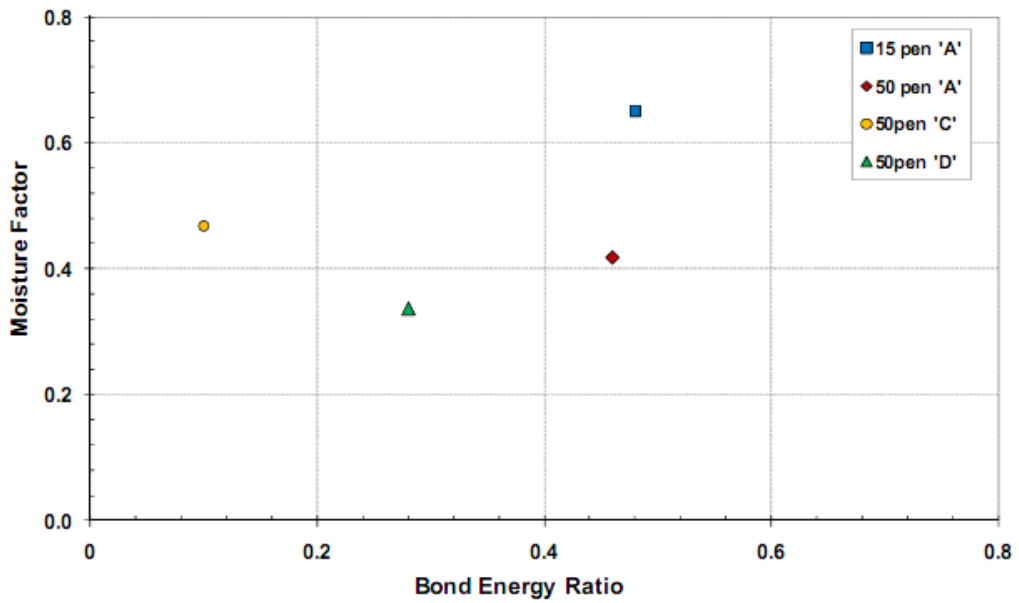


Figure 8-8 SATS Moisture Factors versus SE Bond Ratios [5]

## 8.5 Conclusions

The focus of this chapter is to compare the moisture damage evaluation techniques used in this research. This was done so as to study the correlation between the moisture sensitivity results obtained from different methods and characterise the reliability of each test. The test results obtained from different tests in the dry condition were first combined and compared. Then, the moisture sensitivity results, including the retained fracture energy and retained tensile strength, obtained from the four mechanical tests were compared and correlated with each other. In addition, the moisture sensitivity parameters from the surface energy-based tests were compared with the mechanical tests. The following conclusions were deduced based on the results presented in this chapter.

Based on the mechanical tests used in this research, the fracture energy or tensile strength of different aggregate-bitumen systems are controlled by the bitumen in dry conditions. The work of adhesion and cohesion results obtained from the surface energy tests also demonstrated that the bitumen rather than the aggregate-bitumen interface dominate the failure in dry conditions. All the techniques used in this research, including the mechanical tests and surface energy-based tests, showed the same result in terms of the bonding properties of the aggregate-bitumen systems in the dry condition.

By comparing the retained fracture energy and retained tensile strength values, the reliability and sensitivity of the four mechanical tests were correlated and evaluated. Firstly, the retained fracture energy obtained from the standard peel test and the newly developed CSPT showed good correlation, which demonstrated the reliability of the newly developed test. Furthermore, the PATTI test and the pull-off test also obtained similar rankings as the standard peel test in terms of the moisture sensitivity of different aggregate-bitumen systems. In addition, the failure surfaces of these four mechanical tests showed the same phenomenon with the cohesive failure transforming from cohesive to adhesive after moisture conditioning. So, based on the comparison conducted, the four mechanical tests are all considered to be reliable to evaluate the moisture sensitivity of different aggregate-bitumen systems.

The surface energy-based tests and the newly developed CSPT showed a different ranking in terms of the moisture sensitivity of aggregate-bitumen systems. In addition, the surface energy-based tests and the standard peel test showed different ranking in terms of moisture sensitivity evaluation. Other two mechanical tests, PATTI test and pull-off test also showed different results from the surface energy test. So, for the moisture sensitivity evaluation, the CSPT does not correlate well with the surface energy-based method which in turn does not correlate well with other three mechanical tests. Based on the aggregates considered in this research, the moisture sensitivity parameters obtained from the surface energy tests are suggested to be unreliable to evaluate the moisture sensitivity of aggregate-bitumen systems.

## References

1. Zhang J., Airey G.D. and Grenfell J.R.A. Experimental evaluation of cohesive and adhesive bond strength and fracture energy of bitumen-aggregate systems [J]. *Materials and Structures*, 2015: 1-15.
2. Zhang J., Apegyei A.K., Airey G.D. and Grenfell J.R.A. Influence of aggregate mineralogical composition on water resistance of aggregate-bitumen adhesion [J]. *International Journal of Adhesion and Adhesives*, 2015, 62: 45-54.
3. Blackman B.R.K., Cui S., Kinloch A.J. and Taylor A.C. The development of a novel test method to assess the durability of asphalt road-pavement materials. *International Journal of Adhesion and Adhesives* 2013; 42: 1-10.
4. Bhasin A. Development of Methods to Quantify Bitumen-Aggregate Adhesion and Loss of Adhesion due to Water: PhD dissertation, Texas A&M University, USA. 2006.
5. Ahmad N. Asphalt mixture moisture sensitivity evaluation using surface energy parameters. Ph.D. dissertation. University of Nottingham, 2011.

# 9. Conclusions and Recommendations

## 9.1 Overview

Moisture damage is recognised as one of the major causes of distress in asphalt pavements. During its service life, the presence of moisture can lead to the loss of stiffness and strength of the asphalt pavement layers and eventually the costly failure of the structure. Although not all damage is caused directly by moisture, its presence increases the extent and severity of already existing distresses. When moisture damage occurs, the loss of cohesion in the mastic and/or the loss of adhesion between the bitumen and aggregate interface will reduce the ability of a pavement to support traffic-induced stresses and strains, which can promote the development of cracks and rutting so as to accelerate the deterioration of the asphalt pavement.

Based on the literature review, the aggregate-bitumen interface is considered as a vulnerable boundary and most aggregate-bitumen interfaces are very sensitive to moisture attack. By evaluating the moisture sensitivity of asphalt mixtures, the focus of this research is located on the adhesion between aggregate and bitumen.

Numerous techniques have been developed in the past to evaluate the moisture sensitivity of asphalt mixtures. These tests can broadly be divided into tests performed on the loose coated aggregates and tests performed on compacted asphalt mixtures. Even if these techniques have been widely used and many of them were proved to be reliable to predict the performance of asphalt mixtures in the field, they do not directly evaluate the deterioration of the aggregate-bitumen interface so they cannot understand the mechanisms of moisture damage.

In this research, the moisture sensitivity of aggregate-bitumen combined specimens has been evaluated by directly measuring the bonding strength of the aggregate-bitumen interface before and after moisture conditioning using standard and newly developed mechanical tests. In addition, the surface energy properties of different bitumen and aggregates have been measured to characterise the moisture damage using the calculated moisture sensitivity parameters. Finally, the moisture damage results from

mechanical tests and thermodynamic results were compared and correlated with the physico-chemical properties of the original materials.

## 9.2 Conclusions

Based on the results obtained in this research, the following conclusions were deduced:

According to the surface energy tests presented in Chapter 2, the bonding strength of the aggregate-bitumen interface in the dry condition is controlled by the bitumen as the work of cohesion in the bitumen film is much lower than the work of adhesion at the aggregate-bitumen interface. However, with the presence of moisture, the work of debonding in the bitumen film is much higher than the work at the aggregate-bitumen interface resulting in the failure mechanism transforming from cohesive to adhesive. In addition, the work of debonding at the aggregate-bitumen interface is aggregate dependent demonstrating that moisture sensitivity of asphalt mixtures is dominated by the aggregate properties.

There are four moisture sensitivity parameters calculated based on the surface energy results of bitumen and aggregates. These four parameters show similar moisture sensitivity ranking for the five aggregates considered in this research. However, it should be mentioned that the four moisture sensitivity equations contain absolute values. The definition of these four equations is based on the hypothesis that all work of debonding results consisting of negative values. However, there are two aggregates used in this research that result in positive work of debonding values. It could be misleading if two aggregate-bitumen combinations result in positive and negative work of debonding result but with the same magnitude.

Based on the results from the standard peel test in the dry condition, all specimens showed cohesive failure regime with the bitumen dominating the fracture energy of the aggregate-bitumen bonds. In the dry condition, the bitumen film thickness showed significant influence on the fracture energy values with a thicker bitumen film resulting in higher fracture energy. However, the normalised toughness decreased with increasing film thickness.

After moisture conditioning, the values of fracture energy experienced a decrease for most of the specimens with 40/60 pen bitumen showing better moisture resistance than the 70/100 pen bitumen. The fundamental properties of aggregates, including the mineralogical composition and moisture absorption showed significant influence on the moisture sensitivity of aggregate-bitumen bonds. Strong correlations were also found between mineral compositions and moisture sensitivity with clay and anorthite having strong negative influence while calcite showed positive effect on moisture sensitivity. In terms of similar mineralogical composition, higher moisture absorption of aggregate correlated to lower resistance to moisture damage.

The combination of the PATTI equipment and the environmental chamber means that the tensile strength can be assessed under accurate temperature control. Based on the PATTI test, the tensile strength of aggregate-bitumen bonds was found to be sensitive to temperature. The failure pattern changed from cohesive failure to mixed cohesive/adhesive failure as the test temperature decreased from 40 °C to -10 °C. At the same time, the bitumen failure behaviour changes from brittle to ductile as the temperature increases from -10 °C to 40 °C. These combined effects resulted in the maximum tensile fracture strength for the various bitumen-aggregate combinations occurring at approximately 10 °C.

The tensile strength of different aggregate-bitumen combinations measured with the PATTI test and the pull-off test was shown to be sensitive to moisture conditioning. The failure pattern was shown to change from cohesive to mixed cohesive/adhesive and even adhesive failure as the conditioning time extended. These two tests showed similar ranking in terms of moisture sensitivity but the pull-off test was found to be the most sensitive. The high sensitivity of the pull-off test could be attributed to smaller specimen geometry that allowed faster moisture diffusion into the aggregate-bitumen interface where damage is believed to be initiated.

The newly developed Composite Substrate Peel Test (CSPT) was found to be practicable to combine several asphalt mixture coarse aggregates together and get a flat aggregate surface. The magnitude of the fracture energy in the presence of water was found to be aggregate type dependent rather than bitumen dependent with failure being adhesive in nature. The newly developed CSPT was found to be effective in characterising the moisture resistance of the aggregate-bitumen bond with the tensile

force accurately correlated with the failure mechanisms. The newly developed CSPT and the standard peel test showed the same ranking in terms of the moisture damage evaluation demonstrating that the CSPT is a reliable and feasible design to assess the moisture damage performance of aggregate-bitumen systems.

In the dry condition, all the techniques used in this research, including the mechanical tests and surface energy tests showed the same results in terms of the bonding properties of aggregate-bitumen systems. After moisture conditioning, the four mechanical tests, including standard peel test, CSPT, PATTI test and pull-off test showed similar moisture sensitivity ranking and failure surfaces demonstrating the good correlation of these four tests. In addition, based on the comparison conducted, the four mechanical tests are all considered to be reliable to evaluate the moisture sensitivity of different aggregate-bitumen systems. However, based on the aggregates considered in this research, the moisture sensitivity parameters obtained from the surface energy tests are suggested to be unreliable to evaluate the moisture sensitivity of aggregate-bitumen systems.

### **9.3 Recommendations**

Based on the overall work carried out in this research and the conclusions made in the previous section, the following recommendations are suggested for future research:

- The surface energy-based tests, including dynamic contact angle (DCA) technique and dynamic vapour sorption (DVS) technique should be used for the measurement of surface energy of a wide range of materials. The bitumen should be obtained from different crude oil sources with greater compositional diversity than those used in this research. In addition, modified bitumen should also be evaluated in the future. The aggregates from different quarries with different physico-chemical properties commonly used in asphalt pavement construction should also be investigated. The surface energy results from these two techniques can be used to evaluate the moisture sensitivity of different aggregate-bitumen systems. The moisture sensitivity of different aggregate-bitumen systems should be compared with the mechanical tests so as to further characterise these correlations.

- As mineral filler is one of the most important components in asphalt mixture, its influence on the moisture sensitivity of asphalt mixture should also be characterised. The surface energy of mastic (bitumen + filler) should be measured using the DCA technique so as to evaluate the influence of filler on bitumen surface energy. The surface energy results of mastic can then be combined with the aggregate surface energy to characterise the moisture sensitivity of aggregate-mastic systems.
- Based on the mechanical tests performed in this research, the properties of aggregate rather than the bitumen are the main influential factors for moisture damage of asphalt mixtures. So, the fundamental properties of aggregate, such as the surface micrographs, roughness and texture should be characterised using developed material testing techniques. In addition, the moisture absorption and diffusion properties of aggregates should be evaluated based on the moisture uptake results and correlated with the moisture sensitivity.
- As the bitumen is a visco-elastic material, its properties are very sensitive to temperature change. So, the standard peel test, the newly developed CSPT and the pull-off test should be carried out under accurate temperature control by assembling an environmental chamber in the universal testing machine (UTM). The influence of temperature on the surface energy of aggregate-bitumen bonds can be evaluated by using the standard peel test and the CSPT. Furthermore, the influence of temperature on moisture sensitivity of aggregate-bitumen bonds can also be evaluated by using the UTM with the temperature control system.
- As the speed of air release in the PATTI test is controlled manually, a large variability may be obtained from different researchers for the same sample. So, a modification should be carried out on the PATTI equipment to make sure the high pressure air is released at a constant speed. The bitumen film thickness in the PATTI test is controlled at 0.8 mm by the steel pull stub which cannot be changed like the peel test and pull-off test. So, more pull stubs which can produce different bitumen film thicknesses should be prepared so as to evaluate the influence of bitumen film thickness on tensile strength and moisture sensitivity of aggregate-bitumen systems.

- It was found from the pull-off test that the bitumen film thickness can be accurately controlled by using the modified fixtures which were assembled in the DSR. So, the specimens used for pull-off test can be prepared with different film thicknesses. In this case, the influence of bitumen film thickness on the tensile strength of aggregate-bitumen bonds should be evaluated in the future. In addition, the influence of bitumen film thickness on the moisture sensitivity of aggregate-bitumen systems should also be assessed.
- In this research, the moisture conditioning is only done on samples placed in deionised water at 20 °C for different periods. The limitation of this procedure is that it cannot evaluate the influence of temperature on the moisture sensitivity. So, the moisture damage procedure should be carried out in a water bath which can change the conditioning temperatures.
- Further investigation should be carried out by adding mineral fillers and adhesion promoters (amine based solutions and silanes) in the bitumen so as to evaluate their effects on the moisture sensitivity of the aggregate-bitumen systems.
- As the effect of aggregate on moisture sensitivity of asphalt mixture is more influential than the effect of bitumen, the surface treatment of aggregate should be considered in the future [1]. Surface treatment can make the aggregate surface waterproof and improve its adhesion with bitumen. In addition, surface treatment can change the aggregate surface from hydrophilic to hydrophobic so as to improve the moisture resistance.

## References

1. Mehrara A. and Khodaii A. A review of state of the art on stripping phenomenon in asphalt concrete [J]. Construction and Building Materials 2013 (38): 423-442.

## Appendix A

The influence of bitumen film thickness on fracture energy values

Specimen	Film thickness (mm)	Fracture energy (J/m <sup>2</sup> )				Average	SD
		1	2	3	4		
B1-L1	0.2	704	931	769	720	781	104
	0.25	1020	898	953	1046	979	67
	0.38	1050	1119	999	1056	1056	49
	0.5	1059	1063	1167	1099	1097	50
	0.9	1167	1154	1162	1170	1163	7
B2-L1	0.2	353	339	336	340	342	8
	0.25	438	434	438	408	430	14
	0.38	430	545	416	460	463	58
	0.5	468	572	442	479	490	57
	0.9	510	564	506	530	528	27

Note: SD = standard deviation

## Appendix B

Fracture energy values of all specimens before and after moisture damage

Specimen	Conditioning time (day)	Fracture energy (J/m <sup>2</sup> )				Average	SD
		1	2	3	4		
B1-L1	0	1020	898	953	1046	979	67
	7	759	821	803	835	805	33
	14	804	778	796	757	784	21
B1-L2	0	986	1008	986	906	972	45
	7	984	1024	997	1010	1004	17
	14	867	885	923	862	884	28
B1-G1	0	1055	974	1046	974	1012	44
	7	965	1007	958	966	974	22
	14	921	986	954	920	945	31
B1-G2	0	1171	931	965	965	1008	110
	7	606	671	638	674	647	32
	14	235	209	216	248	227	18
B2-L1	0	438	434	438	408	430	14
	7	297	306	333	315	313	15
	14	305	317	279	296	299	16
B2-L2	0	408	476	457	416	439	33
	7	439	392	407	414	413	20
	14	397	368	385	389	385	12
B2-G1	0	472	390	427	438	432	34
	7	456	407	389	438	423	30
	14	359	368	396	389	378	17
B2-G2	0	468	397	476	434	444	36
	7	106	113	139	132	123	16
	14	113	106	85	105	102	12

Note: SD = standard deviation

## Appendix C

Tensile strength of all specimens before and after moisture damage obtained by PATTI

Specimen	Conditioning time (day)	Tensile strength (kPa)				Average	SD
		1	2	3	4		
B1-L1	0	1578	1738	2064	1898	1820	209
	7	1694	1678	1306	1319	1498	217
	14	1060	1214	1269	839	1096	193
B1-L2	0	1798	1856	1891	1675	1805	95
	7	1269	1457	1528	1278	1383	130
	14	1046	1342	1197	1343	1232	142
B1-G1	0	2014	1683	1794	1832	1831	138
	7	1247	1435	11724	11424	1458	197
	14	1209	1369	1098	1236	1228	111
B1-G2	0	1724	1679	1963	1994	1840	161
	7	1403	1175	1304	1106	1247	132
	14	796	1019	869	786	863	112
B2-L1	0	1375	1265	1436	1358	1359	71
	7	960	1098	976	905	985	81
	14	729	889	811	1109	885	163
B2-L2	0	1496	1539	1512	1434	1495	45
	7	1352	1330	1187	1396	1316	90
	14	1087	1342	1429	1352	1303	149
B2-G1	0	1369	1584	1336	1727	1504	185
	7	1540	1545	1479	1507	1518	31
	14	1370	1594	1463	1512	1485	94
B2-G2	0	1347	1633	1468	1495	1486	117
	7	1203	1352	1115	1319	1247	109
	14	899	1059	568	927	863	209

Note: SD = standard deviation

## Appendix D

Tensile strength of all specimens before and after moisture damage obtained by Pull-off test

Specimen	Conditioning time (day)	Tensile strength (kPa)				Average	SD
		1	2	3	4		
B1-L2	0	1820	1915	2063	1881	1920	103
	1	1332	1605	1277	1344	1390	147
	7	1513	1318	1404	1297	1383	98
B1-G1	0	1701	1868	2164	2044	1947	199
	1	1276	1531	1253	1341	1350	126
	7	1262	1321	1193	1394	1293	86
B1-G2	0	2232	1740	1843	-	1938	259
	1	632	420	505	436	498	84
	7	301	456	316	411	371	75
B2-L2	0	1222	1416	1504	1557	1425	147
	1	1351	1084	1101	1275	1203	131
	7	1009	1106	1152	1045	1078	64
B2-G1	0	1455	1414	1286	1389	1386	72
	1	1187	1380	1264	1156	1247	100
	7	1027	1105	1074	1041	1062	35
B2-G2	0	1589	1371	1407	1284	1413	128
	1	994	1106	1042	1023	1041	47
	7	835	753	741	865	799	61

Note: SD = standard deviation

## Appendix E

Fracture energy of all specimens before and after moisture damage

Specimen	Conditioning time (day)	Fracture energy (J/m <sup>2</sup> )				Average	SD
		1	2	3	4		
B1-L1	0	985	999	-	-	992	9.4
	7	680	712	680	680	688	16.0
	14	568	585	745	650	637	80.3
B1-L2	0	968	1006	-	-	987	26.3
	7	826	812	800	778	804	20.1
	14	799	673	575	798	711	108.4
B1-G1	0	1008	998	-	-	1003	6.7
	7	747	772	696	689	726	40.0
	14	728	722	668	-	706	33.4
B1-G2	0	976	988	-	-	982	7.8
	7	476	216	305	234	308	118.5
	14	208	146	319	203	219	72.0
B1-G3	0	978	988	-	-	983	7.3
	7	568	660	536	626	598	55.9
	14	135	177	194	115	155	36.5

Note: SD = standard deviation

## Relevant Publications

1. Zhang J., Airey G.D. and Grenfell J.R.A. Experimental evaluation of cohesive and adhesive bond strength and fracture energy of bitumen-aggregate systems. *Materials and Structures*, 2015: 1-15.
2. Zhang J., Apegyei A.K., Airey G.D. and Grenfell J.R.A. Influence of aggregate mineralogical composition on water resistance of aggregate-bitumen adhesion. *International Journal of Adhesion and Adhesives*, 2015, 62: 45-54.
3. Zhang J., Apegyei A.K., Grenfell J.R.A and Airey G.D. Experimental Study of Moisture Sensitivity of Aggregate-Bitumen Bonding Strength Using a New Pull-Off Test. 8th RILEM International Symposium on Testing and Characterization of Sustainable and Innovative Bituminous Materials. Springer Netherlands, 2016: 719-733.
4. Zhang J., Apegyei A.K. and Airey G.D. Effect of Aggregate Composition on Moisture Sensitivity of Aggregate-Bitumen Bonds. Transportation Research Board 94th Annual Meeting. 2015 (15-0999).
5. Zhang J., Airey G.D., Grenfell J.R.A., Apegyei A.K. and Barrett M. Development of a composite substrate peel test to assess moisture sensitivity of aggregate-bitumen bonds. *International Journal of Adhesion and Adhesives* (Under review).